2014

Regulation and Targeting of Fyn in Human Cutaneous Squamous Cell Carcinoma

Sarah Fenton
Loyola University Chicago

LOYOLA UNIVERSITY CHICAGO

REGULATION AND TARGETING OF FYN IN HUMAN CUTANEOUS SQUAMOUS CELL CARCINOMA

A DISSERTATION SUBMITTED TO

THE FACULTY OF THE GRADUATE SCHOOL

IN CANDIDACY FOR THE DEGREE OF

DOCTOR OF PHILOSOPHY

PROGRAM IN MOLECULAR BIOLOGY

BY

SARAH E. FENTON

CHICAGO, IL

AUGUST 2014

ACKNOWLEDGEMENTS

This dissertation would not have been possible without the support of many people. I would first like to express my sincere gratitude to Dr. Mitchell F. Denning for his unceasing patience and dedication to my development as a scientist. His commitment to science is a constant inspiration, and I cannot thank him enough for this example that will influence the rest of my career.

I would also like to thank the members of my dissertation committee: Dr. Diaz, Dr. Osipo, Dr. Shimamura and Dr. Callaci. Every meeting was instrumental in the development of this project. I am particularly grateful to the members of the Denning lab, Molecular Biology Program and MD/PhD Program at Loyola University Chicago for their support and constant positive input.

I cannot thank my parents, Jay and Susan Fenton, enough for their unflagging support during these long years of schooling. Without their belief in my capabilities I am confident I could not have completed this degree course. I would also like to thank my husband, Thomas Schuessler, although nothing that I can write here can express my gratitude or the immensity of his constant support. I would also like to thank my sister, Erica Fenton, for her emotional support and belief in my capabilities and my grandmother, Jackie Fenton, for her constant reassurances that nothing worthwhile comes easily.

TABLE OF CONTENTS

LIST OF FIGURES

LIST OF ABBREVIATIONS

AK	Actinic keratosis
BCC	Basal cell carcinoma
CaR	Calcium receptor
CDK	Cyclin dependent kinase
ChIP	Chromatin immunoprecipitation
CML	Chronic myelogenous leukemia
cSCC	Cutaneous squamous cell carcinoma
DAG	Diacylglycerol
DMBA	7,12-Dimethylbenz(a)anthracene
DMEM	Dulbecco's Modified Medium
ECM	Extracellular matrix
EGF	Epidermal growth factor
EGFR	Epidermal growth factor receptor
EMSA	Electrophoretic mobility shift assay
EMT	Epithelial to mesenchymal transition
GAP	GTPase activating protein
GDP	Guanosine diphosphate
GEF	Guanine nucleotide exchange factor

GPCR	G-protein coupled receptor
GTP	Guanosine triphosphate
K1	Keratin 1
KC	Keratinocyte
MMP	Matrix metalloprotease
NAC	N-acetyl-cysteine
NF-κB	Nuclear factor κB
PBS	Phosphate buffered saline
PDGFR	Platelet-derived growth factor receptor
PI	Propidium iodide
PI3K	Phosphatidylinositol 3-kinase
PKC	Protein kinase C
ROS	Reactive oxygen species
RT-qPCR	Quantitative reverse transcriptase polymerase chain reaction
SDS-PAGE	Sodium dodecyl sulphate-polyacrylamide gel electrophoresis
SFK	Src family kinase
SH	Src-homology
SiRNA	Small interfering RNA
TGF-α	Transforming growth factor-α
TPA	12-O-tetradecanoylphorbol 13-acetate
UV	Ultraviolet light

ABSTRACT

Fyn, a member of the Src family kinases (SFK), is an oncogene in murine epidermis and is associated with cell-cell adhesion turnover and migration. Additionally, Fyn is upregulated in multiple tumor types, including human cutaneous squamous cell carcinoma (cSCC). Introduction of active H-Ras(G12V) into the HaCaT human keratinocyte cell line resulted in upregulation of *FYN* mRNA (200-fold) and protein, but did not increase the expression of other SFKs. Using luciferase reporter constructs, we identified two nucleotides 74 bases upstream of the human *FYN* gene transcription start site as necessary for *FYN* upregulation in HaCaT-Ras cells. Following chromatin immunoprecipitation and electrophoretic mobility shift assays, Lef-1 was identified as the transcription factor most likely binding to this site and mediating *FYN* upregulation.

Increased Fyn expression levels following either the transduction of active Ras (HaCaT-Ras) or Fyn (HaCaT-Fyn) into HaCaT cells induced an epithelial-to-mesenchymal transition (EMT), including loss of E-cadherin and cytokeratin expression, gain of vimentin expression and reduced cell-cell adhesion. Introduction of Ras or Fyn also resulted in upregulation of the EMT master regulator, *TWIST1*, demonstrating a potential mechanism driving the transition to a mesenchymal phenotype. The identification of EMT markers in cSCC significantly increases the risk of cancer-related

mortality. Therefore we next chose to inhibit Fyn activity to see if this would reverse or block these characteristics that result in clinically more dangerous cSCCs.

Inhibition of Fyn activity using the clinical SFK inhibitor Dasatinib did not reduce cell viability, proliferation, apoptosis or autophagy in the transformed HaCaT-Ras cells when compared to the parental HaCaT cells. However, Fyn inhibition using siRNA or Dasatinib increased cell-cell adhesion in HaCaT-Ras cells over 6-fold ($p<0.001$) through a rapid (5-60 min.) increase in the cortical F-actin cytoskeleton. Treatment of the HaCaT-Fyn cells with Dasatinib also resulted in upregulation of F-actin. Dasatinib did not restore cytokeratin expression, but induced F-actin colocalized with the adherens junction proteins α-catenin, β-catenin and p120catenin in HaCaT-Ras cells, suggesting that stable adherens junctions were mediating the increase in cell-cell adhesion. Additionally, Dasatinib treatment significantly inhibited cell migration ($p<0.001$). Inhibition of the Rho effector protein Rho-associated protein kinase (ROCK) blocked Dasatinib-induced F-actin and cell-cell adhesion ($p<0.001$) in HaCaT-Fyn and HaCaT-Ras cells, implicating relief of Rho GTPase inhibition as a mechanism of Dasatinib-induced cell-cell adhesion. The ability of Dasatinib to promote F-actin polymerization was a key initiator of cell-cell adhesion, as Dasatinib-induced cell-cell adhesion was blocked by Cytochalasin D ($p<0.001$). Conversely, inhibiting cell-cell adhesion with low Ca^{+2} media did not block Dasatinib-induced F-actin induction.

Finally, topical Dasatinib treatment immediately following UV exposure significantly reduced total tumor burden in the SKH1 mouse model of skin

carcinogenesis ($p<0.05$). Together these results identify the promotion of actin-based cell-cell adhesion as a newly described mechanism of action for Dasatinib and suggest that Fyn inhibition may be an effective therapeutic approach in treating SCC.

CHAPTER I

INTRODUCTION

1.1 The Human Skin

The main function of the skin is to form a first line of defense, protecting the internal structures of an organism from external insults by creating a physical, antimicrobial and immunological barrier (Madison, 2003, Proksch, Brandner and Jensen, 2008). In order to protect the organism, the skin must prevent excessive water loss, participate in thermoregulation and sensory perception and prevent damage induced by ultraviolet radiation, toxins, pathogens and physical trauma (Madison, 2003). These functions of the skin are accomplished due to the unique anatomy of the dermis and epidermis.

1.1.1 The Anatomy of the Skin

The skin is composed of two main layers, the epidermis and the dermis. More specifically, the epidermis makes up the outermost layer of the skin, creating a protective barrier composed primarily of keratinocytes at varying stages of differentiation (Proksch, Brandner and Jensen, 2008). Separating the epidermis from the dermis is the basement membrane, a fibrous sheet composed of the basal and reticular laminae that creates a

surface for the epidermal cells to attach to, as well as a physical barrier against invading pathogens or malignant cells (Figure 1)(Paulsson, 1992, Liotta et al, 1980). The dermis, in turn, is composed of connective and adipose tissue, as well as hair follicles, sweat glands, sebaceous glands, apocrine glands, lymphatic and blood vessels (Pearce and Grimmer, 1972). The dermis protects internal structures from external stress, as well as provides tensile strength to the skin (Figure 1) (Pearce and Grimmer, 1972). Although not technically considered a layer of the skin, the hypodermis lies underneath the dermis, aids in the attachment of the skin to the muscle and bone and is comprised mostly of adipose tissue.

The epidermis is classified as a stratified squamous epithelium, meaning it is composed of several layers of epithelial keratinocytes undergoing a programmed process of squamous differentiation (Fuchs, 2008, Presland and Dale, 2000). The surface layer of the epidermis is the stratum corneum, and is composed completely of fully differentiated, anuclear corneocytes (also known as squames). The stratum corneum creates the most important barrier against water loss and external infiltration, although loss of this layer is not life-threatening (Proksch, Brandner and Jensen, 2008, Elias, Fritsch and Epstein, 1977, Madison, 2003). Underneath the stratum corneum is the stratum lucidum, an area of transition between the dead and living layers of the epidermis (Eckert and Rorke, 1989). Next is the stratum granulosum, where the keratinocytes lose their nuclei (as well as other intracellular organelles) and synthesize lipids to aid in the formation of a lipid

barrier (Eckert and Rorke, 1989, Eckert, 1989). Following the stratum granulosum is the stratum spinosum, characterized by the formation of desmosomes between adjacent keratinocytes that give the layer a "spinous" appearance (Eckert, 1989). This is also the layer where the keratinocytes begin production of suprabasal keratins K1 and K10, important intermediate filament proteins that aid in the cell's tensile strength, as well as many signaling mechanisms (Dotto, 1999). Finally, adjacent to the basement membrane is the stratum basale, a layer of keratinocytes that attach to the basement membrane using hemidesmosomes and proliferate to renew the stem cell pool or yield transit amplifying cells (Nie, Fu and Han, 2013). These transit amplifying cells may also proliferate, but they ultimately begin to differentiate and progress through the overlying epidermal layers (Figure 1)(Houben, De Paepe and Rogiers, 2007, Allen and Potten, 1974, Ghazizadeh and Taichman, 2005).

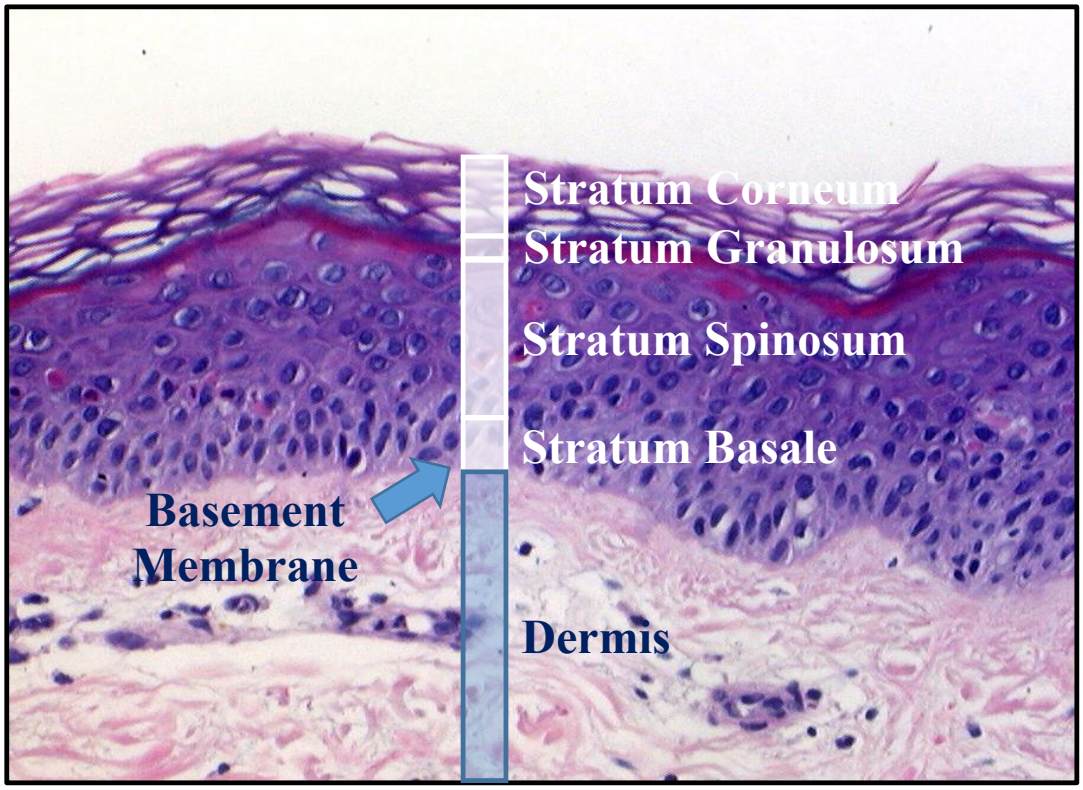

Figure 1: Histology of the Epidermis

A section of the human epidermis stain with Hematoxylin and Eosin is pictured. The Dermis and four layers of the Epidermis are labeled (Stratum Corneum, Stratum Granulosum, Stratum Spinosum, Stratum Basale), as well as the basement membrane. Picture of skin histology courtesy of Mitchell F. Denning.

Although the layers of the epidermis are clearly defined and identifiable microscopically, they are in constant flux. As the stem cells proliferate at the stratum basale, they yield transit amplifying cells whose daughter cells are eventually pushed up from the basement membrane, decreasing their cell-matrix adhesion by downregulating their hemidesmosomes in favor of cell-cell adhesion complexes such as desmosomes and adherens junctions (Dotto, 1999). The increase in cell-cell adhesion complexes is aided by an increasing gradient of extracellular Ca^{+2} from the stratum spinosum to the stratum granulosum, a driving force in keratinocyte differentiation (Tu et al, 2004, Menon et al, 1992, Forslind et al, 1997). Extracellular Ca^{+2} binds to its surface receptor CaR, activating phospholipase C to induce inositol 3 phosphate and diacyl glycerol production, increasing intracellular Ca^{+2} and activating protein kinase C family members, including PKC-α, -δ and –η, to induce cellular differentiation pathways (Dotto, 1999, Denning et al, 1995, Lee et al, 1997, Osada et al, 1993, Tu et al, 2004). Other groups have also shown the importance of retinoic acid and Vitamin D3 in regulating the expression of pro-differentiation factors (Dotto, 1999). As the cells differentiate, they lose their ability to proliferate and begin to express markers such as keratin 1 and 10, involucrin, filaggrin and transglutaminase (Eckert and Rorke, 1989, Dotto, 1999). During differentiation the keratinocytes continue to move through the stratum spinosum to the stratum granulosum where they lose their nuclei to create a tightly bound layer of corneocytes, the outer layers of which can be shed to protect the integrity of the organ. When this carefully

regulated program of differentiation is disturbed the barrier function of the skin is compromised (Eckert and Rorke, 1989).

1.1.2 Skin Cancer Diagnoses and Prevalence

Three main classes of malignancies arise from cells of the epidermis: melanoma, basal cell carcinoma (BCC) and squamous cell carcinoma (cSCC). Over 3.5 million cases of skin cancer were diagnosed in the United States of America in 2010, making non-melanoma skin cancers more common than all other forms of cancer combined (Perera and Sinclair, 2013, Rogers et al, 2010a). Rates of diagnoses for non-melanoma skin cancer have been increasing 3-8% per year since the 1960s, most likely due to increased ultraviolet light (UV) exposure, changes in outdoor activities and clothing styles, increased lifespan and ozone depletion (Gloster and Brodland, 1996, Green, 1992). Current studies have shown an even greater increase (around 300%) in diagnosis rates since 1994 (Perera and Sinclair, 2013, Rogers et al, 2010b). BCCs are histologically very uniform and homogenous tumors, and are also extremely common. 3 out of 10 Caucasians will develop a BCC within their lifetime (Bhawan, 2007, Ratushny et al, 2012). Approximately 20% of non-melanoma skin cancers are cSCCs, and these tumors are differentiated from BCCs by the presence of keratin pearls and other indicators of stratification (Diepgen and Mahler, 2002). 99% of cSCC cases are successfully treated with surgical excision (LeBoeuf and Schmults, 2011, Newman, 1991, Clayman et al, 2005). Melanoma originates from the pigment producing melanocytes and is the least

common type of skin cancer, with 18-20x lower rates of diagnosis than BCC and cSCC (Diepgen and Mahler, 2002). However, melanoma is the most aggressive and most fatal form of skin cancer, causing 75% of skin cancer-related deaths (Jerant et al, 2000).

1.2 Cutaneous Squamous Cell Carcinoma (cSCC)

When keratinocytes from the epidermis undergo malignant transformation and histologically maintain characteristics of squamous differentiation, a tumor classified as a cSCC results. UV exposure, especially UVB, is the most common carcinogen driving the formation of cSCCs (Alam and Ratner, 2001). Additionally, many skin lesions are diagnosed in the precursor phase of cSCC or as an actinic keratosis (AK). Once the malignancy has progressed to the diagnosis of cSCC it is classified as either cSCC *in situ* (also known as Bowen's disease), or as invasive SCC (Figure 2)(Croxton, Ma and Cress, 2002).

1.2.1 Actinic Keratoses (AKs)

AKs are often considered precursor lesions for cSCC and are defined as epidermal dysplasia with enlarged, irregular and hyperchromatic nuclei and disorganized growth and differentiation resulting in a thickened stratum corneum with retained nuclei (Ratushny et al, 2012, Butani, Arbesfeld and Schwartz, 2005). The atypia that

characterizes AKs does not penetrate the full thickness of the epidermis – instead it is usually confined to the deeper layers of the epidermis with overlying parakeratotic and hyperkeratotic cells (Figure 2)(Anwar et al, 2004). 15-20% of AKs progress to cSCCs within 10-25 years (Marks, Rennie and Selwood, 1988). Because most patients present with an average of 6-8 AK lesions, their risk of developing invasive SCC within one year is between 0.15% and 80%. However, within one year AKs have a 26% likelihood of spontaneous regression (Ratushny et al, 2012).

1.2.2 cSCC *in situ*

cSCC *in situ* is often the next step in malignant progression from AKs, where a greater degree of atypia is observed but the abnormal cells have not invaded the basement membrane (Ratushny et al, 2012, Bhawan, 2007). More specifically, the atypia of cSCC *in situ* is seen through all layers of the epidermis, while the atypia of AKs are contained to fewer layers (Figure 2)(Butani, Arbesfeld and Schwartz, 2005). Other lesions that fall underneath the subheading of cSCC *in situ* include Bowen's disease, arsenical keratosis, bowenoid papulosis and erythroplasia of Queyrat (Ratushny et al, 2012, Bhawan, 2007, Anwar et al, 2004). Some dermatologists also consider AKs to be cSCC *in situ*, as clinical criteria to differentiate AKs from cSCC have not been determined (Bhawan, 2007, Moy, 2000). Histologically this malignancy is defined as transepidermal atypia

with loss of polarity, mitotic figures, dyskeratosis, hyperchromasia, abnormal differentiation and nuclear crowding (Bhawan, 2007).

1.2.3 Invasive cSCCs

Once malignant keratinocytes have invaded past the basement membrane and into the dermis they are no longer considered cSCC *in situ* and are instead histologically classified as invasive cSCCs (Figure 2)(Mullen et al, 2006). Clinically, the identification of invasion or a migratory capacity in cSCC decreases the average predicted three year disease free survival rate by thirty percent (Clayman et al, 2005). cSCCs most likely to metastasize fulfill the following clinical parameters: larger than 2 cm, invade more than 6 cm, poorly differentiated, have undergone previous treatment or are located near the nose, ear or lip (Salasche, 2000, Mullen et al, 2006).

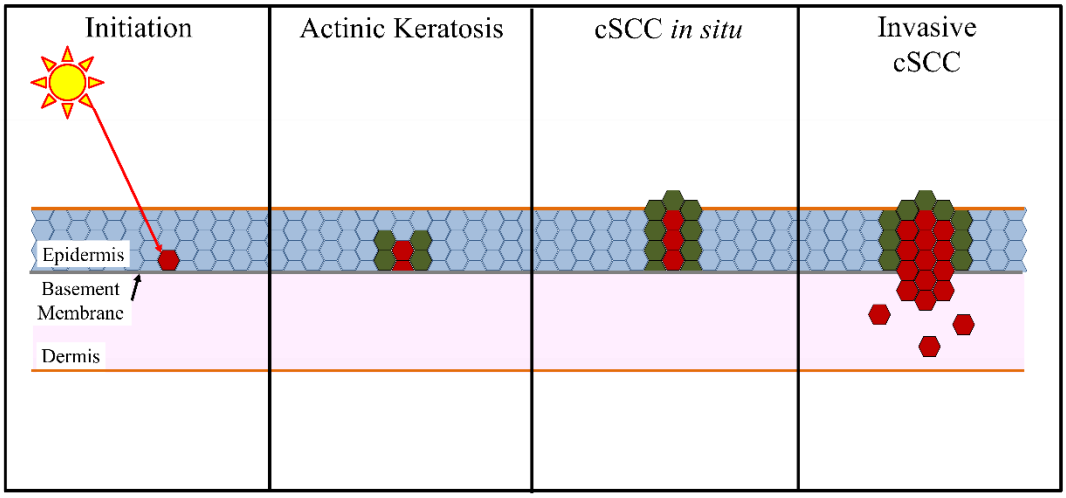

Figure 2: Progression of a cSCC

cSCCs often develop in a stepwise manner, beginning with an initial mutation that is often induced by damage from UV exposure. This mutation confers either a growth or survival advantage, resulting in the development of a patch of keratinocytes containing this mutation. The lesion is diagnosed as an actinic keratosis when it has histological features such as hyperchromatic nuclei, as well as abnormal proliferation or differentiation. However, this atypia does not penetrate the full thickness of the epidermis. Once this atypia does penetrate the entire thickness of the epidermis the lesion is characterized as cSCC *in situ*. Further progression and the acquisition of a migratory phenotype, as well as penetration of the basement membrane, results in a diagnosis of invasive cSCC.

1.2.4 Causes of cSCC

Because the skin is the main mechanism of defense against external insults, it is exposed to a high level of external injury, either physically or through mutagens. Risk factors for cSCC include: therapy with methoxsalen and UVA radiation, exposure to ionizing radiation, infection with human papillomavirus, exposure to chemical carcinogens (ex. arsenic, polycyclic hydrocarbons), immunosuppression, organ transplantation, leukemia and lymphoma, chronically injured or diseased skin, ulcers, osteomyelitis and radiation dermatitis (Alam and Ratner, 2001). Increased risk of cSCC is also associated with certain genetic disorders such as genodermatosis, oculocutaneous albinism, xeroderma pigmentosum, Ferguson-Smith Syndrome, Rothmund-Thomson Syndrome, Fanconi anemia, epidermodysplasia verruciformis, dyskeratosis congenita, Bloom syndrome, Werner syndrome and chronic inflammatory disorders such as dystrophic epidermolysis bullosa (Nikolaou, Stratigos and Tsao, 2012, Alam and Ratner, 2001).

However, the most common cause of cSCC is exposure to ultraviolet radiation, especially UVB and to a lesser extent UVA, two carcinogens considered responsible for 90% of skin cancers (Rogers et al, 2010b, Alam and Ratner, 2001). A patient's photosensitivity or risk of cSCC following UV exposure is clinically assessed using the Fitzpatrick Scale. For example, the highest risk patients have very pale skin with blond or red hair, blue eyes, freckles and they always burn and rarely tan (Ravnbak, 2010). Exposure to the

damaging rays of sunlight results in the formation of pyrimidine dimers, adducts in the DNA that can result in DNA mutation following replication or during repair (Melnikova and Ananthaswamy, 2005). Ozone depletion has played a major role in the increased skin cancer diagnosis rate due to an increased exposure to UV rays. A 2% depletion in ozone concentration was calculated to cause a 6-12% increase in non-melanoma skin cancer (Kripke, 1988, Kelfkens, de Gruijl and van der Leun, 1990). However, during the winter and spring months the ozone layer has been shown to decline 10-40% over the northern hemisphere, causing a predicted 20-60% increase in UV exposure and a 40-120% increase in non-melanoma skin cancer occurrence (Oikarinen and Raitio, 2000). Increased use of tanning beds is also increasing the rate of cSCC diagnosis, particularly in young patients that regularly use tanning beds (International Agency for Research on Cancer Working Group on artificial ultraviolet (UV) light and skin cancer, 2007). Additionally, the risk of cSCC due to immunosuppression is growing. One year following renal transplant the risk of cSCC increases 7%, 45% following 11 years and 70% following 20 years of immunosuppression (Bouwes Bavinck et al, 1996). Pharmacological therapies, for example sorafenib treatment for renal cell carcinoma or BRAF inhibitors, have also been linked to an increased incidence of AKs and cSCCs (Smith et al, 2009, Robert, Arnault and Mateus, 2011).

1.2.5 Pathogenesis of cSCCs

The formation of cSCCs is a multistep process, requiring the mutation of several oncogenes and tumor suppressor genes (Xie and Bikle, 2007). Following chronic exposure to a mutagen (usually UV exposure), the DNA of a keratinocyte undergoes significant damage (Alam and Ratner, 2001). In fact, normal-appearing, sun exposed skin contains thousands of loss-of-function mutations in the most common cSCC tumor suppressor, p53 (Nakazawa et al, 1994, Jonason et al, 1996a, Campbell et al, 1993, Xie and Bikle, 2007). Keratinocytes containing this initial mutation have a growth advantage, as loss of p53 function prevents cell cycle arrest and apoptosis following DNA damage. Through this mechanism patches of mutant keratinocytes form, creating cell populations at increased risk of a secondary mutation following chronic UV exposure (Melnikova and Ananthaswamy, 2005, Jonason et al, 1996b). Abnormal cell growth, in turn, results in epidermal dysplasia and the formation of a precursor AK lesion (Melnikova and Ananthaswamy, 2005). Loss of p53 function is found in over 50% of human cancers (Hollstein et al, 1991). Upon UV exposure p53-/- and p53+/- mice develop AKs and cSCCs more rapidly than wild type mice, reaffirming this tumor suppressor's role in epidermal carcinogenesis (Jiang et al, 1999). Loss of chromosome 9p21 is another common genetic alteration, resulting in loss of p16INK4 and p14ARF, two regulators of p53 (Xie and Bikle, 2007). Mutations in p16 promote increased progression through the cell cycle and an increased risk of genetic mutations due to errors

in mitosis (Xie and Bikle, 2007). Upregulation of the Fas receptor in keratinocytes is another common cause of cSCC, reducing the cell's ability to regulate apoptosis (Melnikova and Ananthaswamy, 2005). Other mutations often seen in cSCC involve c-Myc over-expression and activation of STAT signaling, resulting in tumor angiogenesis and cytokine secretion, respectively (Xie and Bikle, 2007). Mutations in H-Ras or N-Ras are observed in 30-50% of human cSCCs, with H-Ras being the most commonly mutated Ras isoform (Xie and Bikle, 2007, Boukamp, 2005). Increased levels of Src family kinases (SFKs), EGFR and ATF-3 have also been associated with cSCC, as has increased PI3K/Akt activity (Kim et al, 2011, Lentini et al, 2006, Toll et al, 2009, Toll et al, 2010, Sekulic et al, 2010). Additionally, increased Fyn activity has been shown to downregulate p53 activity, increasing the malignant transformation of keratinocytes (Zhao et al, 2009).

1.3 Ras Oncogene

Ras proteins are a member of the RAS-like GTPase family that, in response to external stimuli, alter signaling pathways associated with growth, migration, adhesion, cytoskeletal maintenance, survival and differentiation (Rajalingam et al, 2007). The Ras-like GTPase superfamily has been broken down into five subfamilies of GTPases, including Ras, Rho, Rab, Arf and Gα subunits of heterotrimeric G-proteins. The Ras subfamily, in turn, includes Ras, Rap, Ral and Rheb, among others (Colicelli, 2004).

1.3.1 Ras Structure

A high degree of sequence homology exists between H-, N- and K-Ras, with the majority of variability occurring in the C-terminal hypervariable region. This C-terminal region is the site of posttranslational modifications that allow the protein to anchor at the plasma membrane and aid in intercellular trafficking to the cytoplasmic membrane (Hancock and Parton, 2005). Ras also contains a G domain that regulates binding to GDP/GTP, and mutations in this sequence can turn Ras permanently off or on, depending on whether binding or hydrolysis of GTP is blocked (Vetter and Wittinghofer, 2001).

1.3.2 Regulation of Ras Signaling

Ras is classified as a GTPase, thus the activity of Ras is dependent on whether it is bound to GTP (protein is active or "on") or GDP (protein is inactive or "off"). Although Ras does have a small amount of intrinsic GTPase function, Ras activity is most often regulated by other GTPase activating proteins (GAPs) and guanine nucleotide exchange factors (GEFs). Following posttranslational modification in the endoplasmic reticulum, Ras is trafficked to the cytoplasmic membrane, where it is activated in response to external signals (Rajalingam et al, 2007). For example, following activation of the epidermal growth factor receptor (EGFR), the receptor binds to GRB2 to recruit SOS1 or SOS2, two Ras-GEFs that exchange the Ras-bound GDP for GTP, activating Ras to alter

intracellular signaling pathways (Downward, 2003). Downregulation of Ras signaling requires the activity of Ras-GAPs to hydrolyze GTP to GDP, and alteration in Ras-GAP activity, localization, expression or ability to bind Ras can result in constitutively active Ras (Grewal et al, 2011).

1.3.3 Signaling Downstream of Ras

Increased Ras activity results in the activation of several signaling cascades. Following activation by external growth factors, Ras binds to and activates Raf, ultimately upregulating the MEK/MAPK pathway and altering gene transcription to hasten cell cycle progression and increase cell survival (Rajalingam et al, 2007, Downward, 2003). Ras also activates PI3K to induce the Akt signaling pathway, promoting cell proliferation and survival (Rajalingam et al, 2007). PI3K can directly bind to and activate Rac, a Rho family protein that regulates the stability of the actin cytoskeleton and the migratory capacity of the cell (Downward, 2003).

1.3.4 Ras as an Oncogene

Studies have shown that at least one Ras gene contains an activating mutation in approximately 20% of human cancers (Rajalingam et al, 2007, Downward, 2003). Mutations resulting in oncogenic Ras activity occur primarily at G12, G13 and Q61,

preventing GTP hydrolysis to generate constitutively active Ras (Barbacid, 1987). Additionally, Ras activity is upregulated in tumors without direct Ras mutations due to activating mutations upstream of Ras or loss of GAP expression, increasing Ras signaling. Increased Ras activity results in the dysregulation of signaling pathways governing cell growth, programmed cell death, invasiveness and angiogenesis (Downward, 2003).

1.3.5 Ras in the Epidermis

The three isoforms of Ras are differentially expressed in different tissue systems. H-Ras is primarily expressed in brain, muscle and skin, while K-Ras is expressed in gut, lung and thymus and N-Ras is expressed in the testis and thymus (Rajalingam et al, 2007). Genetic studies of knockout mice indicate that loss of H-Ras and N-Ras do not alter mouse development or tissue homeostasis, while loss of K-Ras is not compatible with life (Umanoff et al, 1995, Esteban et al, 2001, Johnson et al, 1997). However, expression of H-Ras from the K-Ras locus rescues mouse development, suggesting that the distribution of tissue expression is more important than specific differences between Ras isoforms (Drosten, Lechuga and Barbacid, 2013a).

In the epidermis, Ras has been shown to induce cellular proliferation and inhibit differentiation (Dajee et al, 2002, Drosten, Lechuga and Barbacid, 2013b). Interference

with all three Ras isoforms in the basal layer of keratinocytes results in epidermal thinning and hyperkeratosis, indicating a decrease in keratinocyte proliferation (Dajee et al, 2002). Loss of Ras signaling *in vitro* has also been shown to induce downregulation of c-Myc and ΔNp63 (an isoform expressed from the p63 locus), regulators of proliferation, as well as upregulation of p21 and p15, two proteins involved in cell cycle arrest (Drosten, Lechuga and Barbacid, 2013a). Additionally, increased Ras activity in the basal layer of mouse keratinocytes inhibits cellular differentiation and increases proliferation to induce the formation of cSCCs (Vitale-Cross et al, 2004, Khavari and Rinn, 2007). Overall, changes in Ras signaling alter the proliferation and differentiation programs of keratinocytes, two changes that increase the likelihood of cSCC formation (Drosten, Lechuga and Barbacid, 2013b). Thus it is clear that Ras is an important oncogene in the formation of cSCC.

1.3.6 Ras and cSCC

22% of cSCCs contain mutations in at least one Ras gene, most commonly in the H-Ras isoform. Chemical carcinogenesis using DMBA/TPA is a common method of cSCC induction in the lab. DMBA is applied to the skin, causing a mutation in Ras, and then TPA is applied to promote the formation of the tumor (Brown, Buchmann and Balmain, 1990). Expression of constitutively active H-Ras or K-Ras in a murine epidermis resulted in the formation of papillomas that progress to cSCCs, suggesting that abnormal

Ras activity is sufficient to cause skin carcinogenesis. However, expression of constitutively active H-Ras at endogenous levels was not sufficient to induce papilloma formation, indicating that a threshold of Ras expression must be surpassed to induce skin tumors (Drosten, Lechuga and Barbacid, 2013b). Additionally, tumor promotion in the epidermis of H-Ras knockout mice resulted in fewer papillomas than in wild type mice (Ise et al, 2000). Thus, alterations in Ras activity levels play an important role in keratinocyte transformation and skin carcinogenesis.

Adhesion complexes between cells serve as major hubs of signaling in the epidermis and changes in signaling at these locations can alter Ras activity. Components of both the adherens junction and desmosome inhibit signaling from EGFR to induce growth arrest, and downregulation of these complexes following oncogenic transformation results in sustained activation of Ras signaling pathways. During the epithelial to mesenchymal transition (EMT) the stability of these junctions is downregulated, resulting in upregulation of Ras signaling and cellular transformation (Kern, Niault and Baccarini, 2011).

1.4 Src Family Kinases (SFKs)

In 1911 Peyton Rous discovered that injecting tissue homogenate from a spindle cell sarcoma he isolated from a chicken's breast into the breast of a healthy chicken resulted

in tumor formation in the second animal. This occurred whether the injection contained whole cells, desiccated or glycerinated preparations of dead tumor cells or cell free filtrates (Saito et al, 2010, Guarino, 2010). Although Rous believed he had discovered evidence that all tumors were a result of viral infection, he had actually discovered a mutant form of the first known tyrosine kinase, Src (Guarino, 2010). For these discoveries Peyton Rous was awarded the Nobel Prize in 1966, and in 1989 J. Michael Bishop and Harold Varmus won the Nobel Prize for identifying the ability of an active form of c-Src to drive a cancerous phenotype, beginning the field of oncogenesis (Saito et al, 2010).

Clearly, Src has played an important role in our growing understanding of tumorigenesis and cancer biology. Since the identification of Src, other closely related proteins have been identified and added to the Src family. These kinases include Fyn, Lyn, Yes, Blk, Lck, Hck, Fgr and Yrk (Varkaris et al, 2014). Src, Yes and Fyn are highly expressed in platelets, neurons, osteoclasts and epithelial tissues and are ubiquitously expressed in other tissues, while the other SFKs are expressed mainly in hematopoietic cells (Thomas and Brugge, 1997, Guarino, 2010).

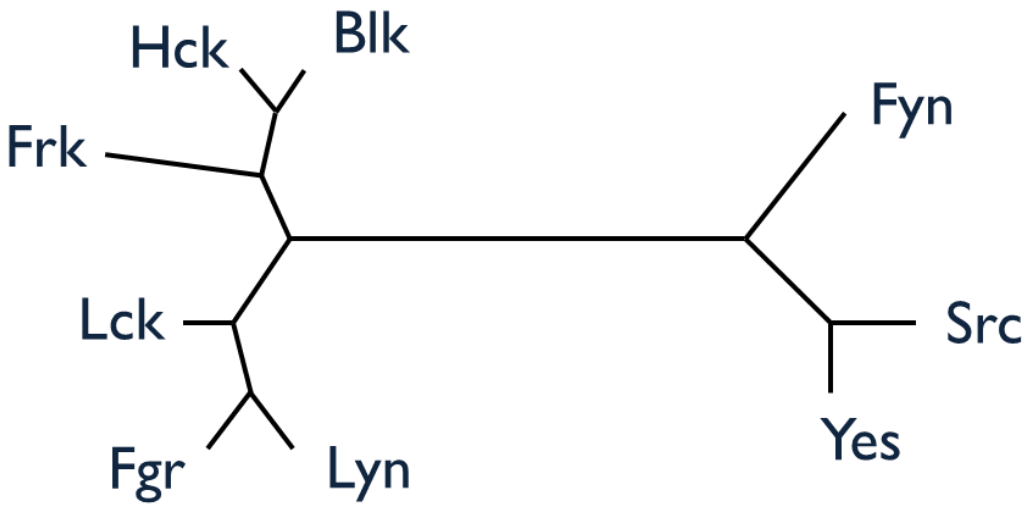

Figure 3: Dendogram of Src Family Kinase Members

This figure demonstrates the relationship between different members of the Src family of protein tyrosine kinases.

1.4.1 Structure of SFKs

The protein structure of all SFKs is highly redundant, resulting in a great deal of functional overlap between family members. From the N- to C- terminal SFKs are composed of an SH4 domain that is myristoylated (and sometimes palmitoylated) to aid in association with the cell membrane, a unique domain specific to each SFK member that directs protein-protein binding, an SH3 domain that binds to proteins with PXXP-like sequences (left-handed polyproline type II sequence motifs), an SH2 domain that binds proteins with phosphotyrosine resides in a pYEE1 sequence, an SH2-kinase linker domain, an SH1 catalytic or kinase domain and a C-terminal regulatory element (Saito et al, 2010). The SH1 domain is composed of two lobes, a small N-terminal lobe that binds ATP and the protein substrate to allow phosphotransfer and a larger C-terminal lobe that controls accessibility to substrates (Saito et al, 2010, Guarino, 2010, Schenone et al, 2011).

1.4.2 Regulation of SFK Signaling

SFK activity is regulated by tyrosine phosphorylation of two tyrosines, commonly referred to by their location within the Src protein. These two sites are Y416 (activating) and Y528 (inhibitory). Phosphorylation of Y528 within the C-terminal regulatory element creates a binding site for the SH2 domain, inhibiting substrate binding. This also

allows the SH2-linker domain to bind to the backside of the SH1 catalytic domain, creating a polyproline type II helix conformation that can bind to the SH3 domain (Brignatz et al, 2009). Ultimately, these conformational changes result in autoinhibition of SFK activity by preventing substrate binding, inhibiting kinase activity and masking the activating Y416 site. However, other proteins containing phosphotyrosine or polyproline helices can compete for the SH2 or SH3 domain, unfolding SFKs from their inhibitory conformation. Once this conformational change has occurred, SFKs can autophosphorylate Y416, resulting in displacement the SH2-kinase linker domain from the SH1 catalytic domain and full kinase activity (Brignatz et al, 2009, Saito et al, 2010, Bjorge, Jakymiw and Fujita, 2000, Li et al, 2005).

Although SFK activity can be regulated by autophosphorylation of Y416 and Y528, association with specific proteins can contribute to SFK activity through their kinase or phosphatase activities (Li et al, 2005, Rengifo-Cam et al, 2004). For example, Srcasm contains optimal ligands for both the SH2 and SH3 domains of SFKs, inducing their activity. However, Srcasm's role in SFK activity is more complex, as results show that Srcasm in fact acts like a rheostat to regulate SFK activity, activating or repressing the SFK based on the ratio of SFK and Srcasm levels in the cell (Li et al, 2005, Li et al, 2007). Csk is an inhibitory protein that is often found in near SFKs and can phosphorylate Y528 to induce autoinhibition (Shima, Nada and Okada, 2003, Bjorge, Jakymiw and Fujita, 2000). SFKs can also be activated by protein tyrosine phosphatases

such as PTPalpha, PTPgamma, SHP-1, SHP-2 and PTP1B that remove the inhibitory Y527 phosphorylation mark (Frame, 2002).

1.4.3 Signaling Downstream of SFKs

SFK signaling has been implicated in a large array of pathways, including those that govern cell metabolism, viability, proliferation, angiogenesis, differentiation and migration (Ingley, 2008, Okada, 2012). Src recruits members of the Gab/IRS family to activate PI3K and ultimately Akt, altering the cell's metabolism, gene transcription, migration and survival (Frame, 2002, Sirvent, Benistant and Roche, 2012). Increased Src activity activates the PI3K and Ras/MEK pathways to suppress p27 and increase CyclinD, CyclinE and CyclinA to speed progression through the cell cycle (Frame, 2002). SFKs directly phosphorylate and activate the transcription factor STAT3 to increase cell growth (Sirvent, Benistant and Roche, 2012). SFKs also increase the expression of pro-angiogenic factors such as VEGF, matrix metalloproteases and interleukin-8. Src reduces the stability of focal adhesions by phosphorylating integrin subunits, inhibiting RhoA and activating FAK, Ras and phosphatidylinositol phosphate kinase (Kim, Song and Haura, 2009, Zhang and Yu, 2012). Furthermore, Src activity is associated with downregulation of E-cadherin synthesis and stability at the cytoplasmic membrane through phosphorylation of p130catenin and FAK (Kim, Song and Haura, 2009). Overall, these signaling changes result in decreased cell adhesion, increased

migration, decreased apoptosis, increased proliferation and increased angiogenesis, all of which promote cellular transformation and tumorigenesis (Frame, 2002, Guarino, 2010).

1.4.4 SFKs in the Epidermis

Two major, yet contradictory, roles have been ascribed to SFKs in the epidermis (Avizienyte and Frame, 2005). During keratinocyte differentiation and stratification, elevated extracellular Ca^{+2} induces the formation of adherens junctions, initiating signaling cascades necessary for cell polarization and desmosome formation. Tyrosine phosphorylation by SFKs is necessary for this initial assembly of the adherens junction structure (Calautti et al, 1998). Therefore, one of the most important functions of the SFKs in the epidermis is the assembly of adhesion structures to aid in keratinocyte differentiation. Contradictory to this, SFKs have also been implicated in the dissolution of epidermal junctions, as the stability of adherens junctions *in vitro* increases upon inhibition of SFK activity (Owens et al, 2000). Supporting Src's pro-migratory role, staining for active SFKs revealed increased activity in skin samples from patients suffering from psoriasis, AKs, cSCC *in situ* and cSCCs when compared to adjacent skin, most likely due to aberrant activation of EGFR (Ayli et al, 2008).

1.4.5 Prevalence of SFK Activity in cSCC

Somatic mutations in SFKs have only been recorded in a study of human colorectal cancer (Irby et al, 1999). Despite the rarity of SFK mutations in human cancers, most solid tumors have increased SFK activity, and this upregulation often correlates with advanced disease progression (Varkaris et al, 2014, Yeatman, 2004, Frame, 2004, Mandal et al, 2008). More specifically, Src over-expression or activation has been identified in head and neck, breast, colon, bladder, stomach, ovary, lung, prostate, glioma, melanoma and pancreatic tumors, among others (Matsumoto et al, 2004, Guarino, 2010). Increased SFK activity has also been detected in human cSCC tumors when compared to adjacent skin samples (Lee et al, 2010). SFK activity is frequently upregulated following alterations in one of its upstream activators such as PDGFR, EGFR or FGFR, reversing the inhibitory conformation of the SFKs to induce their activity (Okada, 2012, Bromann, Korkaya and Courtneidge, 2004). The introduction of constitutively active Src to the basal keratinocytes of the murine epidermis resulted in severe epidermal hyperplasia and death within three weeks of birth. Over-expression of wild type Src resulted in epidermal hyperplasia, spontaneous cSCCs and increased susceptibility to chemical carcinogenesis with increased risk of metastasis (Matsumoto et al, 2004). Inhibition of SFK activity using AZD0530 during chemical carcinogenesis significantly reduced keratinocyte hyperproliferation and papilloma formation (Serrels et al, 2009). Additionally, increased SFK activity through conditional knockout of the SFK

inhibitor Csk resulted in chronic inflammation and epithelial hyperplasia with disorganized keratinocyte stratification (Yagi et al, 2007). Src function has also been identified as a driver of EMT in epithelial cells, a conversion associated with loss of cell-cell adhesion (Avizienyte and Frame, 2005, Mandal et al, 2008). Increased SFK activity in keratinocytes resulted in activation of Rac1, upregulation of Snail and Twist, as well as inhibition of RhoA, all drivers of EMT (Yagi et al, 2007). Thus there is significant evidence suggesting that increased SFK activity plays an important role in keratinocyte malignancies.

1.5 Fyn

In 1986 Fyn was cloned based on its homology to the Src family kinase (SFK) member Yes (Semba et al, 1986, Davidson, Viallet and Veillette, 1994). Fyn is a 59 kDa protein composed of 537 amino acids and the 200 kb gene coding for its expression is found on chromosome 6q21 (Saito et al, 2010). Like its Src family members, Fyn tyrosine phosphorylates residues on target proteins in response to extracellular signals to alter gene regulation or induce changes in cell adhesion (Guarino, 2010).

1.5.1 Regulation of Fyn Expression

Three isoforms of Fyn have been identified that differ in the SH2-linker region through alternative splicing of exon 7 (Brignatz et al, 2009, Goldsmith, Hall and Atkinson, 2002). Fyn(B) is predominantly expressed in the central nervous system and includes exon 7a, a region that is believed to have been derived through a recombinatorial event with another gene. Fyn(T) is predominantly expressed in T-cells and contains exon 7b, a sequence that creates a smaller contact surface with the SH3 domain and therefore is less efficient at autoinhibition and more efficient at phosphorylating downstream targets and inducing cellular transformation. FynΔ7, the third isoform, lacks exon 7 and is not translated to protein. Despite the high levels of expression of Fyn(B) and Fyn(T) in neurons and T-cells, respectively, both isoforms are ubiquitously expressed in other tissues (Brignatz et al, 2009, Goldsmith, Hall and Atkinson, 2002).

Although Fyn is overexpressed in many cancers, detailed study of *FYN* regulation has only been undertaken in chronic myelogenous leukemia, where the oncogene Bcr-ABL drives reactive oxygen species production, activating the transcription factors Egr1 and Sp1 to upregulate *FYN* gene transcription (Saito et al, 2010, Zhao et al, 2009, Ban et al, 2008, Lu et al, 2009, Posadas et al, 2009, Talantov et al, 2005, Gao et al, 2009). Vipin Yadav from the Denning lab also found that in cSCC the introduction of constitutively

active H-Ras results in Fyn upregulation through a PI3K-Akt dependent mechanism (Yadav and Denning, 2011).

1.5.2 Fyn in Keratinocyte Differentiation

Fyn activity has been implicated in both KC differentiation and oncogenesis. Differentiation signals, such as activation of the Ca^{+2} receptor by extracellular Ca^{+2}, induce Fyn activity and recruitment to the plasma membrane (Calautti et al, 1995, Tu et al, 2008). Once localized to the membrane, Fyn phosphorylates tyrosines on members of the adherens junction to stabilize its formation (Tu et al, 2008, Calautti et al, 1998, Calautti et al, 2002, Tu, Chang and Bikle, 2011). Following adhesion initiation, Fyn activates signaling cascades involving phospholipase C/PI3K/Akt and PKCη that ultimately induce KC differentiation (Tu et al, 2008, Cabodi et al, 2000). Loss of Fyn expression *in vivo* alters the differentiation program, as primary KCs from Fyn -/- mice do not stratify in culture and express lower levels of the differentiation markers transglutaminase, keratin 1 and filaggrin (Ilic et al, 1997, Calautti et al, 1995). The skin of Fyn -/- mice also expresses reduced levels of these markers and has impaired cell-cell junctions, particularly adherens junctions (Calautti et al, 1995, Calautti et al, 1998). KCs from mice that overexpress Fyn have increased transglutaminase activity following Ca^{+2} exposure, suggesting increased KC differentiation (Zhao et al, 2009, Cabodi et al, 2000, Li et al, 2007). Taken together, these findings indicate that Fyn activity is involved in

KC differentiation, as this process is impaired upon loss of Fyn and increased with Fyn over-expression.

1.5.3 Fyn in cSCC and Keratinocyte Oncogenesis (EMT)

While Fyn is a participant in the KC differentiation program, Fyn activity has also been implicated in KC transformation and oncogenesis (Zhao et al, 2009, Calautti et al, 1995, Tu et al, 2008). A survey of human cSCCs showed increased SFK expression through all layers of the tumors (Ayli et al, 2008). Over-expression of constitutively active Fyn(Y528F) in murine epidermis using the Keratin 14 promoter resulted in the formation of keratotic tumors and actinic keratoses that progress to squamous cell carcinoma, most likely through Fyn-mediated downregulation of the tumor suppressors Notch1 and p53 (Zhao et al, 2009). Additionally, introduction of oncogenic H-Ras in the KC cell line HaCaT resulted in upregulation of Fyn expression via a PI3K/Akt signaling mechanism, increasing the migratory and invasive capacity of the cells (Yadav and Denning, 2011). Increased Fyn activity has also been associated with the epithelial to mesenchymal transition and migratory capacity of oral squamous cell carcinoma cell lines (Lewin et al, 2010).

1.5.4 Fyn in Keratinocyte Adhesion

Fyn's function in both KC differentiation and transformation is strongly associated with its role in cellular adhesion. To mediate KC differentiation, Fyn activity aids in the initiation and formation of cell-cell adhesions, while in oncogenesis Fyn aids in the dissolution of adhesions. These opposing roles for Fyn in KC biology may at first appear contradictory, but a careful analysis of the literature suggests several possible mechanisms to integrate these divergent functions.

1.5.4.1 Fyn's Role at the Adherens Junction

Once KCs leave the stratum basale, they maintain the integrity of the epidermis primarily through two cell-cell adhesion complexes, the adherens junction and the desmosome. Formation of an immature or transient adherens junction is initiated when E-cadherin proteins from adjacent cells bind homophilically through their extracellular domain. Following E-cadherin-mediated adhesion, p120catenin associates with the cadherin at its juxtamembrane domain (Grosheva et al, 2001, Mariner, Davis and Reynolds, 2004, Alema and Salvatore, 2007). Fyn associates with the adherens junction by binding to p120catenin, where it phosphorylates several downstream targets, including β- and α-catenin, to induce their association with the cadherin and increase the stability of the complex (Figure 4)(Tu et al, 2008, Calautti et al, 1998, Tu, Chang and Bikle, 2011,

Calautti et al, 2002, Grosheva et al, 2001, Piedra et al, 2003, Lilien and Balsamo, 2005, Lampugnani et al, 1997, Hu, O'Keefe and Rubenstein, 2001). However, the adherens junction can mediate cell adhesion without the cytoplasmic tail of E-cadherin or its associated proteins, implying that Fyn activity is not necessary for adherens junction formation but may increase the efficiency of this process (Lampugnani et al, 1997).

Counter to these findings, SFK activity is also required for the dissolution of adherens junctions. KCs are constantly forming transient adhesions upon intercellular contact that must remain dynamic enough to allow movement of the KC through the layers of the epidermis (Lewis, Jensen and Wheelock, 1994, Tao et al, 1996). However, if SFK activity is inhibited, KCs cannot free themselves from these dynamic adhesions, reducing cell motility (Owens et al, 2000). Fyn phosphorylates β-catenin on tyrosine 142, disrupting the association between β-catenin and α-catenin and breaking apart the complex that connects the adherens junction to the actin cytoskeleton (Figure 4). Other SFKs, especially Src and Yes, phosphorylate β-catenin more efficiently on Y654, triggering dissociation of β-catenin from E-cadherin (Roura et al, 1999). Although Fyn exhibits greater preference for phosphorylation of β-catenin at Y142, it can also simultaneously phosphorylate β-catenin at Y654, resulting in complete dissociation of β-catenin from the adherens junction and potential translocation of β-catenin to the nucleus where it can upregulate expression of TCF/LEF target genes (Piedra et al, 2003, Castano et al, 2007). Overall, these findings indicate that within the epidermis, where KCs must

be able to adhere to each other but maintain these contacts in a fluid state, Fyn plays a dual role mediating adherens junction formation and dissolution.

The biochemical consequences of Fyn-mediated p120catenin phosphorylation have not been completely resolved. When Fyn phosphorylates p120catenin on Y112, the association of RhoA is blocked, resulting in increased RhoA activity, increased stress fiber formation and decreased conversion of the adherens junction from a strong to a weak state (Castano et al, 2007, Grosheva et al, 2001). However, Fyn has also been shown to phosphorylate p120catenin and induce its dissociation from the adherens junction, resulting in activation of Cdc42 and Rac and inhibition of Rho activity (Figure 4)(Grosheva et al, 2001, Anastasiadis et al, 2000). Therefore Fyn has been shown to both increase and decrease Rho activity. However, because Fyn activity primarily promotes the induction of a migratory phenotype, it appears more likely that Fyn is inhibiting Rho activity to reduce adhesion stability (Rengifo-Cam et al, 2004). Finally, Fyn has been shown to phosphorylate E-cadherin to induce the association of Hakai, an E3 ligase that ubiquitinates E-cadherin and β-catenin to direct endocytosis of the adherens junction (Figure 4)(Fujita et al, 2002, Chen et al, 2009a). Increased Src activity has also been shown to inhibit E-cadherin recycling back to the cell membrane, instead directing E-cadherin to degradation in the lysosome (Wadhawan et al, 2011, Serrels et al, 2011). Although Fyn's role in E-cadherin stability has not been completely determined, based on significant overlap in the function of SFK family members it is probable that Fyn also

reduces E-cadherin stability at the cell membrane (Alt-Holland et al, 2008). Overall, Fyn-mediated phosphorylation of adherens junction proteins induces rearrangement of the actin cytoskeleton away from the adherens junction and toward focal contacts to initiate a more migratory phenotype (Rengifo-Cam et al, 2004).

The experimental dermatologist is thus presented with two bodies of literature that characterize Fyn's role in both the formation and dissolution of adherens junctions. We propose that Fyn may initially increase the efficiency of adherens junction formation, recruiting key proteins to the cadherin to initiate binding with the actin cytoskeleton. After adherens junction assembly and with delayed kinetics, Fyn activity then results in the dissolution of the adherens junction through phosphorylation of β-catenin and p120catenin. This apparently futile cycle may be responsible for the dynamic nature of the epidermal adherens junction.

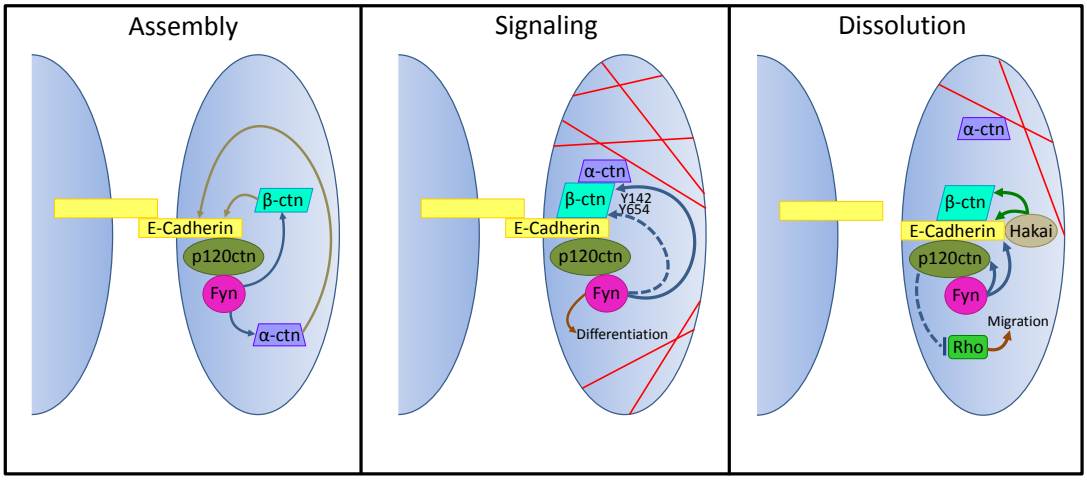

Figure 4: Fyn at the Adherens Junction

Assembly: During adherens junction assembly p120catenin associates with E-cadherin, stabilizing the junction and creating a docking site for Fyn. Fyn then tyrosine phosphorylates α-catenin and β-catenin to induce their association with the complex.
Signaling: Once the adherens junction has assembled, Fyn activates signaling pathways resulting in KC differentiation and tyrosine phosphorylates β-catenin at Y142 and Y654* to disrupt the contact between the junction and the actin cytoskeleton.
Dissolution: Fyn phosphorylates E-cadherin to induce Hakai association. Hakai binds to and ubiquitinates (green arrows) E-cadherin and β-catenin to promote their internalization and degradation. Fyn also phosphorylates p120catenin to inhibit Rho activity*, increasing the migratory capacity of the cells.
* Dotted lines denote putative phosphorylation events.

1.5.4.2 Fyn's Role at the Focal Adhesion

Fyn activity shifts adhesion away from adherens junctions toward more migratory focal adhesions, where it plays an important role in maintaining the dynamic state of this complex (Rengifo-Cam et al, 2004). Once integrins contact extracellular matrix proteins such as fibronectin they cluster, resulting in transient dimerization of the integrin-associated protein FAK and auto- or transphosphorylation of FAK at Y397 (Figure 5)(Schaller, Hildebrand and Parsons, 1999, Zeng et al, 2003). Fyn activity has been implicated in this process; however FAK recruitment and phosphorylation at Y397 can occur in the absence of SFKs (Cary, Chang and Guan, 1996). Similar to adherens junctions, Fyn activity may increase the efficiency of focal contact formation by aiding in FAK phosphorylation (Cary et al, 2002, Playford and Schaller, 2004). Interaction between Fyn and FAK results in loss of Fyn's inhibitory Y528 phosphorylation and autophosphorylation of the activating Y416 site. Fyn then phosphorylates Y576/577 on FAK to maximize FAK's enzymatic activity. Fyn also phosphorylates FAK at Y925 to recruit Grb2, Y861 to recruit Paxillin or Talin, and Y407 (Figure 5)(Schaller, Hildebrand and Parsons, 1999, Yeo et al, 2011). Although all of the SFKs are capable of phosphorylating FAK at these sites, Fyn induces focal contact formation more efficiently than Src or Yes due to its double palmitoylation (cysteine 3 and 6), which increases targeting to the plasma membrane and therefore the likelihood of association with FAK (Kostic and Sheetz, 2006).

At the focal adhesion Fyn recruits and phosphorylates several proteins that play a role in promoting cellular migration. Fyn binds to and phosphorylates paxillin and p130Cas, both of which act to recruit Crk1, ultimately acting through the guanine exchange factor DOCK180 to activate Rac1 and inhibit RhoA, promoting cellular migration and facilitating adhesion turnover (Zeng et al, 2003, Sharma and Mayer, 2008, Peng and Guan, 2011). Fyn also phosphorylates Shc to activate the Grb/mSOS/Ras/Raf/MEK/MAPK/ERK/MLCK pathway, promoting myosin and actin engagement to generate the force required for cell movement (Sharma and Mayer, 2008, Peng and Guan, 2011). Ultimately, these signaling pathways result in the recruitment of dynamin to Grb2 and FAK at Y397. Dynamin binds to microtubules and mediates the endocytosis of the integrin/FAK complex, disassembling the focal adhesion (Figure 5)(Webb et al, 2004). Thus, by aiding in focal adhesion formation Fyn paradoxically initiates signaling pathways that will ultimately result in junctional turnover.

From the signaling mechanisms detailed above, it is clear that Fyn is necessary for the dynamic cycle of formation and dissolution at the focal contact. This process is perturbed in the absence of Fyn as Fyn-/- FAK+/- KCs attach to the extracellular matrix but form atypically dense bundles of actin stress fibers, suggesting abnormally robust focal contact maturation (Schober et al, 2007). When SFK phosphorylation sites on FAK are mutated, the cells can form protrusions but cannot disassemble focal contacts to allow the cell body to move forward (Brunton et al, 2005). Further studies show that increased

SFK activity maintains focal complexes in an immature, dynamic state and induces their turnover (Guarino, 2010, Mitra and Schlaepfer, 2006). Lamellipodia and filopodia, two migratory structures, are associated with smaller, more immature focal adhesions. FAK/SFK mediated inhibition of RhoA activity maintains these structures in their immature state and activates a signaling cascade that ultimately leads to focal adhesion endocytosis and dissolution (Playford and Schaller, 2004, Sharma and Mayer, 2008, Peng and Guan, 2011). Because focal adhesions aid in migration, they must constantly be assembled at the leading edge of the cell and disassembled at the trailing edge. Upregulated Fyn activity induces KC migration by increasing the efficiency both of focal adhesion formation and dissolution. As of this publication, Fyn subcellular localization and activity have not been studied in migrating cells, but such spatially and temporally resolved information may uncover a role for Fyn in the formation of focal adhesions at the leading edge of the cell and in focal adhesion dissolution at the trailing edge.

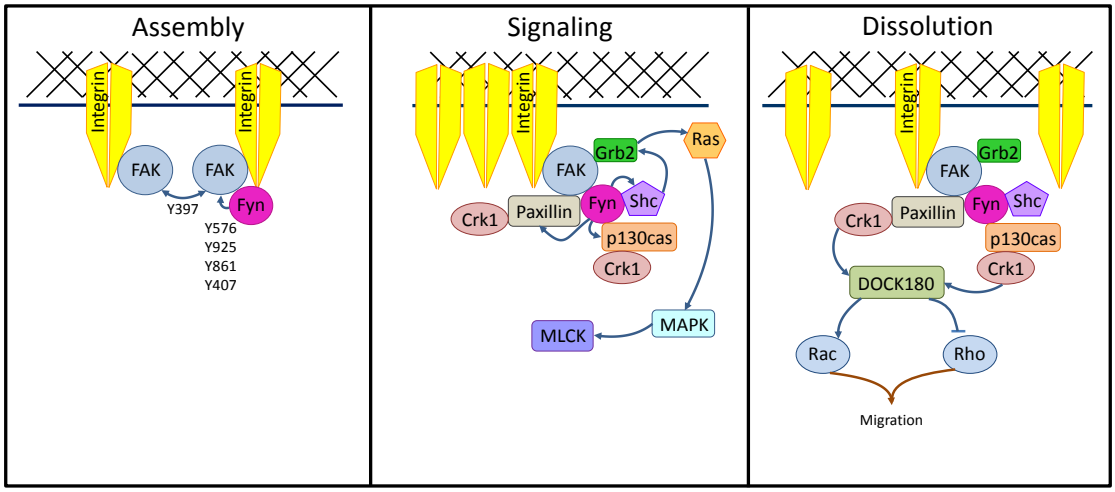

Figure 5: Fyn at the Focal Adhesion

Assembly: Following integrin binding to extracellular matrix proteins, FAK molecules are brought in close proximity where they can auto- or trans-phosphorylate Y397. Phosphorylation of FAK Y397 induces loss of Fyn auto-inhibition and Fyn-mediated phosphorylation of FAK at Y576, Y925, Y861 and Y407, maximizing FAK activity.
Signaling: Fyn-mediated FAK phosphorylation results in the recruitment of Grb2 and Paxillin. Fyn then tyrosine phosphorylates p130cas and Paxillin to induce the association of Crk1. Fyn also phosphorylates Shc to induce Grb2-mediated activation of the Ras/MAPK/MLCK pathway.
Dissolution: Crk1 recruits DOCK180 to increase Rac activity and inhibit Rho activity. Together these signaling mechanisms result in focal adhesion turnover and increased cell migration.

1.5.4.3 Fyn's Role at the Desmosome and Hemidesmosome

Less is known about the role of Fyn at the desmosome and hemidesmosome. However, it appears that Fyn plays a similar dichotomous role at these sites as it does in adherens junctions and focal adhesions by increasing the efficiency of adhesion initiation, then ultimately aiding in hemidesmosomal and desmosomal dissolution (Mariotti et al, 2001, Spinardi et al, 2004, Gagnoux-Palacios et al, 2003). Blocking SFK activity inhibits hemidesmosome formation, while inhibition of Fyn also increases the stability of the hemidesmosome once they are formed (Spinardi et al, 2004). Fyn activation has been shown to trigger desmosome dissolution through the Shc/Grb2/mSOS/Ras/RAF/MEK/ERK pathway and Shc/Grb1/mSOS/Ras/PI3K/Rac/JNK pathway (Mariotti et al, 2001, Gagnoux-Palacios et al, 2003)

1.6 The Epithelial-to-Mesenchymal Transition (EMT)

Epithelial tissues are made up of polarized, tightly adherent cells that form continuous sheets to protect underlying structures, regulate the exchange of chemicals and other substances, secrete hormones and body products and provide sensation. For various biological reasons, these epithelial cells can undergo a transition to a mesenchymal cell phenotype, increasing their migratory capacity, invasiveness, resistance to apoptosis and secretion of extracellular matrix proteins (Kalluri and Weinberg, 2009a). This change in

cell phenotype is called the epithelial-to-mesenchymal transition, or EMT, and it occurs in three different biological settings. The first, termed Type I EMT, occurs during embryo formation and organ development (Zeisberg and Neilson, 2009). Type II EMT is associated with wound healing, tissue regeneration and organ fibrosis (Kalluri and Weinberg, 2009a). The most pertinent to this project, Type III EMT occurs in transformed, neoplastic cells, increasing their malignant potential and allowing these cells to detach from the basement membrane and invade the circulatory system to form distant metastases (Thiery, 2002). This process is more of a spectrum than an on/off switch, with cells undergoing different degrees of transition towards the mesenchymal phenotype. Ultimately, changes in cell signaling and gene expression result in downregulation of cell-cell and cell-matrix junctions, a switch from apical-basal polarity to front-rear polarity and a reorganization of the cytoskeleton to change the cell shape and allow the formation of cell protrusions (Lamouille, Xu and Derynck, 2014).

1.6.1 EMT in cSCC

All three types of EMT are seen in the skin. During embryogenesis, Type I EMT is necessary for the formation of the epidermis and dermis. Type II EMT is necessary during wound healing, when keratinocytes reduce their adhesions and migrate into the wound margin to aid in closure (Nakamura and Tokura, 2011). Type III EMT is also seen in cSCC, although it is considered to be a rare event as only 5% of cSCCs

metastasize (Toll et al, 2013). Those cSCCs that do undergo EMT are most often part of a particularly malignant subgroup defined as spindle cell carcinomas. Spindle cell carcinomas are histologically defined by the presence of elongated keratinocytes that invade the dermis as individual cells (Nakamura and Tokura, 2011, Klein-Szanto, 1989, Shimokawa et al, 2013). Despite the low occurrence of EMT in cSCC, loss of E-cadherin, an important marker of EMT, is associated with advanced cSCC progression, metastasis and poor clinical prognosis (Alt-Holland et al, 2008).

1.6.2 Signaling in EMT

Paradoxically, many commonly accepted oncogenes such as Ras induce senescence following their upregulation or activation in normal cells. Activation of the EMT process, however, increases cellular resistance to senescence, ultimately promoting the survival of the tumor and increasing the ability of the transformed cell to travel to other sites (Smit and Peeper, 2008, Ansieau et al, 2008, Weinberg, 2008). Extracellular growth factors such as HGF, EGF, PDGF and TGF-β, as well as WNT and Notch signaling, activate transcription factors such as Snail, Slug, ZEB1, Twist, Goosecoid and FOXC2 to drive the changes in gene expression that result in EMT (Kalluri and Weinberg, 2009b, Yilmaz and Christofori, 2009). Ultimately these alterations activate signaling pathways involving ERK, MAPK, PI3K, Akt, Smads, Rho, β-catenin, LEF, Ras, c-FOS, β4 integrins, α5β1 integrin and αVβ6 integrin (Tse and Kalluri, 2007). Reduction of

adherens junction and focal adhesion stability result in an increased migratory capacity, facilitating the transition to a mesenchymal phenotype (Kalluri and Weinberg, 2009b). EMT also induces the expression of NCAM, which interacts with Fyn to increase focal adhesion assembly and cell migration (Lehembre et al, 2008).

1.6.3 Transcription Factors Mediating EMT

EMT requires activation of genes that characterize a mesenchymal phenotype and repression of genes that characterize an epithelial phenotype. This global change in gene expression is regulated primarily through three families of transcription factors: Snail, Twist and Zeb. The Snail family of transcription factors includes Snail (SNAI1) and Slug (SNAI2). Snail acts to bind the E-box sequence of the *CDH1* promoter region, where it recruits the Polycomb repressive complex 2 to acetylate histone H3K9 and methylate histones H3K9, H3K27 and H3K4. Methylation of H3K9 and H3K27 repress *CDH1* (E-cadherin) transcription, while methylation of H3K4 and acetylation of H3K9 activate *CDH1* transcription. Through this combination of repressive and activating modifications Snail creates a state of repression, while still allowing rapid activation of transcription and reversal of EMT. The Snail family of transcription factors is activated by the TGF-β-SMAD2, WNT-β-catenin, Notch, PI3K-Akt, NF-κB, EGF and FGF signaling pathways. Together, Snail and Slug downregulate the expression of E-cadherin, Claudins, Occludin, Crumbs3, Pals1, Cytokeratins, Desmoplakin and

Plakophilin while upregulating expression of Fibronectin, N-cadherin, Collagen, MMP15, MMP2, MMP9, Twist, Id1, Id2, Zeb1 and Zeb2 (Lamouille, Xu and Derynck, 2014). Activation of the ZEB family of transcription factors by Snail, TGFβ-SMAD3, WNT-β-catenin or Ras-MAPK or through repression of the microRNA-200 family results in downregulation of E-cadherin, Zo1, Crumbs3 and Plakophilin expression and upregulation of N-cadherin and matrix metalloproteases (Lamouille, Xu and Derynck, 2014, Enkhbaatar et al, 2013). Twist acts through Snail-independent mechanisms to recruit SET8 to target promoters and methylate histone H4K20, repressing E-cadherin and upregulating N-cadherin expression (Lamouille, Xu and Derynck, 2014). Twist family members are activated by β-catenin and the MAPK signaling pathway to downregulate E-cadherin, Claudins, Occludins, Desmoplakin and Plakoglobin expression and upregulate Fibronectin, N-cadherin and α5 integrin (Lamouille, Xu and Derynck, 2014, Scanlon et al, 2013).

SFKs also regulate expression of Slug, Snail and Twist. Although little is known about the interaction of Fyn and these transcription factors, increased SFK activity directly targets Slug and Twist to induce EMT. In both breast and lung cancer cell lines, inhibition of SFK activity reversed characteristics of the EMT phenotype and downregulated expression of Slug, suggesting Src activity was driving Slug expression levels (Liu and Feng, 2010, Joannes et al, 2014). SFK activity has also been shown to

increase the transcription and activity of Twist in leukemia and breast cancer cells (Bourguignon et al, 2010, Kim et al, 2013, Cheng et al, 2008).

1.6.4 Changes in Adhesion and Cytoskeletal Structure

One of the hallmarks of EMT is the downregulation of stable cell-cell junctions, including tight junctions, desmosomes and adherens junctions. Adherens junction stability is decreased both by reducing levels of E-cadherin at the cell membrane and inhibiting E-cadherin gene transcription. The stability of E-cadherin at the cell membrane is decreased through cleavage of its cytoplasmic domain, increasing levels of free cytoplasmic β-catenin and p120catenin to alter the cell's transcriptional program (Lamouille, Xu and Derynck, 2014). Levels of E-cadherin at the cell membrane are also decreased through endocytosis and Src-mediated ubiquitination and degradation (Yilmaz and Christofori, 2009, Fujita et al, 2002). Downregulation of E-cadherin expression is countered by increased expression of the mesenchymal neural cadherin N-cadherin, often called the cadherin switch, resulting in increased affinity for mesenchymal cells and decreased strength of cell-cell adhesions (Yilmaz and Christofori, 2009, Lamouille, Xu and Derynck, 2014).

Establishing a front-rear polarity allows differential regulation of the actin cytoskeleton at the front and back of the cell. Following the initial activation of the EMT program,

RhoA and its downstream effectors ROCK and DIA1 are activated to increase the formation of actin stress fibers (Lamouille, Xu and Derynck, 2014). RhoA continues to be active at the rear of the cell, where it promotes the disassembly of cell-matrix adhesions and initiates cell retraction (Nelson, 2009). At the front edges of the cell the downregulation of adherens junctions increases the amount of cytoplasmic p120catenin, inhibiting RhoA activity and increasing the instability of cell junctions in this region. Activation of Rac1 and CDC42 at the front of the cell increases the formation of lamellipodia and filopodia, increasing the motility of the cell (Whale et al, 2011, Anastasiadis and Reynolds, 2001). Together these processes result in cell movement and migration.

SFKs inhibit RhoA and activate Rac1 to alter the structure of the actin cytoskeleton (Yagi et al, 2007). During adhesion initiation, Src complexes with FAK to recruit Rac-activating GEFs such as Tiam1, DOCK180, Vav and PIX at immature focal adhesions, activating Rac to induce lamellipodia formation (Huveneers and Danen, 2009). Src also activates p190RhoGAP, increasing levels of GDP-bound Rho and inhibiting Rho activity (Brandt et al, 2002). In cancer cell metastases, Src suppresses RhoA to relax the actin cytoskeleton and allow podosome formation (Clark et al, 2007). During oligodendrocyte differentiation, Fyn phosphorylates p190RhoGAP to decrease Rho activity. Fyn also activates Rac and Cdc42, and together with Rho inhibition these signaling changes induce process extension and differentiation of the oligodendrocytes (Wolf et al, 2001,

Liang, Draghi and Resh, 2004). Fyn-mediated phosphorylation of p250GAP in neurons has also been implicated in Rho inhibition and oligodendrocyte differentiation (Taniguchi et al, 2003).

1.6.5 SFKs and EMT

SFKs are involved in cell processes that regulate proliferation, survival, regulation of the cytoskeleton and cell shape, maintenance of cell-cell and cell-matrix adhesions, motility and migration (Guarino, Rubino and Ballabio, 2007). Therefore, when proteins from this family are dysregulated it alters many of the characteristics important in EMT. In head and neck SCCs there is a correlation between Src over-expression and E-cadherin downregulation, vimentin upregulation and invasiveness (Mandal et al, 2008). Src activation plays a key role in the induction of EMT by upregulating the production of matrix metalloproteases, phosphorylating caspase-8 to induce its pro-migratory function and disrupting cell-cell junctions (Rivat et al, 2003, Frisch, 2008, Behrens et al, 1993). More specifically, Src phosphorylates β-catenin, disrupting the interaction between E-cadherin and β-catenin and reducing the stability of the adherens junction (Behrens et al, 1993). β-catenin can then travel to the nucleus where it upregulates pro-EMT genes such as Snail, Vimentin and matrix metalloproteases (Guarino, Rubino and Ballabio, 2007). Sequestration of β-catenin in adherens junctions suppresses tumor formation through contact inhibition, and the liberation of β-catenin by SFKs contributes to the oncogenic

activity of this family of proteins. Src also phosphorylates E-cadherin to target the adherens junction protein for endocytosis and degradation (Avizienyte and Frame, 2005, Palacios et al, 2005). Upregulation of Fyn activity has been associated with the induction of EMT in oral SCC through downregulation of Cytokeratin and E-cadherin and upregulation of N-cadherin and vimentin (Lewin et al, 2010). Increased Fyn activity has also been associated with the induction of EMT in colorectal cancer (Wang et al, 2012). Thus it is clear that SFKs, including Fyn, play an important role in the transformation from an epithelial to a mesenchymal cell phenotype.

1.7 Dasatinib

Dasatinib (BMS-354825, Sprycel®; Bristol Myers Squibb) is a small molecule tyrosine kinase inhibitor that blocks SFK, BCR-ABL, EphA2, c-FMS, PDGFR and c-Kit activity by binding to the ATP-binding site of these tyrosine kinases and competitively inhibiting ATP binding (Aguilera and Tsimberidou, 2009, Gnoni et al, 2011). Despite the fact that Dasatinib has a broad specificity, the *in vitro* IC_{50} necessary to inhibit SFK activity is 0.5 nM, lower than any of its other targets (Aguilera and Tsimberidou, 2009, Lombardo et al, 2004). The most clinically studied SFK inhibitor, Dasatinib is already used in clinics to treat Imatinib-resistant chronic myelogenous leukemia (CML) and Philadelphia chromosome positive acute lymphoblastic leukemia (ALL), and is being evaluated in clinical trials to treat a variety of solid tumors (Araujo and Logothetis, 2010, Gnoni et al,

2011).

Dasatinib is orally administered drug that reaches its maximum plasma concentration within 3-5 hours and has a half-life of 3-5 hours. Highly protein bound, Dasatinib reaches extensive distribution in the extravascular space but has poor brain penetration. The majority of Dasatinib is metabolized in the liver by CYP3A4 to produce the pharmacologically active metabolites M4, M5, M6, M20 and M24. Following its metabolism, 96% of Dasatinib is excreted in the feces and 4% is excreted in the urine (van Erp, Gelderblom and Guchelaar, 2009). When administered every twelve hours for 5 consecutive days followed by 2 non-treatment days for the treatment of solid tumors the maximum tolerated dose was 120 mg. When administered continuously twice daily for the treatment of solid tumors the maximum tolerated dose was 70 mg. Dose limiting toxicities included nausea, fatigue and anorexia (Demetri et al, 2009).

1.7.1 Role for Dasatinib in the Treatment of Cancer

Dasatinib was originally developed as an inhibitor of SFKs, although its initial clinical use was as an inhibitor of BCR-ABL in CML and ALL (Montero et al, 2011). SFKs are upregulated in most solid tumors; therefore targeting this dysregulation using Dasatinib is a promising clinical therapy (Varkaris et al, 2014, Yeatman, 2004, Frame, 2004, Mandal et al, 2008). Studies in prostate cancer have shown that Dasatinib-mediated SFK

inhibition directly blocks properties associated with cellular metastasis. Furthermore, prostate tumors from mice treated with Dasatinib were smaller and resulted in a reduced incidence of lymph node metastases (Park et al, 2008). Dasatinib treatment in triple negative breast cancer cell lines (MDA-MB-231 cells) inhibited cell cycle progression and stimulated apoptosis while also inhibiting cellular invasion and migration (Nautiyal et al, 2009). Studies of non-small cell lung cancer, colorectal cancer, pancreatic cancer, head and neck squamous cell carcinoma and melanoma have recapitulated these results, indicating Dasatinib treatment inhibits cell migration and invasion, with variable ability to inhibit cell proliferation and survival (Araujo and Logothetis, 2010, Montero et al, 2011). Additionally, Dasatinib exposure results in significantly reduced osteoclast activity through inhibition of FMS, the tyrosine kinase receptor of the macrophage colony-stimulating factor (Brownlow et al, 2009). Therefore, Dasatinib both reduces the ability of cells to migrate from the primary tumor and the process of osteolysis that creates an attractive environment for bone metastasis (Araujo and Logothetis, 2010, Montero et al, 2011).

1.8 Hypothesis and Aims

More than 700,000 patients are diagnosed with cSCC every year, and this number is only growing as UV exposure increases due to changing lifestyles and a thinning ozone layer. Despite the personal and economic impact of cSCC, there are no targeted therapies to treat this type of tumor. The introduction of H-Ras, a common oncogene in cSCC, is sufficient to selectively upregulate Fyn expression in HaCaT cells, a human keratinocyte cell line. SFKs activity is upregulated in most tumor types (including cSCC), and this increase is associated with tumor progression and decreased survival. The introduction of active Fyn to the epidermis of a mouse is sufficient to induce the formation of AKs and cSCCs. For these reasons, targeting Fyn activity may be an effective clinical therapy in the treatment of cSCC.

1.8.1 Hypothesis

Fyn expression and activity in keratinocytes is upregulated following the introduction of active Ras, a common oncogene in cSCC. Within the context of cellular transformation and oncogenesis, Fyn activity is associated with the transition from an epithelial to mesenchymal phenotype, as well as an increase in the migratory capacity of tumorigenic cells. Targeting Fyn in Ras-transformed keratinocytes may serve as a potential therapy in

the treatment of cSCC, as well as increase our understanding of how increased Fyn activity drives the malignant phenotype of keratinocytes.

1.8.2 Aims

1.8.2.1 Aim 1

Although Fyn is overexpressed in many tumors, the signaling mechanism controlling the transcriptional regulation of Fyn expression has only been identified in leukemic white blood cells. Therefore, we will determine the mechanism regulating Fyn over-expression in HaCaT cells stably expressing constitutively active H-Ras.

1.8.2.2 Aim 2

Increased Fyn activity has been linked to many of the characteristics associated with tumors that have an increased migratory and metastatic capacity. Progression to a pro-migratory phenotype is associated with poor clinical outcomes in cSCC. Therefore, we will determine whether targeting Fyn can reverse these pro-migratory characteristics and elucidate the mechanism by which Fyn inhibition decreases cell mobility.

1.8.2.3 Aim 3

Increased Fyn activity is associated with increased tumor formation in the epidermis, and inhibition of SFKs decreases papilloma formation following chemical carcinogenesis. Therefore, we will determine whether Dasatinib treatment following UV exposure, a common carcinogen in cSCC, reduces tumor formation *in vivo*.

CHAPTER II

MATERIALS AND METHODS

2.1 Cell Culture and Reagents

HaCaT, HaCaT-Ras and HaCaT-Fyn cell lines were grown in DMEM with 10% FBS, 1% penicillin/streptomycin or Media 154 (0.07 mM Ca^{2+}) for low Ca^{2+} experiments (Invitrogen, Grand Island, NY). MDA-MB231 cells were grown in IMEM with 5% FBS, 1% penicillin/streptomycin, 1% L-Glutamine and 1% non-essential amino acids (Invitrogen, Grand Island, NY). Active H-Ras(G12V) was expressed from the LZRS retroviral vector, while active Fyn (I338T) was expressed from the pMV7 retroviral vector (Yadav and Denning, 2011). Dasatinib (LC Laboratories, Woburn, MA), Cytochalasin D (Santa Cruz Biotechnology Inc., Dallas, TX) and Y27632 (Millipore Inc., Billerica, MA) were purchased from the companies indicated.

2.2 Reverse Transcriptase qPCR

Total RNA was isolated using Trizol (Invitrogen, Grand Island, NY). Complementary DNA was synthesized using the Superscript First Strand Synthesis system (Invitrogen, Grand Island, NY). Quantitative RT-PCR was performed using a GeneAmp 5700

sequence detection system (Applied Biosystems, Carlsbad, CA) with Platinum SYBR Green PCR reagents (Invitrogen, Grand Island, NY). GAPDH or β-actin was used to normalize expression levels and relative mRNA expression was calculated using the ΔΔCt method. More specifically, ΔΔCt was calculated by subtracting the average Ct values of the gene of interest from the average Ct values of the housekeeping control gene to generate the ΔCt value. The control sample was used to compare all other samples to and the ΔCt of this control sample was subtracted from the ΔCt value of all other samples to generate ΔΔCt values. Data is represented as mean ΔΔCt ± standard deviation. Positive standard deviations were calculated by subtracting 2 raised to – ΔΔCt from 2 raised to –(ΔΔCt – the square root of the standard deviation of the Ct values of the gene of interest squared plus the standard deviation of the Ct values of the control housekeeping gene squared). Negative standard deviations were calculated by subtracting 2 raised to –(ΔΔCt plus the square root of the standard deviation of the Ct values of the gene of interest squared plus the standard deviation of the Ct values of the control housekeeping gene squared) from 2 raised to –ΔΔCt.

The RT-qPCR primers used are as follows:

Src Forward: 5'-GTCAAGCTGGGCCAGGGCTG-3'

Src Reverse: 5'-TGACCTGGGCCTCCTGCAGG-3'

Fyn Forward: 5'-GGCAGCCCTGTACGGGAGGT-3'

Fyn Reverse: 5'-GCTCCACCTGCTCCAGCACC-3'

Fyn(B) Forward: 5'-GCCGCTAGTAGTTCCCTGT-3'

Fyn(T) Forward: 5’-AGATGCTTGGGAAGTTGCAC-3’

Fyn(B)/(T) Reverse: CTTCATGATCTGCGCTTCCT-3’

Yes Forward: 5’-GACTCATGAGAGCGCGGCCG-3’

Yes Reverse: 5’-TGGCTCACACTTGTACTGACAGGCT-3’

FGR Forward: 5’-ATCATGCCGCAGCCCCACTG-3’

FGR Reverse: 5’-CGTGGCCACCGGCTCCAATT-3’

Lyn Forward: 5’-GCGCTGGGCAGTTTGGGGAA-3’

Lyn Reverse: 5’-GGGCTCCTCCCTGGTGACCA-3’

Hck Forward: 5’-GCCACCCGGAAGGAGGGCTA-3’

Hck Reverse: 5’-AGCCAGCAGGTTGGCGCTCTG-3’

Lck Forward: 5’-CACGGCCGCATCCCTTACCC-3’

Lck Reverse: 5’-CTGGGCGCTCCTTCCAGCAC-3’

Blk Forward: 5’-GGCGGCCAACATCCTGGTGT-3’

Blk Reverse: 5’-ATGGCTTCCGGGGCTGTCCA-3’

GATA1 Forward: 5’- CTCCGCAACCACCAGCCCAG-3’

GATA1 Reverse: 5’-GCATCCAAGCCCTCAGGCCC-3’

GATA2 Forward: 5’-GACCGGCCTCCAGCTTCACC-3’

GATA2 Reverse: 5’-AGGCCACAGGCATTGCACAGG-3’

GATA3 Forward: 5’-CAAGGCCCGCTCCAGCACAG-3’

GATA3 Reverse: 5’-CCGCAGGCGTTGCACAGGTA-3’

LEF1 Forward: 5’-TGCAGCCATCCCATGCGGTC-3’

LEF1 Reverse: 5’-ACACCACCCGGAGACAAGGGA-3’

TCF4 Forward 5’-GAGCCATGGGTGGTCTGGGC-3’

TCF4 Reverse 5’-CTGCCTCTCAGGGGCCACGC-3’

β-catenin Forward 5’-TTGTCCCGCAAATCATGCAC-3’

β-catenin Reverse 5’-GCTAGGATGTGAAGGGCTCC-3’

Snail (Snai1) Forward 5’-CAAGATGCACATCCGAAGCC-3’

Snail (Snai1) Reverse 5’-CATCTGAGTGGGTCTGGAGG-3’

Slug (Snai2) Forward 5’-CATCTTTGGGGCGAGTGAGT-3’

Slug (Snai2) Reverse 5’-ATGGCATGGGGGTCTGAAAG-3’

Twist1 Forward 5’-TCTACCAGGTCCTCCAGAGC-3’

Twist1 Reverse 5’-CTCCATCCTCCAGACCGAGA-3’

GAPDH Forward: 5’-CGACCGTCAAGGCTGAGAAC-3’

GAPDH Reverse: 5’-GCCTTCTCCATGGTGGTGAA-3’

Fyn promoter Forward: 5’-TGCCACAGTAACGCTCAACCCACT-3’

Fyn promoter Reverse: 5’-CCCGGCTGCCCTATCAAAGA-3’

2.3 Luciferase Assays

The pFynPromoterCheck reporter plasmid was a gift from Dr. Joya Chandra (MD Anderson, Houston, TX) (Gao et al, 2009). A 2 kb segment of the human *FYN* promoter was excised from the pFynPromoterCheck plasmid using BglII and HindIII and then

ligated into a pGL3-Basic plasmid (Promega, Madison, WI) to generate pFyn2000. Plasmids containing 1 kb, 0.5 kb, 0.1 kb and 0.05 kb of the *FYN* promoter were generated using the same method. A pFyn2000 plasmid containing a mutation at the site of interest was generated using the QuikChange Lighting Site-Directed Mutagenesis kit (cat# 210518, Agilent Technologies, Santa Clara, CA) (Forward primer 5'CCAAGGGCTCTTTCTTAGGGCAGCCGGG-3' Reverse primer 5'-CCCGGCTGCCCTAAGAAAGAGCCCCTTGGG-3'). 200,000 cells/well in a 12 well plate were transfected with 1.4 μg DNA/well (1.2 μg firefly and 0.2 μg renilla luciferase plasmids) using 4 μL TransIT-2020/well (Mirus Bio LLC, Madison, WI) in Opti-MEM (Invitrogen, Grand Island, NY) with a final volume of 200 μL/well. Reporter plasmid activity was assessed 48 hours post-transfection using the Dual Luciferase Reporter Assay (Promega, Madison, WI) with transfection efficiency normalized using the pRL-TK renilla luciferase plasmids (Promega, Madison, WI). Luciferase was measured using the Femtomaster FB15 (Zylux Corporation, Oak Ridge, TN). Data is represented as mean firefly luciferase/renilla luciferase ± standard deviation.

2.4 Transcription Factor Prediction Analysis

Predicted transcription factor binding was performed by entering the sequence of the promoter region of interest into the following websites:

TF Search: http://www.cbrc.jp/research/db/TFSEARCH.html

ALGGEN/PROMO: http://alggen.lsi.upc.es/cgi-bin/promo_v3/promo/promoinit.cgi?dirDB=TF_8.3

TFBind: http://tfbind.hgc.jp/

TFSiteScan: http://www.ifti.org/cgi-bin/ifti/Tfsitescan.pl

2.5 Chromatin Immuno-Precipitation Assay

The Chromatin Immunoprecipitation (ChIP) assay was performed using the EZ-ChIP kit (cat#17-371 Millipore Inc., Billerica, MA). Briefly, the cells were incubated in 1% formaldehyde for 10 minutes. The reaction was neutralized by incubation in 1% glycine for 5 minutes. The cells were then lysed in SDS lysis buffer and sonicated at 50% power for 10 seconds 8-10x on ice. Cross-linked protein and DNA were incubated overnight at 4°C with rotation and with 2 μg of one of the antibodies listed below. Protein G agarose beads were added and the mixture was incubated for one hour at 4°C with rotation. The isolates were washed with low-salt immune complex buffer, high-salt immune complex buffer, LiCl immune complex buffer and TE buffer. The cross-linked protein and DNA were eluted from the beads by incubating the isolates with elution buffer at room temperature for 15 minutes. Crosslinking was reversed by incubating the isolate with 5M NaCl at 65°C for 5 hours. The DNA was isolated using spin filters provided. The Fyn promoter sequence was detected by performing qPCR as described above.

Antibodies used:

Gata2 SC-9008 Santa Cruz Biotechnology Inc., Dallas, TX

Gata3 SC-22206 Santa Cruz Biotechnology Inc., Dallas, TX

Lef-1 SC-8591 Santa Cruz Biotechnology Inc., Dallas, TX

β-catenin SC-7199 Santa Cruz Biotechnology Inc., Dallas, TX

2.6 Electrophoretic Mobility Shift Assay (EMSA)

EMSA was performed by first annealing the oligonucleotides corresponding to the region of interest. Oligonucleotides were purchased from IDT with the IRdye700 added to the 5' end and were HPLC purified. Equal molar quantities of the forward and reverse oligonucleotide were heated in a 100°C heating block for 3 minutes in the dark. The block was then turned off and the oligonucleotides were allowed to slowly come to room temperature. Following the annealing of the oligonucleotides, a 4% native agarose gel was made. The oligonucleotides were combined with 10x binding buffer (100 mM Tris, 500 mM KCl, 10 mM DTT, pH 7.5), 1 ug/uL poly(dI-dC), 25 mM DTT/2.5% Tween20, 7.5 ug nuclear extract and enough water to total 20 uL. 30% glycerol was added and the mixture was allowed to incubate in the dark for 30 minutes. Alternatively, if a supershift was desired everything but the oligonucleotide was mixed and allowed to incubate for 10 minutes. Then the oligonucleotide was added and the mixture was allowed to incubate for 30 minutes. The sample was then loaded into the native gel with a mixture of glycerol and bromphenol blue in an adjacent lane and was run at 40V until the dye

reached 2/3 of the way down the gel. Agarose gels were visualized using the LI-COR Infrared Imaging System (Li-Cor Biosciences, Lincoln, NE).

Antibodies used: Lef-1 SC-8591 Santa Cruz Biotechnology Inc., Dallas, TX

Oligonucleotide sequences:

EMSA Fyn pro forward: 5'-/5IRD700/GGCTCTTTGATAGGGCAGCC-3'

EMSA Fyn pro reverse: 5'-5IRD700/GGCTGCCCTATCAAAGAGCC-3'

2.7 Immunoblotting

Western blotting was performed as described previously (D'Costa et al, 2006). Cell lysates were collected by scraping cultured cells in RIPA buffer (50mM Tris, ph7.5, 150 mM NaCl, 1% Triton X-100, 0.1% SDS, 1% Sodium Deoxycholate) and were cleared by centrifuging at 14,000 rpm at 4°C for 5 minutes. Protein concentrations were determined using Bradford reagents (Bio-Rad, Hercules, CA). Antibodies were obtained from the companies indicated: Fyn-59 (SC-73388, Santa Cruz Biotechnology Inc., Dallas, TX), E-cadherin (INV135700, Invitrogen, Grand Island, NY), pan-cytokeratin AE1/AE3 (SIG-3464, Covance, Princeton, NJ), vimentin (AMF-17b, Developmental Studies Hybridoma Bank, Iowa City, IA) and β-actin (MP691002, MP Biomedicals, Santa Ana, CA). Secondary antibodies used were goat anti-rabbit IgG-Alexa Fluor 680 or 800 and goat anti-mouse IgG-AlexaFluor 680 or 800 (Invitrogen, Grand Island, NY). Western blots

were visualized using the LI-COR Infrared Imaging System (Li-Cor Biosciences, Lincoln, NE).

F-actin and G-actin fractionation was performed as described by Rasmussen et al. (Rasmussen et al, 2010). Cells were lysed in cold actin stabilization buffer (0.1 M PIPES, 10% glycerol, 20x DMSO, 1 μM $MgSO_4$, 2 μM EGTA, 1% TX-100, 10x ATP and 25x complete protease inhibitor) on ice for 10 minutes. G-actin was isolated by centrifuging the sample at 12,500 rpm in the Beckman TL-100 Ultracentrifuge (Beckman Coulter, Inc., Brea, CA) for 75 minutes at 4°C. The pellet was then resolubilized in actin depolymerization buffer (0.1M PIPES, 1 μM $MgSO_4$, 10 μM $CaCl_2$ and 5 μM Cytochalasin D) for 10 minutes at room temperature to obtain F-actin. Samples were run on a Western blot as described above. Bands were quantitated using Image-J Software.

2.8 SFK Activation Assay

SFK activation was determined using the Milliplex Map 8-Plex Human Src Family Kinase Phosphoprotein kit (Millipore Inc., Billerica, MA) and the Flexmap 3D Luminex system (Luminex Corporation, Austin, TX) as directed by the manufacturer.

2.9 AlamarBlue Assay

Cell viability was measured by incubating the cells with alamarBlue (Invitrogen, Grand Island, NY). Following treatment, alamarBlue was introduced to the cell culture at a 1:20 dilution in growth media. The cells were then allowed to incubate at 37°C for 2 hours. Changes in fluorescence were measured using a POLARstar Omega plate reader (BMG Labtech, Ortenberg, Germany) by detecting fluorescence from the bottom of the plate. Excitation was set at 530 nm and emission was set at 590 nm.

2.10 DNA Quantitation Assay

Cellular proliferation was measured using the DNA Quantitation Kit from Bio-Rad (cat # 1702480, Bio-Rad, Hercules, CA). Following treatment cells were exposed to PBS- with 0.1% EDTA for 10 minutes. The cell lysate was then mixed with Hoechst dye in a 96 well plate and a standard curve with control DNA was set up adjacent to the samples. DNA quantitation was performed by detecting fluorescence emission using a POLARstar Omega plate reader (BMG Labtech, Ortenberg, Germany) with the excitation filter set at 360 nm and the emission filter set to 460.

2.11 Thymidine Incorporation Assay

Cellular proliferation was measured by incubating the cells in media containing 5 μCi radioactive thymidine overnight. The cells were then trypsinized, transferred to 96 well UniFilters (PerkinElmer, Waltham, MA) and read on a scintillation reader.

2.12 DNA-PI Staining

Cell cycle analysis was performed by trypsinizing the cells and placing them in flow cytometry tubes. The cells were washed with cold FACS buffer (PBS+ with 5% FBS and 0.2% sodium azide), then incubated 30 minutes on ice with 85% cold EtOH. After washing the cells with another aliquot of FACS buffer, the cells were treated with 10 μg/mL RNaseA for 15 minutes at 37°C and 5 minutes at room temperature. An equal volume of propidium iodide (100 μg/mL) was then added and the cells were incubated in the dark at 4°C for 1 hour. Propidium iodide staining was measured using either a Coulter Epics XL-MCL flow cytometer (Beckman Coulter, Brea, CA) or a BD FACSCANTO II flow cytometer (BD Biosciences, San Jose, CA).

2.13 Annexin-PI Staining

Apoptosis was measured using the Dead Cell Apoptosis Kit (cat # V13245, Invitrogen, Grand Island, NY) by trypsinizing the cells and placing them in flow cytometry tubes. The cells were washed with cold PBS- and were resuspended in cold binding buffer. Annexin and propidium iodide were added to the cell suspension and the mixture was allowed to incubate in the dark for 15 minutes. Cold binding buffer was added and apoptosis was measured using a Coulter Epics XL-MCL flow cytometer within one hour (Beckman Coulter, Brea, CA).

2.14 Acridine Orange Staining

Autophagy was measured using Acridine Orange (cat # A1301, Invitrogen, Grand Island, NY). Cells were incubated in a 1μg/mL solution of Acridine Orange in DMEM media for 20 minutes at 37°C. The cells were trypsinized and resuspended in PBS+. Autophagy was measured using a Coulter Epics XL-MCL flow cytometer (Beckman Coulter, Brea, CA).

2.15 Cell-Cell Adhesion Assay

Cell-cell adhesion was assayed using a dispase assay with minor modifications (Hobbs et al, 2011). Cells were allowed to grow to confluency and then treated as indicated. Following treatment, the cells were washed with PBS- and incubated with Dispase II (2.4 Units/mL, Roche Diagnostics, Indianapolis, IN) at 37°C for 30 minutes. Following detachment from the culture plate, the cells were spun into a pellet, and then resuspended in PBS-. The number of single cells in each sample was counted using a hemocytometer. The cells were spun down again and resuspended in 0.25% Trypsin. Following 10 minutes at 37°C, the number of total cells was counted using the hemocytometer. Percent single cells were calculated by dividing the number of single cells per sample by the number of total cells. Three counts were taken per well for both the single and total cell counts. Data is represented as mean % single cells ± standard deviation.

2.16 siRNA Transfection

Fyn siRNA (cat # SC29321), GATA3 (cat # SC29331), Lef-2 (cat # SC35804) and control siRNA (cat # SC37007) with no significant homology to the human transcriptome were obtained from Santa Cruz Biotechnology Inc. (Santa Cruz, CA). β-catenin siRNA was obtained from Cell Signaling (cat # 6225, Danvers, MA). To transfect 325,000 cells/well in a 6 well plate 6 μL Lipofectamine transfection reagent (Invitrogen, Grand

Island, NY) was mixed with 10 μL of 10 μM siRNA and 300 μL Opti-MEM/well. Knockdown was assessed 48-72 hours following transfection.

2.17 Migration Assay

Migration assays were performed using a 24-well HTS Multiwell Insert System (BD Falcon, San Jose, CA). 4 x 10^5 cells were seeded in serum-free DMEM into the upper chamber of each well and DMEM with 10% fetal bovine serum was added to the lower chamber. Following 6 hours of incubation at 37°C to allow attachment Dasatinib was added to the upper and lower chamber of each well. Cells were allowed to migrate for 24 hours, then were fixed in 16% formaldehyde and stained with 0.05% crystal violet. Cell counts from one visual field in three separate wells were averaged with error bars denoting standard deviation.

2.18 Immunofluorescence and Quantitation

Cells were grown on glass coverslips or cytospun onto slides, followed by fixation with 4% paraformaldehyde and permeabilization with 0.1% Triton X-100. Following fixation, the cells were blocked with 5% normal goat serum and then stained with Rhodamine-phalloidin (100 nM, PHDR1, Cytoskeleton Inc., Denver, CO), α-catenin (CS-7894 Cell Signaling Technology Inc., Danvers, MA), β-catenin (SC-7963 Santa Cruz

Biotechnology Inc., Dallas, TX) or p120catenin (SC-13957 Santa Cruz Biotechnology Inc., Dallas, TX) and DAPI (0.1 μg/ml). Following antibody staining, secondary antibodies conjugated to AlexaFluor 488 were applied and nuclei were stained with DAPI. Microscopy and photography were performed on an Olympus AX80 microscope (Olympus Corporation, Center Valley, PA) with a QImaging Retiga 4000R CCD camera (QImaging, Surrey, BC, Canada) and the images were colorized and merged using Adobe Photoshop 6.0. Quantitation of Rhodamine-phalloidin staining was performed by quantitating the fluorescence in three fields of equal area in the same image divided by the number of nuclei in each field. Data is represented as mean fluorescence intensity/# nuclei ± standard deviation.

2.19 Mouse Study

Thirty-six SKH1 (Charles River, Chicago, IL) female 4-week old mice were divided into three groups of twelve and allowed to acclimate for 2 weeks. Following acclimation, the mice were exposed to increasing doses of UVB three times a week from two Kodacel-filtered FS20T12/UVB bulbs (National Biological, Beachwood, OH). The doses began at 30 mJ/cm² and were increased by 25% each week up to 150 mJ/cm². Immediately following each UV exposure, the mice were topically treated with 200 μL of acetone, acetone with 10 nmole Dasatinib or acetone with 100 nmole Dasatinib. There was no measurable difference in mouse weight between treatment groups. After twenty-three

weeks of UV exposure, the mice were allowed to recover for a week and then were euthanized using CO_2 gas. Tumors were recovered and processed for analysis. H&E staining was performed by the Pathology Histology Core at Loyola University Chicago. Assessment of tumor type from coded slides was performed by a board-certified dermatopathologist (Kelli A. Hutchens, MD). All experiments were approved by the Loyola University Chicago Institutional Animal Care and Use Committee.

2.20 Statistical Analysis

To determine whether differences in generated data were significant, Student's T-Tests were performed. These T-Tests were calculated on unpaired data with two tails.
To determine whether Dasatinib treatment resulted in a significant difference in the differentiation status of UVB-induced tumors a Fisher's Exact Test was used.

CHAPTER III

REGULATION OF FYN EXPRESSION IN HUMAN cSCC

3.1 Abstract

Fyn over-expression has been identified in cSCC, glioblastoma multiforme, head and neck squamous cell carcinoma, melanoma, sarcomas, lymphoma, breast, pancreatic and prostate cancer (Zhao et al, 2009, Saito et al, 2010, Ban et al, 2008, Lu et al, 2009, Posadas et al, 2009, Talantov et al, 2005, Palomero et al, 2014, Takayama et al, 1993, Martin et al, 2010). In fact, the majority of human carcinomas contain upregulated SFK activity when compared to corresponding non-neoplastic tissue (Zhao et al, 2009). Despite the recurring nature of Fyn over-expression, the mechanism driving Fyn transcription and translation has only been studied at length in chronic myelogenous leukemia (CML), where Gao et al. found that BCR-ABL mediated reactive oxygen species (ROS) production drove Fyn expression through the transcription factors Egr1 and Sp1 (Gao et al, 2009). The signaling pathway regulating Fyn over-expression in other tumor types has not been reported, and may overlap or diverge from these findings in leukemic white blood cells. In this study, we established a cell culture system where Ras-transformed HaCaT cells (a non-transformed, immortalized human keratinocyte cell

line) have selectively upregulated Fyn expression. Using this model we identified a region of the *FYN* promoter necessary for Fyn upregulation, as well as putative transcription factors that may bind to this site *in vivo*.

3.2 qPCR Analysis of SFK Expression

Activating mutations in the Ras gene have been detected in 58% of human cSCCs (Pierceall et al, 1991), suggesting Ras is a common oncogene in these malignancies. Following the stable introduction of constitutively active H-Ras(G12V) to HaCaT cells (Yadav and Denning, 2011) we used RT-qPCR to measure expression levels of all members of the *SFK* family. Only *SRC*, *FYN*, *YES* and *LYN* were expressed at detectable levels; expression levels of *LCK*, *FGR*, *HCK* and *BLK* were not detectable (Figure 6, data not shown). *FYN* mRNA was upregulated over 200-fold in HaCaT-Ras cells (stably express H-Ras(G12V)) compared with HaCaT cells, while expression levels of *SRC, YES* and *LYN* remained unchanged (Figure 6). Two isoforms of the Fyn protein, Fyn(B) and Fyn(T), are differentially expressed in the brain and T-cells but are expressed at similar levels in other tissues. These isoforms arise through alternative splicing of exon 7 within the SH2-linker region of the *FYN* gene (Brignatz et al, 2009, Goldsmith, Hall and Atkinson, 2002). We measured expression of *FYN(B)* and *FYN(T)* in our parental HaCaT and HaCaT-Ras cell lines using RT-qPCR and splice isoform-specific primers. In HaCaT cells, the ratio of *FYN(B)* to *FYN(T)* mRNA was 7.4, indicating that *FYN(T)* was the

predominant isoform of Fyn expressed (Figure 7). However, in the HaCaT-Ras cells, which have much higher levels of overall Fyn expression, the ratio of *FYN(B)* and *FYN(T)* mRNA was nearly equal to 1, indicating that expression of both isoforms was upregulated (Figure 7).

RT-qPCR analysis of SFK expression in HaCaT-Ras cells indicated that *FYN* expression was selectively upregulated (Figure 6). Increased mRNA levels may be due to increased activity at the *FYN* promoter, a transcriptional mechanism, or it may be due to increased stability of the *FYN* mRNA transcript, a translational mechanism. We introduced a luciferase reporter plasmid containing a 2 kb segment of the *FYN* promoter (referred to as pFyn2000) into HaCaT and HaCaT-Ras cells and measured luciferase expression levels as an indicator of transcriptional activity at the *FYN* promoter. HaCaT-Ras cells had 10x higher levels of luciferase activity, indicating *FYN* mRNA levels were upregulated through a transcriptional, and not translational, mechanism (Figure 8). Previous studies have shown that *FYN* expression is upregulated by the production of reactive oxygen species (ROS) (Gao et al, 2009). Additionally, many of the oncogenic functions of Ras are regulated by the ability of Ras to drive ROS production (Hole et al, 2010). Following the introduction of pFyn2000 to HaCaT and HaCaT-Ras cells, we measured whether exposure to N-Acetyl-Cysteine (NAC), a free radical scavenger, reduced *FYN* expression levels in HaCaT-Ras cells. Treatment with the anti-oxidant NAC in culture did not reduce *FYN* expression in either the HaCaT or HaCaT-Ras cells, suggesting that *FYN*

expression was regulated by a different mechanism than that defined by Gao et al. (Figure 8) (Gao et al, 2009).

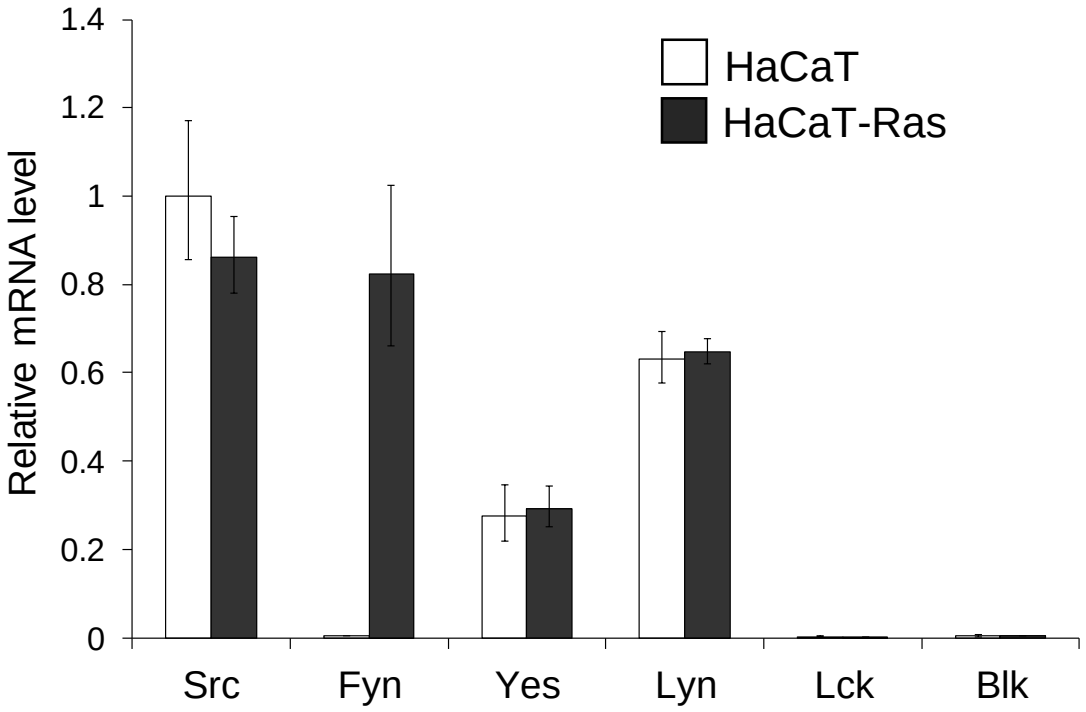

Figure 6: *FYN* Expression is Selectively Upregulated in HaCaT-Ras Cells

Total RNA was isolated from HaCaT and HaCaT-Ras cells and analyzed for SFK RNA by RT-qPCR. RNA levels were normalized to β-actin. Data shown is a representative experiment that was performed in triplicate.

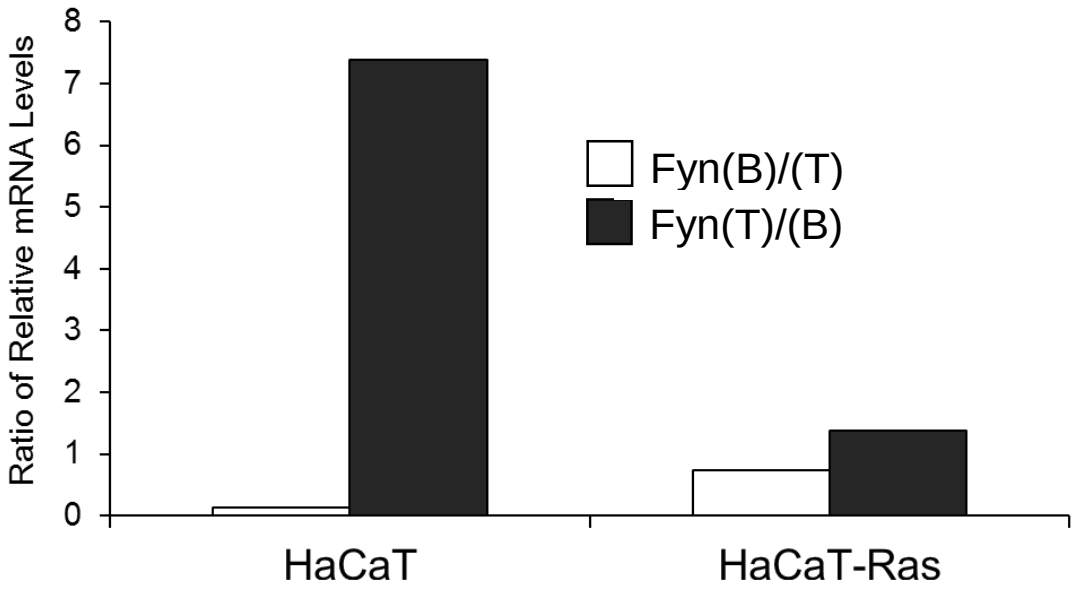

Figure 7: *FYN(B)* and *FYN(T)* are Both Upregulated in HaCaT-Ras Cells

Total RNA was isolated from HaCaT and HaCaT-Ras cells and analyzed for *FYN(B)* and *FYN(T)* RNA by RT-qPCR. RNA levels were normalized to *GAPDH*. Data is expressed as a ratio of relative *FYN(B)* to *FYN(T)* mRNA levels. Data shown is a representative experiment that was performed in duplicate.

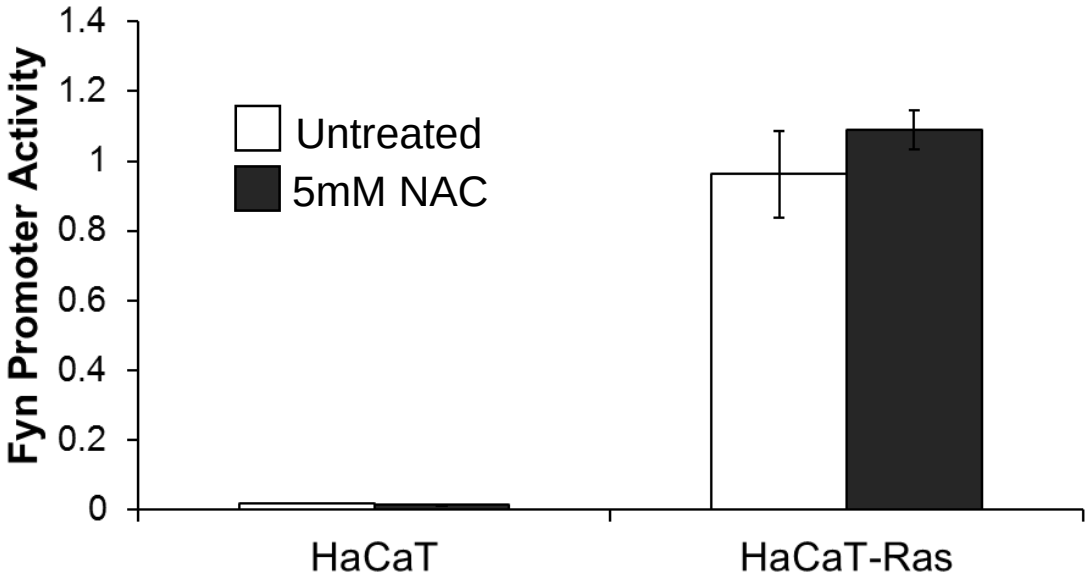

Figure 8: *FYN* Promoter Activity is Not Reduced By ROS Depletion

pFyn2000, a plasmid containing 2 kb of the *FYN* promoter in front of a firefly luciferase gene, and pRL-TK were transiently co-transfected in HaCaT and HaCaT-Ras cells. 5mM N-Acetyl-Cysteine (NAC) was added with the DMEM media prior to transfection. After 48 hours luciferase activity in cell lysates was measured. Data shown is a representative experiment that was performed in triplicate.

3.3 Analysis of the *FYN* Promoter Using Luciferase Reporter Plasmids

To identify potential transcription factors mediating *FYN* upregulation, we first created a series of luciferase reporter plasmids containing segments of the *FYN* promoter. The largest plasmid contained 2 kb of the *FYN* promoter (pFyn2000), and the other plasmids each contained progressively smaller segments of this sequence, with the smallest segment beginning 50 bases before the *FYN* transcription start site (pFyn50) (Figure 9a). Introduction of the full length (2 kb) *FYN* reporter plasmid (as shown in Figure 8) resulted in higher luciferase expression in HaCaT-Ras cells as compared to HaCaT cells, reaffirming our qPCR data (Figure 6 & 9b). Additionally, the region -100 to -50 bases before the transcription start site was proven necessary for *FYN* upregulation in HaCaT-Ras cells, as loss of this region resulted in decreased luciferase expression (Figure 9b).

Careful analysis of the region of interest in the *FYN* promoter using online transcription factor prediction software such as TFSearch, PROMO, TFBind and TFSiteScan identified several transcription factors that were predicted to bind within an approximately 20 base region -65 to -85 base pairs before the transcription start site. Following mutation of the dinucleotide GA sequence located -74 bases upstream of the transcription start site to a CT in the pFyn2000 plasmid (Figure 10a), *FYN* reporter activity in the HaCaT-Ras cells was reduced, indicating this sequence was necessary for *FYN* over-expression (Figure 10b). Furthermore, when nuclear cell lysate from HaCaT and HaCaT-Ras cells was

allowed to bind to a double-stranded oligonucleotide corresponding to the region of interest (-63 to -83 bases upstream of the transcription start site) in the *FYN* promoter, electrophoretic mobility shift assay (EMSA) analysis showed a greater amount of binding in the HaCaT-Ras lysate than the HaCaT lysate (Figure 11). Incubation with an oligonucleotide containing a GA→CT mutation at the -74 base site (Figure 10a) resulted in loss of binding when incubated with HaCaT-Ras cell lysate, as can be seen by loss of the band denoted with an asterisk (Figure 11). Despite the remaining presence of nonspecific bands, these results reaffirmed the importance of this site in *FYN* gene regulation (Figure 11).

A.

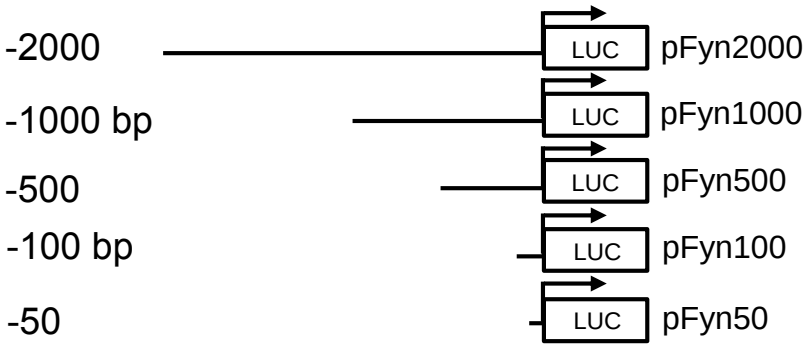

B.

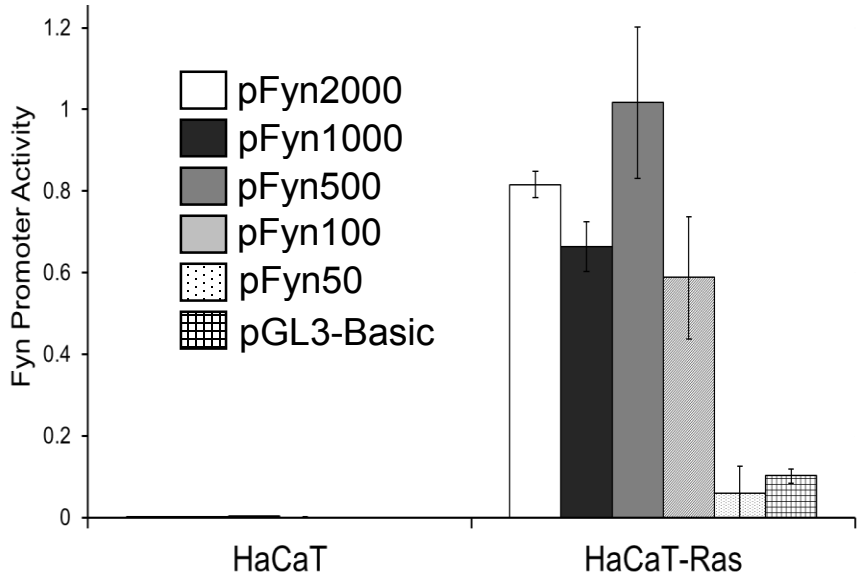

Figure 9: The -100 to -50 Region of the *FYN* Promoter is Necessary for *FYN* Expression in HaCaT-Ras Cells

A. Schematic of the luciferase reporter constructs created to identify regions of the human *FYN* promoter necessary for *FYN* expression. Segments corresponding to regions beginning -2000 bases down to -50 bases before the *FYN* transcription start site were ligated into the pGL3-Basic plasmid. Figure courtesy of Dr. Mitchell F. Denning.
B. *FYN* reporter plasmids were transiently co-transfected with pRL-TK into HaCaT and HaCaT-Ras cells. pGL3-Basic was used as a negative control, as it does not contain any part of the *FYN* promoter. Luciferase levels were measured 48 hours following transfection. Data shown is a representative experiment that was performed in triplicate.

A.

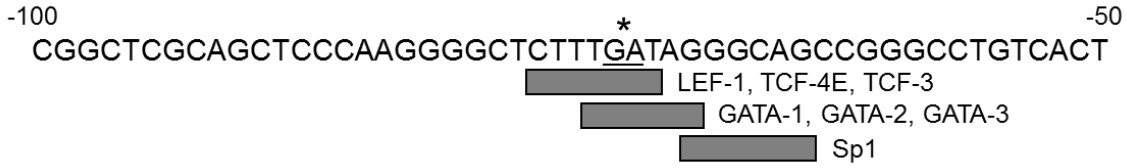

B.

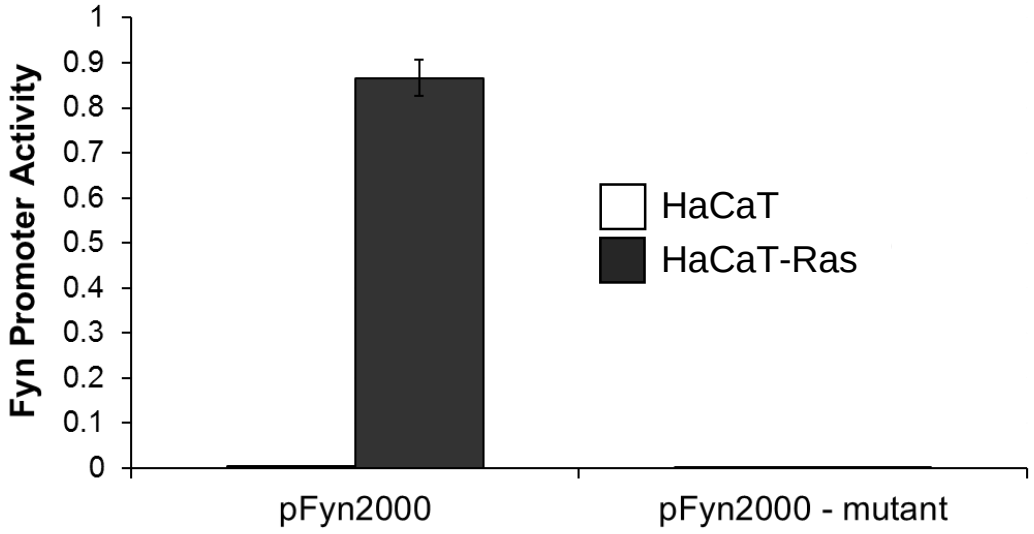

Figure 10: Mutation of the GA Sequence in the *FYN* Promoter Reduces *FYN* Expression in HaCaT-Ras Cells

A. Schematic of the *FYN* promoter region of interest between -100 and -50 bases before the transcription start site. Transcription factors with high likelihood of binding are shown. The pFyn2000-mutant reporter plasmid was created by mutating the GA sequence at -74 to CT (*). Figure courtesy of Dr. Mitchell F. Denning

B. pFyn2000 or pFyn2000-mutant was transiently co-transfected with pRL-TK into HaCaT and HaCaT-Ras cells. Luciferase levels were measured 48 hours following transfection. Data shown is a representative experiment that was performed in triplicate.

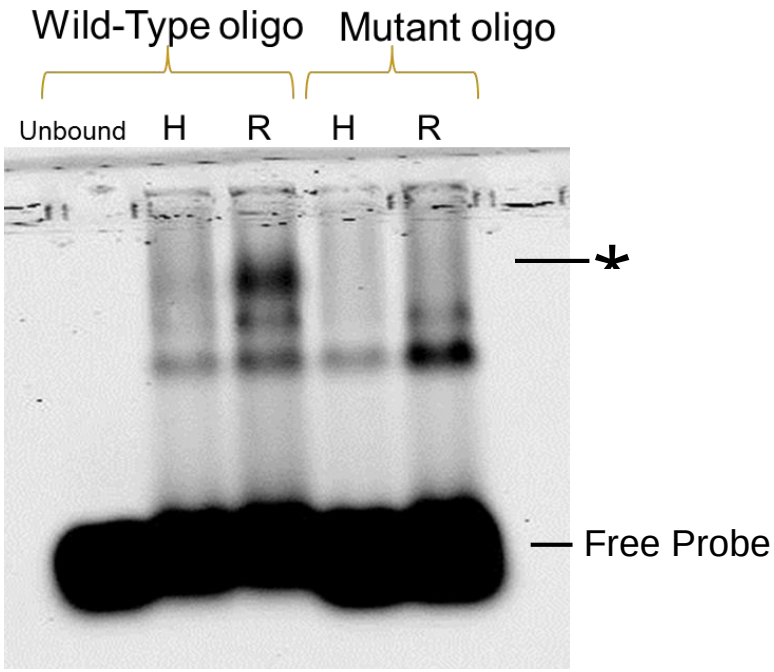

Figure 11: EMSA Analysis of Binding to the *FYN* Promoter

Oligonucleotides corresponding to the region of interest (-63 to-83 bases upstream of the transcription start site) in the *FYN* promoter, as well as the mutated region of interest (-74GA→CT), were incubated with nuclear cell lysates from HaCaT and HaCaT-Ras cells and then were run on a 4% agarose gel to detect binding. H corresponds to HaCaT cell lysate and R corresponds to HaCaT-Ras cell lysate. Unbound oligonucleotide was run on the left as a control. Free probe is designated at the bottom. The band lost upon incubation with the mutant probe is indicated by an *. Data shown is a representative experiment that was performed in triplicate.

3.4 Transcription Factor Expression Levels in HaCaT and HaCaT-Ras Cells

Using the online programs TFSearch, PROMO, TFBind and TFSiteScan, we identified several transcription factors predicted to bind to the region of interest -65 to -85 bases before the transcription start site in the *FYN* promoter (Figure 10a). To determine if any of these factors were upregulated in the HaCaT-Ras cells, we used RT-qPCR to measure expression levels of the *GATA* family, *TCF4* and *LEF1* genes. Expression levels of *GATA1*, *GATA2*, *GATA3* and *TCF4* mRNAs were not significantly upregulated in the HaCaT-Ras cells as compared to the parental HaCaT cells (Figures 12 & 13). However, expression levels of *LEF1* mRNA were increased over 2000-fold in the HaCaT-Ras cell line, suggesting that this transcription factor may be responsible for high Fyn expression in HaCaT-Ras cells (Figure 13).

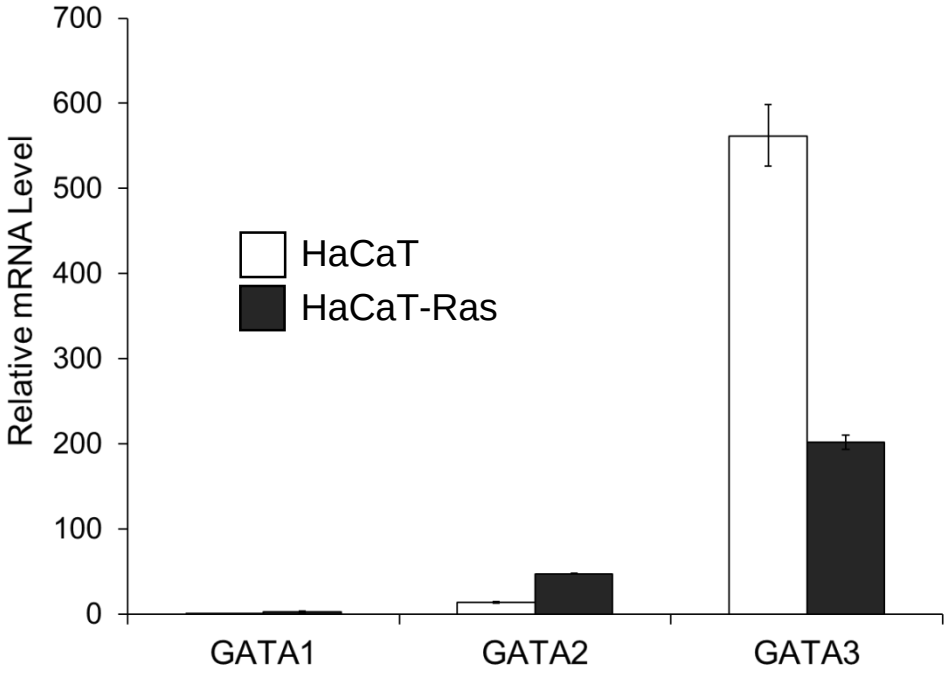

Figure 12: *GATA1, 2* and *3* Expression in HaCaT and HaCaT-Ras Cells

Total RNA was isolated from HaCaT and HaCaT-Ras cells and analyzed for *GATA1*, *GATA2* and *GATA3* RNA by RT-qPCR. RNA levels were normalized to *GAPDH*. Data shown is a representative experiment that was performed in duplicate.

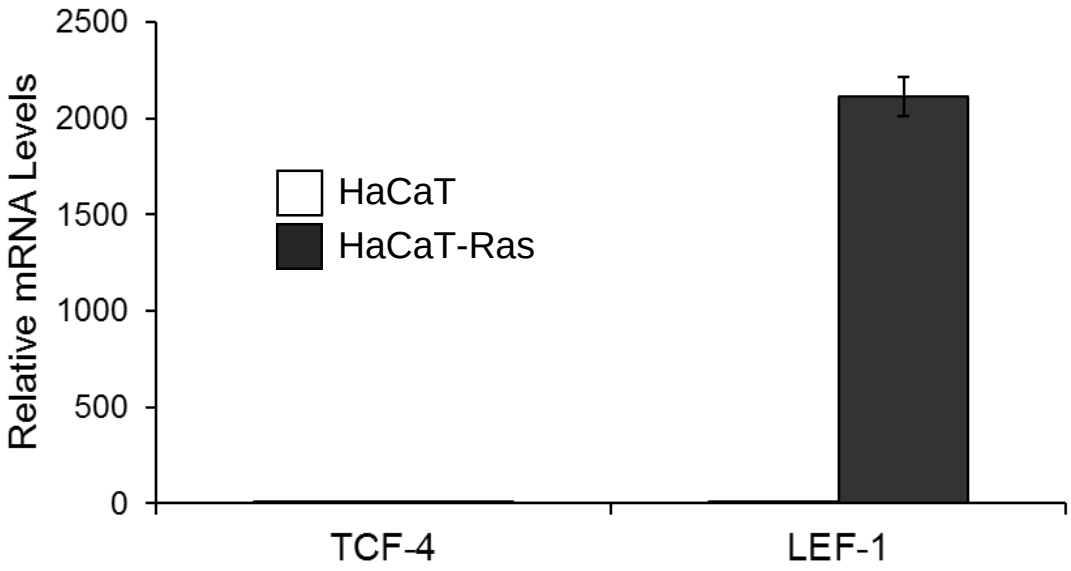

Figure 13: *TCF4* and *LEF1* Expression in HaCaT and HaCaT-Ras Cells

Total RNA was isolated from HaCaT and HaCaT-Ras cells and analyzed for *TCF4* and *LEF1* RNA by RT-qPCR. RNA levels were normalized to *GAPDH*. Data shown is a representative experiment that was performed in duplicate.

3.5 Analysis of Transcription Factor Binding at the Fyn Promoter

Based on the results of our *FYN* promoter analysis (Figure 9a) and RT-qPCR data (Figure 13), we next performed ChIP to detect binding of any of these potential transcription factors to the *FYN* promoter. We also assessed binding levels of β-catenin at this site, as β-catenin is an essential binding partner of the TCF family and is necessary for regulation of gene expression. Experiments performed in triplicate indicated that higher levels of Lef-1 and β-catenin bound to the *FYN* promoter in HaCaT cells as compared to HaCaT-Ras cells (Figure 14). Similarly, experiments performed in triplicate indicated that higher levels of GATA-2 and GATA-3 bound to the *FYN* promoter in HaCaT cells as compared to HaCaT-Ras cells (Figure 15). The nonspecific mouse IgG negative controls in both experiments resulted in low detection of binding. Despite the fact that all of the binding levels were above the mouse IgG control, the percent input for Lef-1, β-catenin, GATA-2 and GATA-3 was very low (< 1% input), suggesting the difference in binding between HaCaT and HaCaT-Ras cells may not be biologically meaningful.

Using EMSA we assessed the ability of antibodies corresponding to the transcription factors of interest to alter binding of the cell lysate to the *FYN* promoter oligonucleotide. Following incubation of the HaCaT-Ras cell nuclear lysate and the -63 to -83 Fyn oligonucleotide with an antibody against Lef-1, the previously detected band indicating association between the lysate and oligonucleotide was lost, suggesting the Lef-1

antibody was interfering with this interaction and Lef-1 may be the transcription factor mediating *FYN* transcriptional regulation (Figure 16). Incubation with antibodies against GATA-2 and GATA-3 did not alter the association between the Fyn oligonucleotide and nuclear cell lysate (Figure 16).

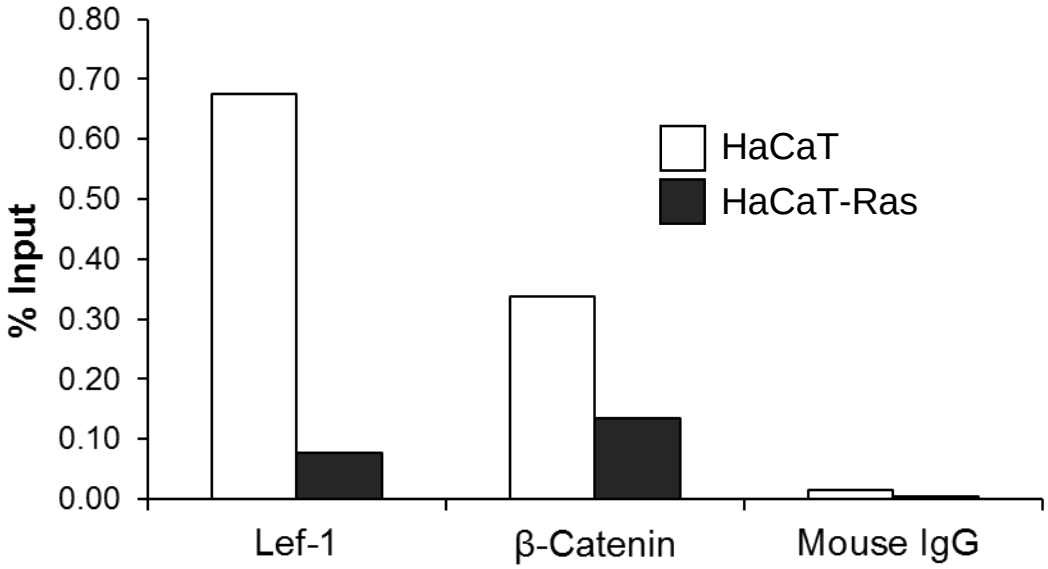

Figure 14: ChIP Analysis of Lef-1 and β-Catenin Binding to the *FYN* Promoter

ChIP assay was performed on lysates from formaldehyde cross-linked HaCaT and HaCaT-Ras cells using antibodies against Lef-1 and β-catenin. Precipitated *FYN* promoter DNA was quantitated by RT-qPCR. Precipitation with mouse IgG is shown as a negative control. Data shown is a representative experiment that was performed in triplicate.

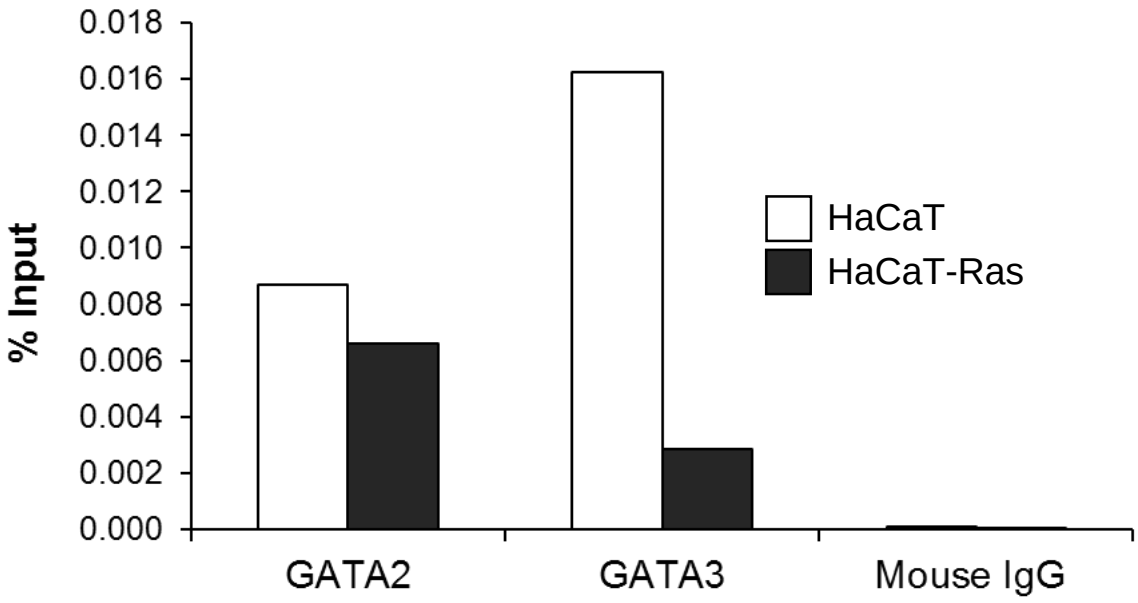

Figure 15: ChIP Analysis of GATA-2 and GATA-3 Binding to the *FYN* Promoter

ChIP assay was performed on lysates from formaldehyde cross-linked HaCaT and HaCaT-Ras cells using antibodies against GATA-2 and GATA-3. Precipitated *FYN* promoter DNA was quantitated by RT-qPCR. Precipitation with mouse IgG is shown as a negative control. Data shown is a representative experiment that was performed in triplicate.

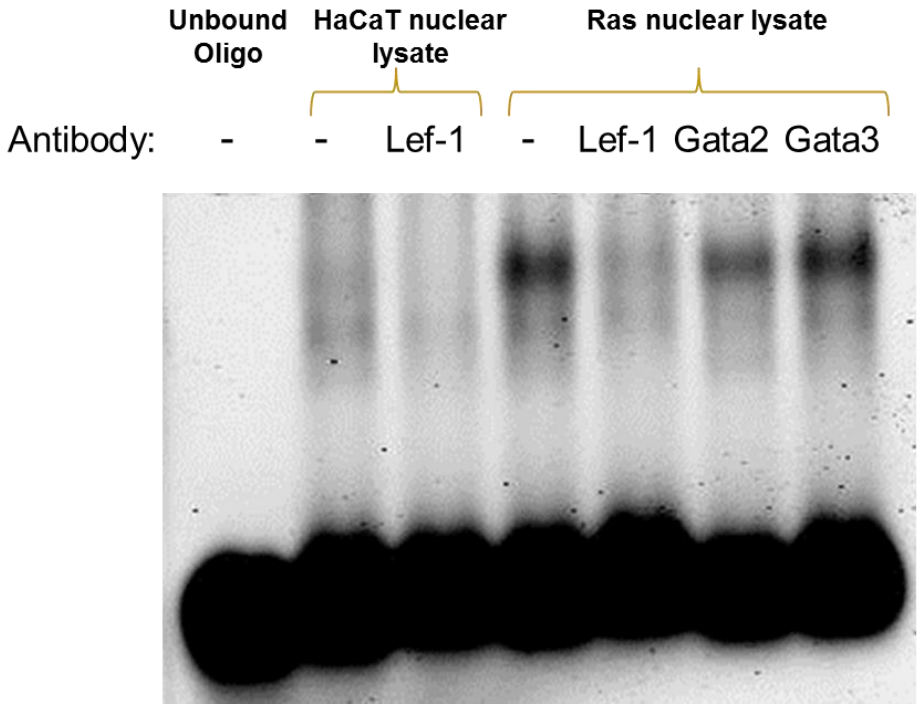

Figure 16: EMSA Analysis of Antibody Interference with Binding to the *FYN* Promoter

Oligonucleotides corresponding to the region of interest in the *FYN* promoter (-63 to -83 bases upstream of the transcription start site) were incubated with nuclear lysates from HaCaT and HaCaT-Ras cells as well as antibodies against the predicted transcription factors. The lysates were then run on a 4% agarose gel to detect binding. Unbound oligonucleotide was run on the left as a control. Data shown is a representative experiment that was performed in triplicate.

3.6 Assessment of Fyn Expression Following Knockdown of Transcription Factors

Following the EMSA analysis of transcription factor binding, we used siRNA to knock down Lef-1 expression (Figure 17a). 72-hours after siRNA transfection we measured *FYN* expression levels in HaCaT and HaCaT-Ras cells using RT-qPCR (Figure 17b). Despite the fact that *LEF1* mRNA levels were reduced over 80%, *FYN* expression levels were not decreased by reduced *LEF1* expression (Figure 17b). However, a careful analysis of the literature suggested that other TCF family members may replace Lef-1 activity, maintaining transcriptional regulation of their target genes (Staal and Clevers, 2000). To address this potential complicating factor we then knocked down β-catenin, a required binding partner of the TCF family of transcription factors. 72-hours after transfection with β-catenin siRNA in HaCaT-Ras cells *FYN* expression levels were not decreased (Figure 18).

A.

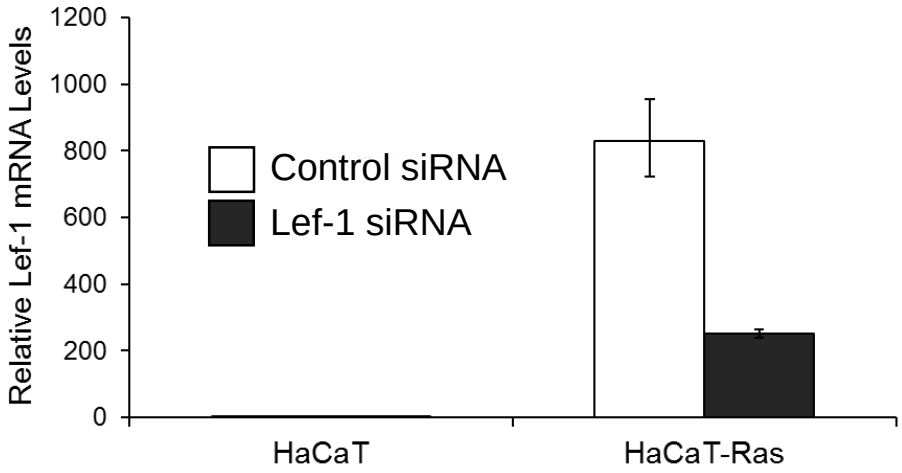

B.

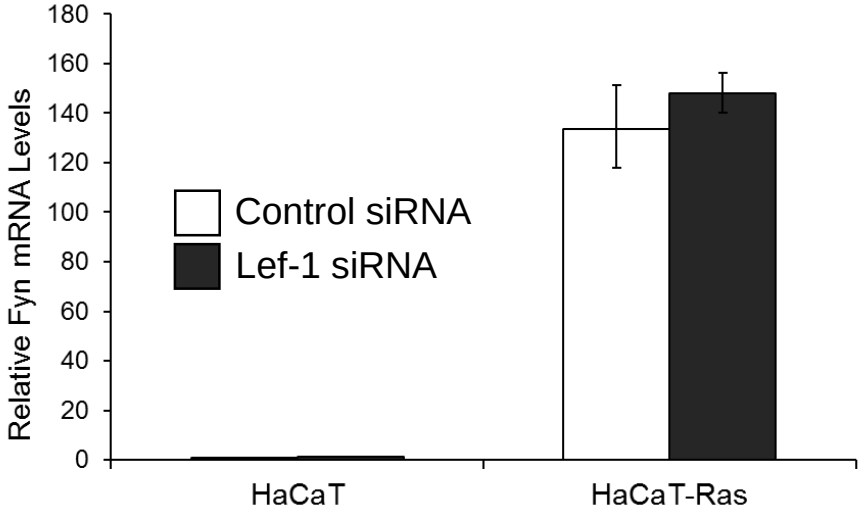

Figure 17: *FYN* Expression is Not Reduced Following Lef-1 Knockdown in HaCaT and HaCaT-Ras Cells

A. HaCaT and HaCaT-Ras cells were transfected with siRNA against Lef-1. 72 hours later total RNA was isolated and analyzed for *LEF1* RNA by RT-qPCR. RNA levels were normalized to *GAPDH*. Data shown is a representative experiment that was performed in duplicate.
B. HaCaT and HaCaT-Ras cells were transfected with siRNA against Lef-1. 72 hours later total RNA was isolated and analyzed for *FYN* RNA by RT-qPCR. RNA levels were normalized to *GAPDH*. Data shown is a representative experiment that was performed in duplicate.

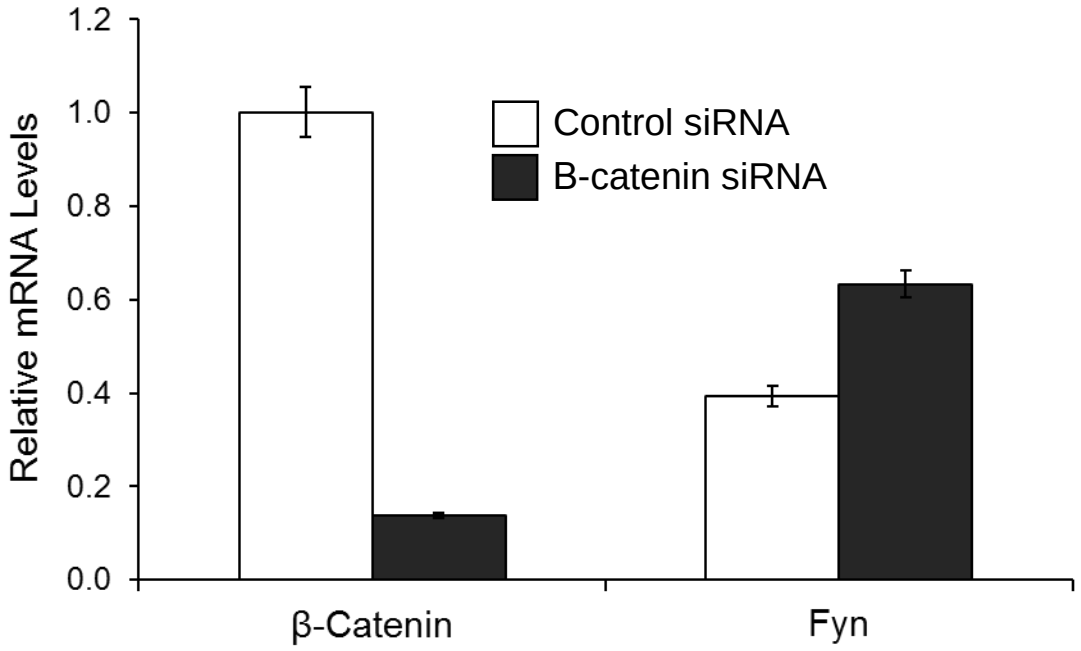

Figure 18: *FYN* Expression is Not Decreased Following β-catenin Knockdown in HaCaT-Ras Cells

HaCaT-Ras cells were transfected with siRNA against β-catenin. 72 hours later total RNA was isolated and analyzed for *βCATENIN* and *FYN* RNA by RT-qPCR. RNA levels were normalized to *GAPDH*. Data shown is a representative experiment that was performed in duplicate.

3.7 Summary

Previous findings concerning Fyn over-expression in BCR-ABL transformed cells indicated that ROS and the transcription factors Sp1 and Egr1 regulated Fyn levels. However, in our system, where increased Ras activity is upstream of Fyn expression, treatment with NAC did not decrease Fyn expression levels (Figure 8). Instead, we identified a region -50 to -100 bases upstream of the transcription start site as critical for Fyn regulation and further identified two bases that, when mutated, significantly reduce Fyn expression (Figures 9b & 10b). Binding analyses studies indicated that the transcription factor Lef-1 was likely regulating this induction of Fyn expression (Figure 16). However, *in vivo* assays such as ChIP and siRNA knockdown did not support our *in vitro* results (Figures 14, 17 & 18).

CHAPTER IV

EFFECT OF DASATINIB ON HACAT AND HACAT-RAS CELL PHENOTYPE

4.1 Abstract

Fyn upregulation has been implicated in cellular transformation and oncogenesis in many tissues (Zhao et al, 2009, Calautti et al, 1995, Tu et al, 2008). Increased Fyn activity in oral SCC cell lines is sufficient to induce a transition from an epithelial to a mesenchymal phenotype, resulting in an increased migratory capacity (Lewin et al, 2010). In the murine epidermis, over-expression of constitutively active Fyn(Y528F) results in downregulation of the tumor suppressors Notch1 and p53, ultimately inducing the formation of keratotic tumors and AKs that progress to SCCs (Zhao et al, 2009). Increased Fyn activity has also been shown to increase cellular proliferation and inhibit apoptosis (Singh et al, 2012, Kim et al, 2010). Additionally, Fyn expression is upregulated in HaCaT cells following the introduction of oncogenic H-Ras, increasing the migratory and invasive capacity of the cells (Yadav and Denning, 2011). Due to Fyn's predicted role as an oncogene, inhibition of Fyn activity may be an effective therapy in the treatment of cSCC.

To inhibit Fyn activity, we treated the HaCaT and HaCaT-Ras cells with Dasatinib, a small molecule tyrosine kinase inhibitor that binds to the ATP-binding site to inhibit SFK, BCR-ABL, EphA2, PDGFR and c-Kit activity (Aguilera and Tsimberidou, 2009). Dasatinib was chosen to inhibit Fyn because it is an orally administered, FDA-approved anti-cancer drug with known pharmacology and side effects. Following Dasatinib treatment we measured cell viability, proliferation, cell cycle distribution, apoptosis and autophagy. Although Dasatinib treatment did cause a reduction in cell viability, it did not alter cell viability in the transformed HaCaT-Ras cells to a greater extent than in the parental HaCaT cells (Figure 23).

4.2 Increased Fyn Protein is Sufficient to Induce the Epithelial to Mesenchymal Transition (EMT)

Previous studies in oral SCC have shown that Fyn activity is sufficient to drive a switch from an epithelial to a mesenchymal morphology, commonly known as the epithelial to mesenchymal transition or EMT (Lewin et al, 2010). Simply put, EMT is a biological process where a polarized epithelial cell assumes a more migratory, mesenchymal phenotype. Although this change has many functions in normal physiological processes such as embryonic development and wound healing, it is also understood to be an important step in the progression of malignancies (Kalluri and Weinberg, 2009b). Using Western blot techniques, we assessed E-cadherin, cytokeratin and vimentin expression, all markers used to asses EMT. HaCaT-Ras cells had decreased protein levels of E-

cadherin and pan-cytokeratin and increased levels of vimentin compared to parental HaCaT cells, which in combination with their small, stellate appearance indicated the HaCaT-Ras cells had undergone EMT (Figures 19 & 20). To test if Fyn over-expression was sufficient to induce EMT in HaCaT cells, we stably introduced active Fyn(I338T) to HaCaT cells (HaCaT-Fyn cells) by retroviral transduction, resulting in a similar level of Fyn expression when compared to the HaCaT-Ras cells. The introduction of active Fyn reduced E-cadherin and cytokeratin levels and increased vimentin expression, indicating that Fyn was sufficient to induce EMT in HaCaT cells (Figure 19).

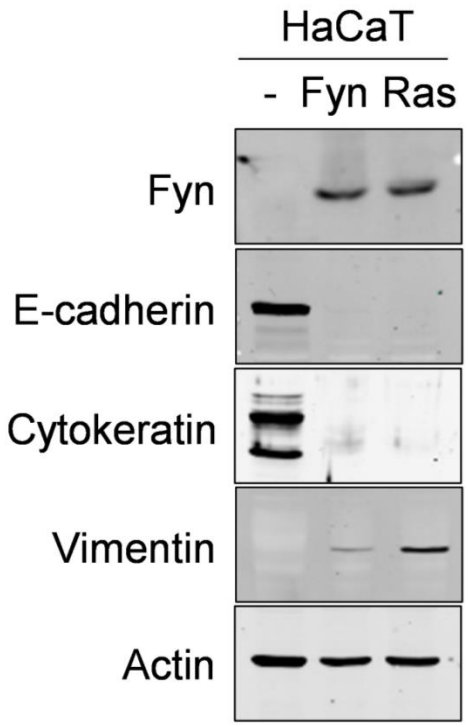

Figure 19. Introduction of Active Ras or Fyn is Sufficient to Induce EMT

Protein levels of Fyn and the EMT markers E-cadherin, pan-cytokeratin and vimentin were measured using a Western blot on lysates from HaCaT, HaCaT-Fyn and HaCaT-Ras cells. β-actin was used as a loading control. Data shown is a representative experiment that was performed in triplicate.

4.3 Dasatinib Treatment Inhibits Fyn and Alters Cell Morphology But Does Not Reverse EMT

Following 24 hours of Dasatinib exposure, HaCaT cells maintained their epithelial phenotype while HaCaT-Ras and HaCaT-Fyn cells underwent a marked change in appearance (Figure 20). HaCaT-Ras and HaCaT-Fyn cells normally grow in a poorly adherent, even distribution in the cell culture plate, but Dasatinib treatment caused both cell types to form tight cell aggregates that frequently detached from the plate. To ensure that Dasatinib treatment was inhibiting Fyn activity we performed a Luminex Milliplex Map 8-Plex Human Src Family Kinase Phosphoprotein assay assessing the activating phosphorylation status of all SFKs. Phosphorylation of the activating tyrosine (Y418) on Fyn, as well as other SFKs, was significantly inhibited by 50-100 nM Dasatinib in HaCaT-Ras cells ($p<0.01$) (Figure 21). Following the change in cellular morphology caused by Dasatinib treatment, we assessed whether EMT was being reversed through SFK inhibition. Using Western blot techniques we again measured E-cadherin, cytokeratin and vimentin expression. Expression of E-cadherin was not restored and vimentin expression was not reduced, suggesting Dasatinib treatment is not sufficient to reverse EMT (Figure 22). To determine the mechanism driving EMT in Ras and Fyn-transformed cells, we used RT-qPCR to measure mRNA levels of three EMT master regulators: Slug, Snail and Twist. Slug was significantly upregulated in HaCaT-Fyn ($p<0.01$) and HaCaT-Ras cells ($p<0.005$). Snail was also significantly upregulated in the HaCaT-Fyn ($p<0.01$) and HaCaT-Ras ($p<0.001$) cells. However, Twist was the most

markedly upregulated, with an over 45-fold induction in both the HaCaT-Fyn ($p<0.005$) and HaCaT-Ras ($p<0.001$) cells (Figure 23). Following 24 hours of 1 μM Dasatinib treatment, expression levels of Twist were not reduced to levels similar to those seen in parental HaCaT cells, again suggesting Dasatinib treatment is not sufficient to reverse EMT (Figure 23).

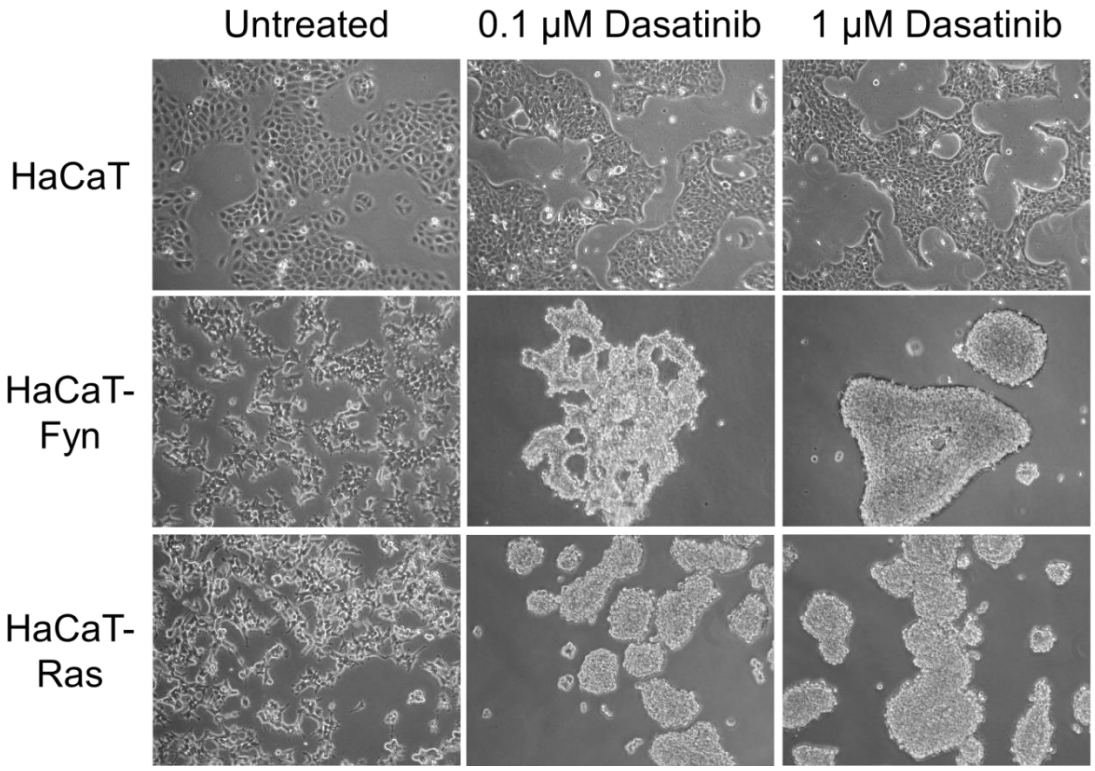

Figure 20. Dasatinib Treatment Results in a Morphology Change in HaCaT-Fyn and HaCaT-Ras Cells But Not HaCaT Cells

Phase-contrast pictures of HaCaT, HaCaT-Fyn and HaCaT-Ras cells untreated or following 24 hours of 0.1 μM or 1.0 μM Dasatinib treatment. HaCaT cells maintain their cobblestone epithelial morphology, while Dasatinib exposed HaCaT-Fyn and HaCaT-Ras cells form aggregates in the culture dish.

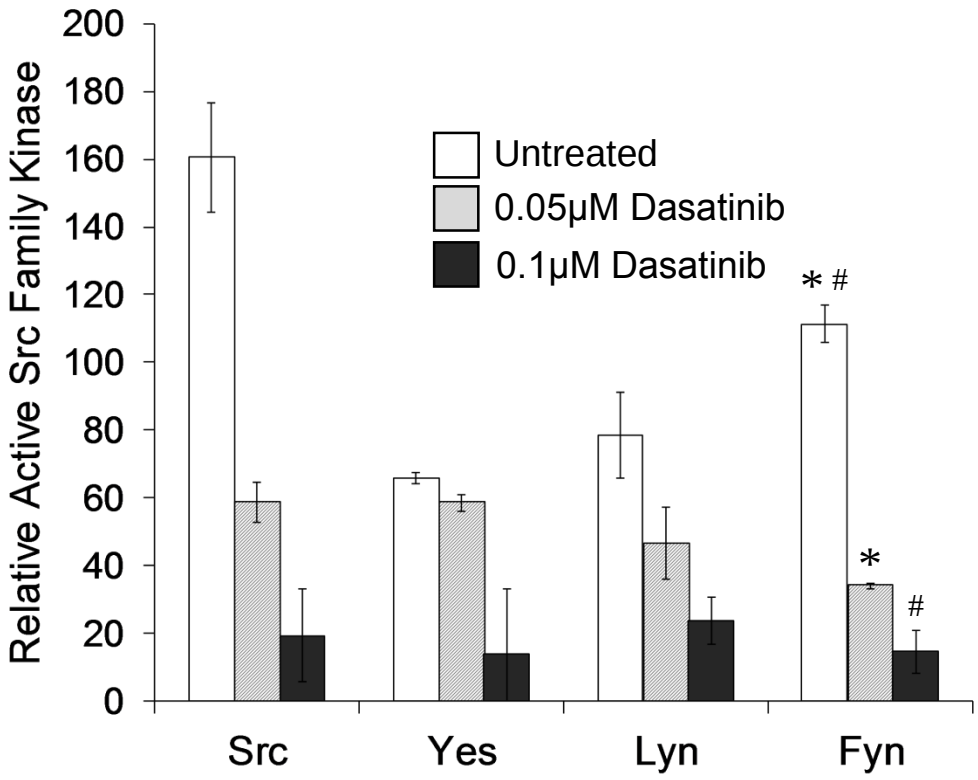

Figure 21. Dasatinib Treatment Inhibits SFK Activity in HaCaT-Ras Cells

Levels of phosphorylation at the SFK activation site (Y418) for all SFKs were assessed using a Milliplex Map 8-Plex Human Src Family Kinase Phosphoprotein kit and a Luminex plate reader. Significant reduction of Fyn activity was induced by 0.05 μM Dasatinib treatment (*$p<0.01$) and 0.1 μM Dasatinib treatment ($^{\#}p<0.01$). Data shown is a representative experiment that was performed in duplicate.

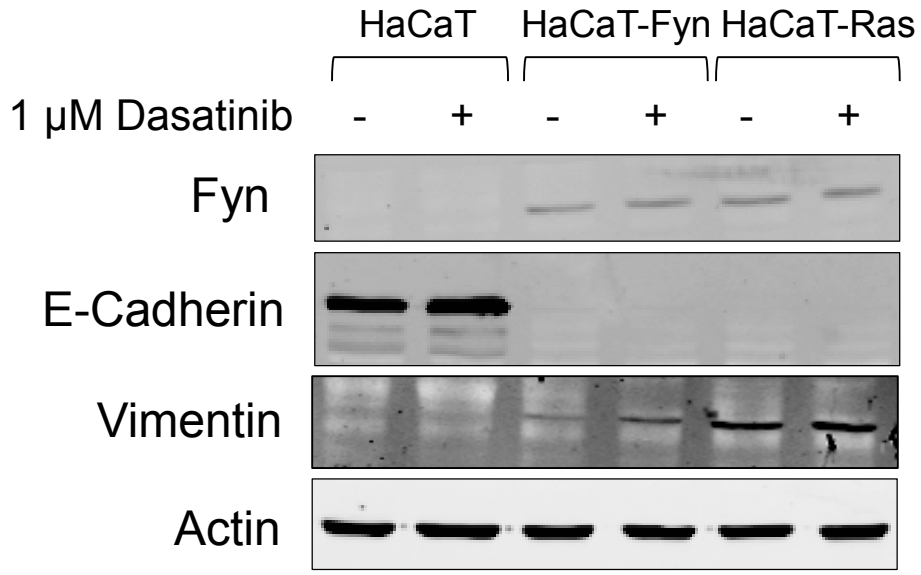

Figure 22. Treatment with Dasatinib for 24 Hours Does Not Reverse EMT

Following treatment with 1 μM Dasatinib for 24 hours, protein levels of Fyn and the EMT markers E-cadherin and vimentin were measured using Western blot techniques on lysates from HaCaT, HaCaT-Fyn and HaCaT-Ras cells. β-actin was used as a loading control. Data shown is a representative experiment that was performed in duplicate.

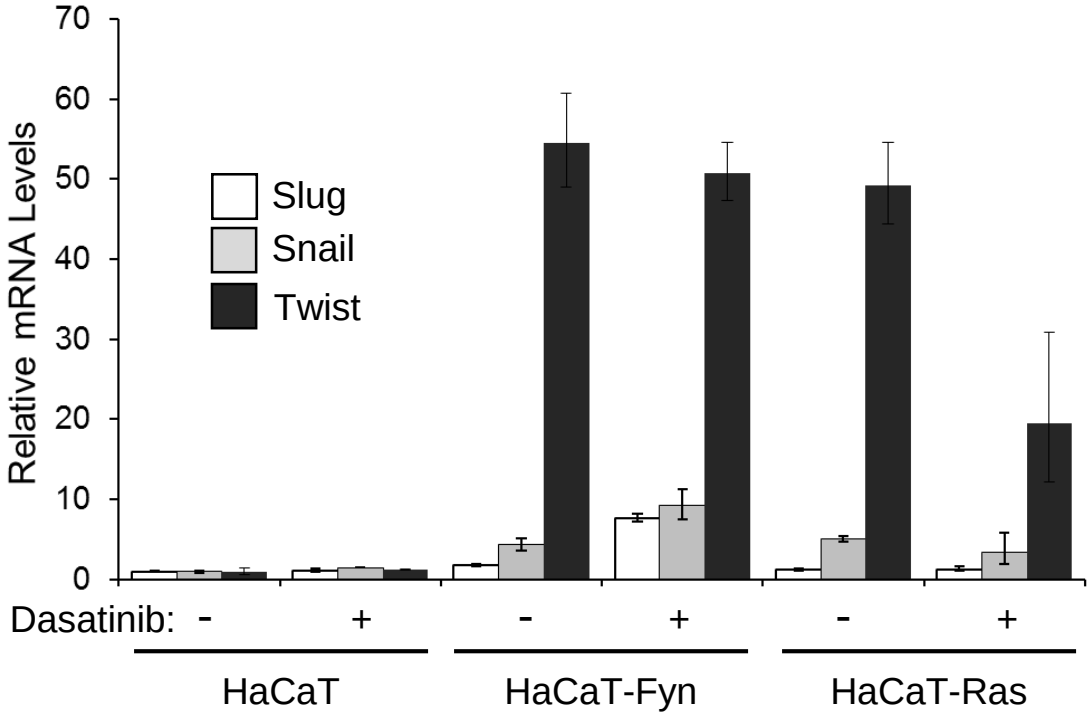

Figure 23: Twist is Upregulated In HaCaT-Fyn and HaCaT-Ras Cells and Dasatinib Treatment Does Not Restore Expression to Levels Seen in HaCaT Cells

Total RNA was isolated from HaCaT, HaCaT-Fyn and HaCaT-Ras cells following no treatment or 24 hours in 1 μM Dasatinib and analyzed for Snail, Slug and Twist RNA by RT-qPCR. RNA levels were normalized to GAPDH. Data shown is a representative experiment that was performed in triplicate.

4.4 Dasatinib Treatment Reduces Cell Viability and Cellular Proliferation to a Similar Extent in HaCaT and HaCaT-Ras Cells

Fyn activity has been linked to increased cellular proliferation and reduced apoptosis (Singh et al, 2012, Kim et al, 2010, Chen et al, 2011). Following Dasatinib treatment and Fyn inhibition, HaCaT-Ras cells undergo a dramatic change in cellular morphology, detaching from the culture dish and forming aggregates that float in the media (Figure 20). It is possible that this change in appearance was due to a decrease in cell viability following Dasatinib treatment. To assess changes in cell viability, we treated the cells with Dasatinib for 24 hours, then stained the attached and floating cells with Trypan Blue or removed the Dasatinib from the culture environment and replated the cells. Similar levels of positive Trypan Blue staining (i.e. apoptotic cells) were seen in the treated and untreated HaCaT and HaCaT-Ras cells, and both cell types grew as usual following replating in Dasatinib-free media, indicating that Dasatinib was not inducing cell death (data not show). We also assessed Dasatinib's ability to decrease cell viability by introducing alamarBlue to our cell culture medium. AlamarBlue is a cell health indicator composed of resazurin, a blue compound that when taken up by a healthy or viable cell is reduced to resorufin, a red compound. Therefore, by measuring fluorescence following incubation with alamarBlue we can directly measure the cell population's ability to proliferate, maintain normal metabolism and survive after Dasatinib treatment. Following 48 hours in 0.1 μM or 1 μM Dasatinib cell viability was comparably reduced in both the HaCaT and HaCaT-Ras cells (Figure 24). Similar results were found

following Dasatinib treatment for 24 and 72 hours (data not shown). We also measured cellular proliferation by quantitating the amount of DNA present in the cell population following Dasatinib treatment, and did not measure a significant reduction in cellular proliferation in either the HaCaT or HaCaT-Ras cells (Figure 25). We also measured cellular proliferation through the incorporation of radioactive ^{3}H-thymidine into DNA strands during S-phase following Dasatinib treatment. Again, we did not find a significant reduction in cellular proliferation following 24 hours in either 0.1 μM or 1 μM Dasatinib (Figure 26). Finally, we assessed cell cycle progression in untreated and Dasatinib treated HaCaT and HaCaT-Ras cells by staining the cells with propidium iodide (PI), a fluorescent intercalating agent that binds to DNA to give a stoichiometric measure of the amount of DNA present in the cell. Therefore, cells in the S phase of the cell cycle will have a greater DNA content than cells in G1 and through this method the different phases of the cell cycle can be identified. Treatment with 0.1 or 1 μM Dasatinib for 24 hours slightly increased the number of HaCaT cells in the sub-G0 phase (apoptotic cells), but otherwise did not alter cell cycle distribution in either the HaCaT or HaCaT-Ras cells (Figure 27).

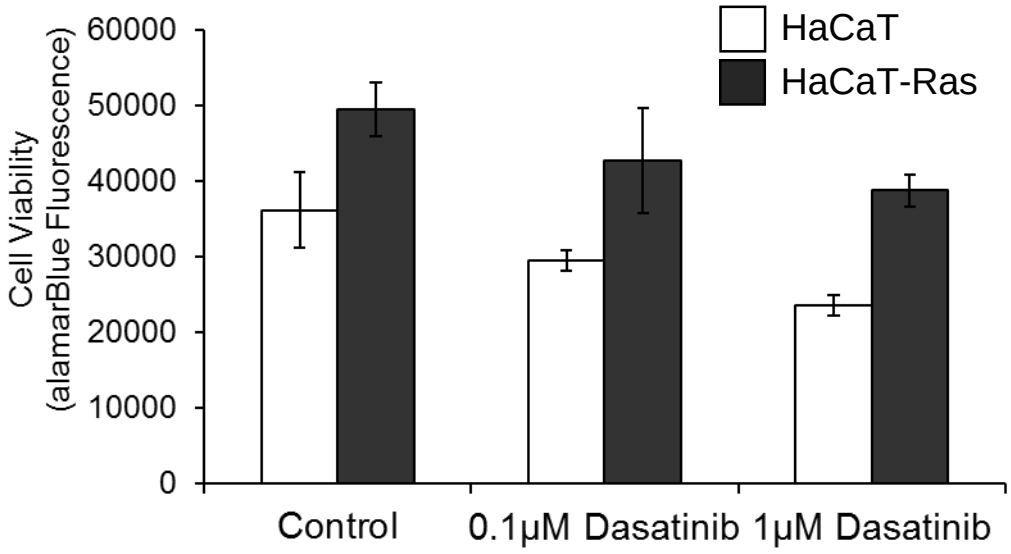

Figure 24: Treatment with Dasatinib Reduced Cellular Viability to a Similar Extent in both HaCaT and HaCaT-Ras Cells

Following treatment with either 0.1 μM or 1 μM Dasatinib for 48 hours alamarBlue was added to the cell culture medium and allowed to incubate for 2 hours. Fluorescence was then measured to determine the amount of alamarBlue that had been metabolized by viable cells. Data shown is a representative experiment that was performed in triplicate.

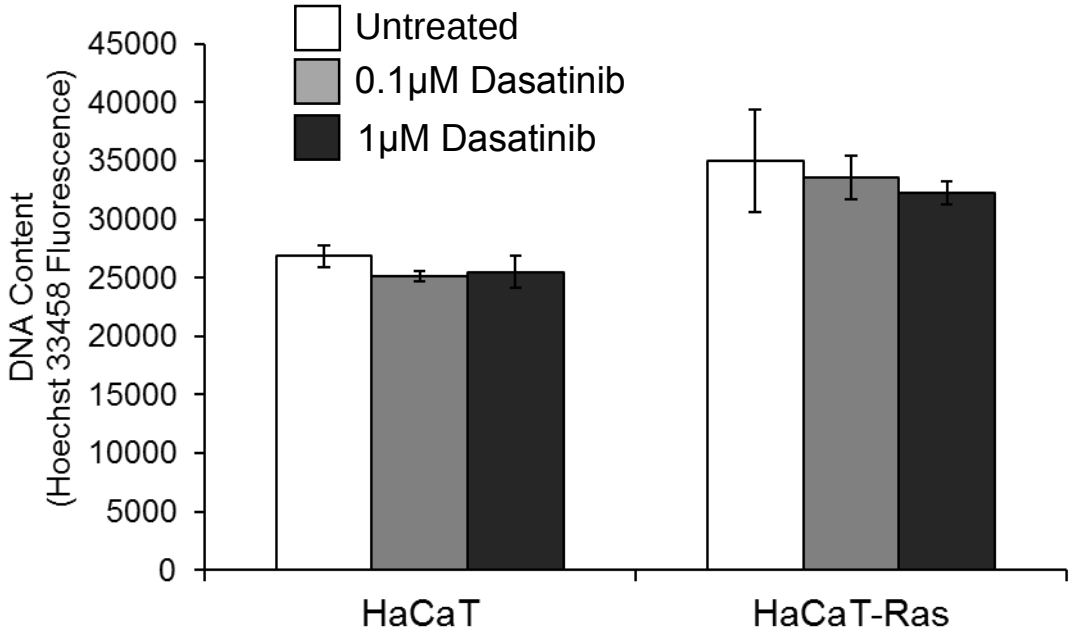

Figure 25: Treatment with Dasatinib Did Not Reduce Cellular Proliferation in Either HaCaT or HaCaT-Ras Cells

Following treatment with either 0.1 μM or 1 μM Dasatinib for 24 hours DNA was stained with the fluorescent dye Hoechst 33458 and quantitated. Data shown is a representative experiment that was performed in triplicate.

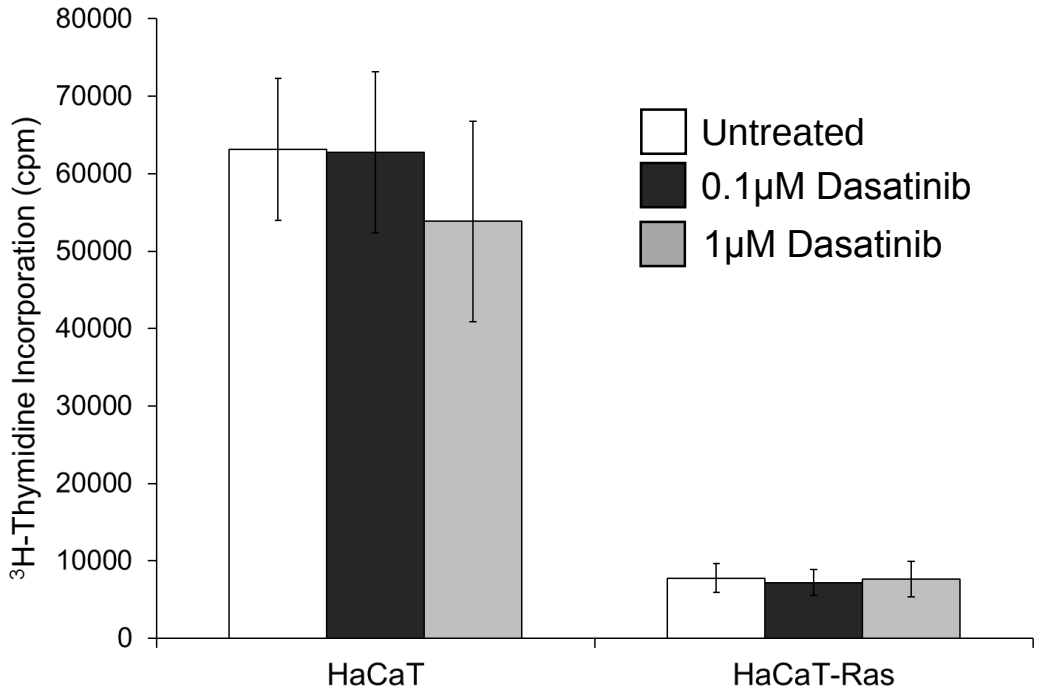

Figure 26: Treatment with Dasatinib Did Not Reduce Cellular Proliferation in Either HaCaT or HaCaT-Ras Cells

Following treatment with either 0.1 μM or 1 μM Dasatinib and concurrent incubation with ^{3}H-thymidine for 24 hours, incorporation of radioactive thymidine into the DNA was measured. Data is expressed as counts per minute (cpm). Data shown is a representative experiment that was performed in triplicate.

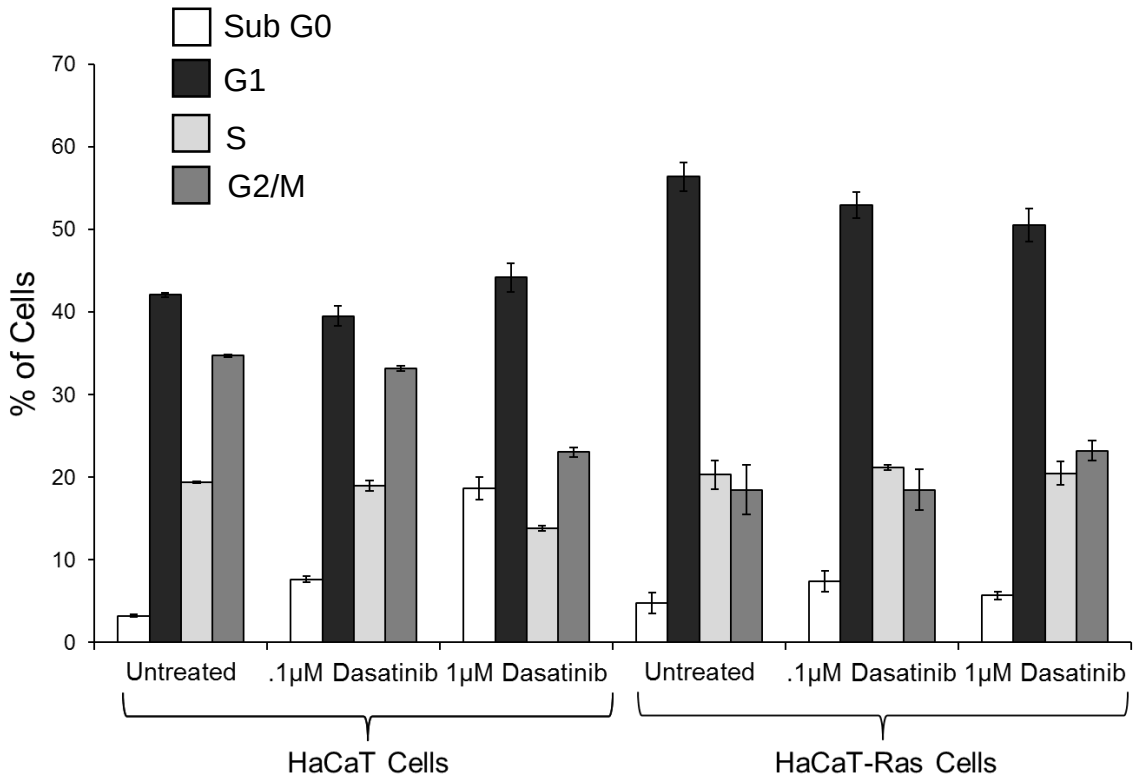

Figure 27: Treatment with Dasatinib Did Not Alter Cell Cycle Distribution in HaCaT-Ras Cells

Following treatment with either 0.1 μM or 1 μM Dasatinib for 24 hours DNA was stained with propidium iodide and quantitated using flow cytometry. Data shown is a representative experiment that was performed in triplicate.

4.5 Dasatinib Treatment Induces Apoptosis to a Similar Extent in HaCaT and HaCaT-Ras Cells and Does Not Induce Autophagy

Increased Fyn activity provides a protective effect against apoptosis and cell death through increased phosphorylation of Sam68 and expression of HnRNPA2B1 (Chen et al, 2011). Inhibition of Fyn, either directly using siRNA or by Dasatinib treatment, has also been shown to induce autophagy in T-cells, chronic lymphocytic leukemia, ovarian cancer and gliomas (Harr et al, 2010, Krause and Hallek, 2011, Le et al, 2010, Milano et al, 2009). Based on these findings we assessed levels of apoptosis and autophagy in HaCaT and HaCaT-Ras cells following Dasatinib treatment. To measure apoptosis we stained the cells with Annexin V-FITC and propidium iodide (Figure 28). When cells are in early apoptosis they begin to expose phosphatidylserine on the external cytoplasmic membrane. Annexin V-FITC binds to the external phosphatidylserine and emits a green fluorescence. When cells are in late apoptosis or are necrotic, the integrity of the cytoplasmic membrane is decreased, allowing the entry of PI, which binds to the DNA and emits a red fluorescence. Through this staining technique populations of early and late apoptotic cells can be detected and measured. Following 24 hours in 0.1 μM or 1 μM Dasatinib apoptosis was induced in both the HaCaT and HaCaT-Ras cells (Figure 28). However, there was no selective effect in the transformed HaCaT-Ras cells – both cell lines induced apoptosis at comparable levels (Figure 28). Similar to apoptosis, autophagy is an alternative process of cell death involving targeted degradation of necessary cellular components (Glick, Barth and Macleod, 2010). Acridine orange is a green fluorescent

molecule that accumulates in acidic organelles, where it becomes protonated and emits a red fluorescence. Because autophagy involves the degradation of cellular components through the lysosomal pathway, large amounts of acridine orange become trapped in the acidified lysosome and can be detected by flow cytometry. Dasatinib treatment did not induce autophagy in either the HaCaT or HaCaT-Ras cells following 24 hours of exposure (Figure 29).

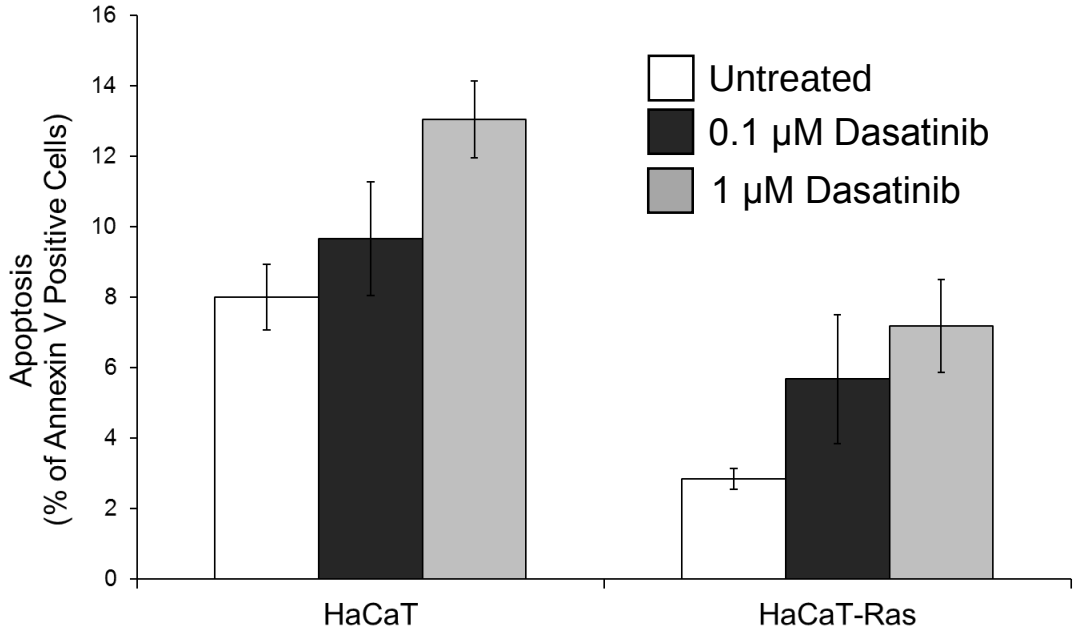

Figure 28: Treatment with Dasatinib Induced Apoptosis to a Similar Extent in both HaCaT and HaCaT-Ras Cells

Following treatment with either 0.1 μM or 1 μM Dasatinib for 24 hours cells were stained with Annexin V and propidium iodide. Fluorescence was measured on a flow cytometer. Data shown is a representative experiment that was performed in triplicate.

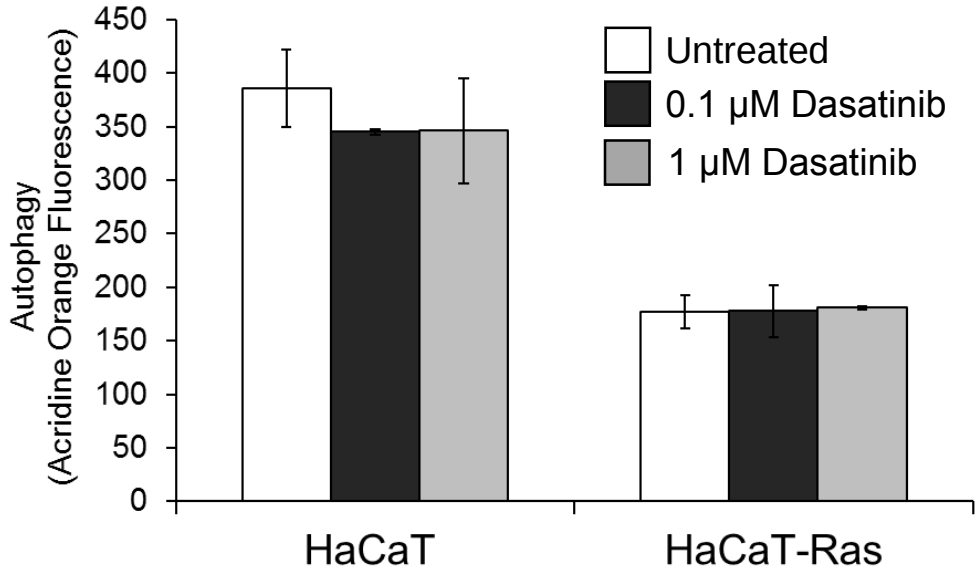

Figure 29: Treatment with Dasatinib Did Not Induce Autophagy in Either HaCaT or HaCaT-Ras Cells

Following treatment with either 0.1 μM or 1 μM Dasatinib for 24 hours Acridine Orange was added to the cell culture plate and allowed to incubate for 20 minutes. Fluorescence was measured on a flow cytometer. Data shown is a representative experiment that was performed in triplicate.

4.6 Dasatinib Treatment Increases Levels of Apoptosis in HaCaT Cells Following UVB Exposure

Dasatinib treatment alone increased levels of apoptotic HaCaT cells less than 6% (Figure 28). These results were surprising, as Fyn activity is known to protect against apoptosis (Chen et al, 2011). One would therefore expect inhibition of Fyn and the SFK family to significantly increase the amount of cell death present in the HaCaT and HaCaT-Ras cells. We postulated that this effect may only be seen with the addition of another stressor, for example a genotoxic insult that is known to result in apoptosis in keratinocytes, UVB. To accomplish this, we exposed HaCaT cells to 10 mJ/cm^2 UVB and followed immediately with 1 μM Dasatinib treatment. After 24 hours we assessed levels of early and late apoptotic cells using an Annexin-V/propidium iodide staining assay. As seen previously, Dasatinib treatment alone resulted in a slight increase in apoptosis (Figure 28 & 30). UVB exposure induced higher levels of total apoptosis, but Dasatinib treatment following UVB exposure resulted in significantly higher levels of apoptotic cells ($p<0.01$) (Figure 30). These results suggest that Dasatinib has an additive effect, increasing the likelihood of a cell undergoing apoptosis following UVB exposure.

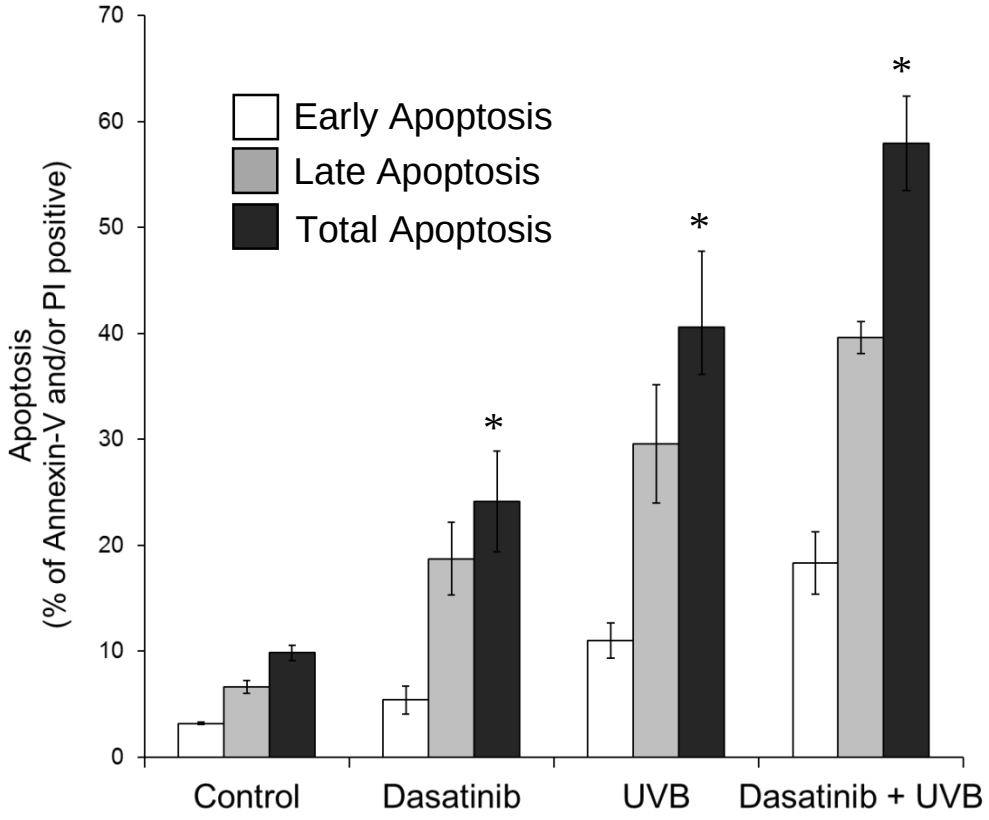

Figure 30: Treatment with Dasatinib Following UVB Exposure Resulted in Greater Levels of Apoptosis Then Either Treatment Alone

Following exposure to 10mJ/cm^2 UVB the cells were treated with 1 μM Dasatinib. After 24 hours the cells were stained with Annexin V and propidium iodide. Fluorescence was measured on a flow cytometer. Levels of total apoptosis were significantly higher in the Dasatinib + UVB treated group than in the Dasatinib or UVB-alone groups (*$p<0.01$). Data shown is a representative experiment that was performed in duplicate.

4.7 Summary

Upregulation of Fyn expression, either directly or indirectly through the Ras oncogene, induces EMT in HaCaT cells (Figure 19). Exposure of the HaCaT-Ras and HaCaT-Fyn cells to the SFK inhibitor Dasatinib drives a marked change in cell morphology, but does not reverse EMT, alter cell viability, proliferation or cell cycle distribution, or induce apoptosis or autophagy to a greater extent than that seen in the parental HaCaT cells (Figures 20, 22, 23, 24, 25, 26, 27, 28 & 29). However, Dasatinib treatment immediately after UVB exposure results in greater cell death than either Dasatinib treatment or UVB exposure alone, suggesting an additive effect (Figure 30).

CHAPTER V

DASATINIB INDUCES F-ACTIN AND ADHERENS JUNCTION FORMATION IN HACAT-RAS CELLS

5.1 Abstract

Fyn acts as an oncogene in murine epidermis and has been associated with cell-cell adhesion turnover and the induction of a migratory phenotype. Inhibition of Fyn activity in HaCaT-Fyn and HaCaT-Ras cells, using either siRNA or the therapeutic SFK inhibitor Dasatinib, increased cell-cell adhesion through a rapid increase in the cortical F-actin cytoskeleton and reduced cellular migration (Figures 31, 32, 34, 36 & 38). In Dasatinib-treated HaCaT-Ras cells, F-actin colocalized with adherens junction proteins, suggesting that stable adherens junctions were mediating the increase in cell-cell adhesion (Figure 40). Inhibition of the Rho effector kinase ROCK blocked Dasatinib-induced F-actin and cell-cell adhesion, implicating relief of Rho GTPase inhibition as a mechanism of Dasatinib-induced cell-cell adhesion (Figure 41). F-actin polymerization was a key initiator of cell-cell adhesion, as Dasatinib-induced cell-cell adhesion could be blocked by Cytochalasin D, an inhibitor of actin polymerization (Figure 44). Conversely, inhibiting cell-cell adhesion with low Ca^{2+} media did not block Dasatinib-induced F-actin polymerization (Figure 45). Together these results identify the promotion of actin-based

cell-cell adhesion as a newly described mechanism of action for Dasatinib, and suggest that Fyn inhibition may be an effective therapeutic approach in treating cSCC.

5.2 Dasatinib Treatment Increases Cell-Cell Adhesion in HaCaT-Ras Cells and Inhibits Migration

Because Fyn is oncogenic in keratinocytes (Zhao et al, 2009, Li et al, 2007) and its activity is sufficient to induce EMT, we evaluated the effects of the clinical SFK inhibitor Dasatinib on HaCaT, HaCaT-Ras and HaCaT-Fyn cells. HaCaT-Ras and HaCaT-Fyn cells normally grow in a poorly adherent, even distribution in the cell culture plate, but Dasatinib caused both cell types to form tight cell aggregates that frequently detached from the plate (Figure 20). The detachment was pronounced in areas of confluency that have extensive cell-cell contacts. Using a quantitative cell-cell adhesion assay, we determined that 0.1 and 1 μM Dasatinib exposure for 24 hours decreased the percent of single cells in HaCaT-Fyn and HaCaT-Ras cells by over 6-fold, indicating Dasatinib treatment increased cell-cell adhesion (Figure 31). Furthermore, Fyn inhibition using siRNA was sufficient to induce a 6-fold increase in cell-cell adhesion 72 hours following transfection in both HaCaT-Ras and HaCaT-Fyn cells, but did not increase cell-cell adhesion in HaCaT cells (Figure 32). Fyn siRNA also induced cell-cell adhesion in MDA-MB-231 cells, a human breast cancer cell line with elevated Fyn (Figure 33) (Yadav and Denning, 2011). Consistent with their EMT phenotype, both HaCaT-Fyn and HaCaT-Ras cells had enhanced migration compared to HaCaT cells, and Dasatinib

treatment significantly inhibited the migration of HaCaT-Fyn and HaCaT-Ras cells ($p<0.001$) (Figure 34).

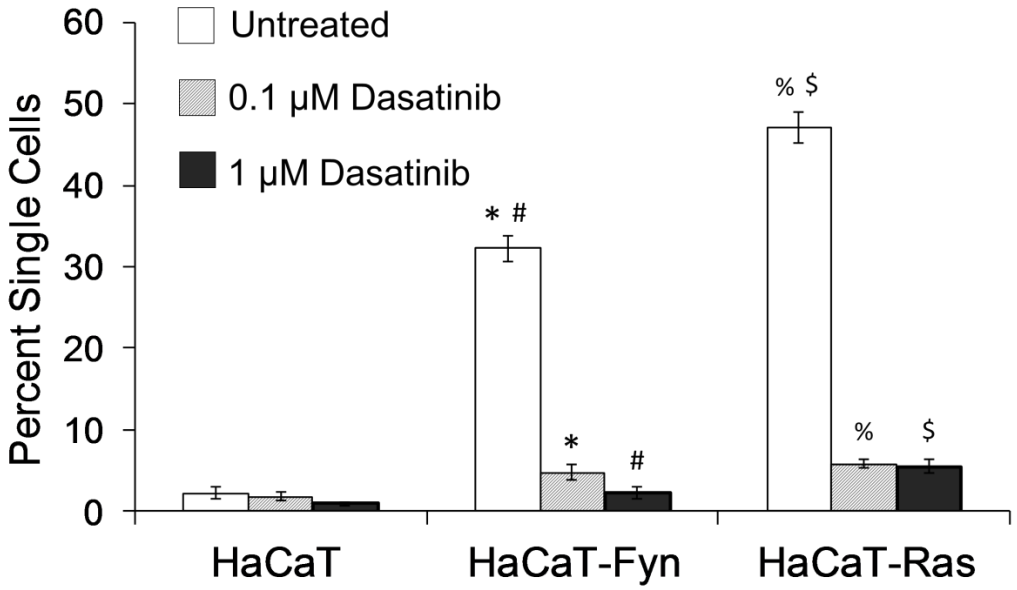

Figure 31: Dasatinib Treatment Induces Cell-Cell Adhesion in HaCaT-Fyn and HaCaT-Ras Cells

HaCaT, HaCaT-Fyn and HaCaT-Ras cell-cell adhesion was measured in untreated cells or following 24 hours of 0.1 µM or 1.0 µM Dasatinib treatment using a dispase assay. Note that a low percentage of single cells corresponds to high cell-cell adhesion. Cell-cell adhesion was significantly increased in the HaCaT-Fyn and HaCaT-Ras cells following 0.1 µM Dasatinib treatment ($^{*,\%}p<0.001$) and 1.0 µM Dasatinib ($^{\#,\$}p<0.001$) treatment. Data shown is a representative experiment that was performed in triplicate.

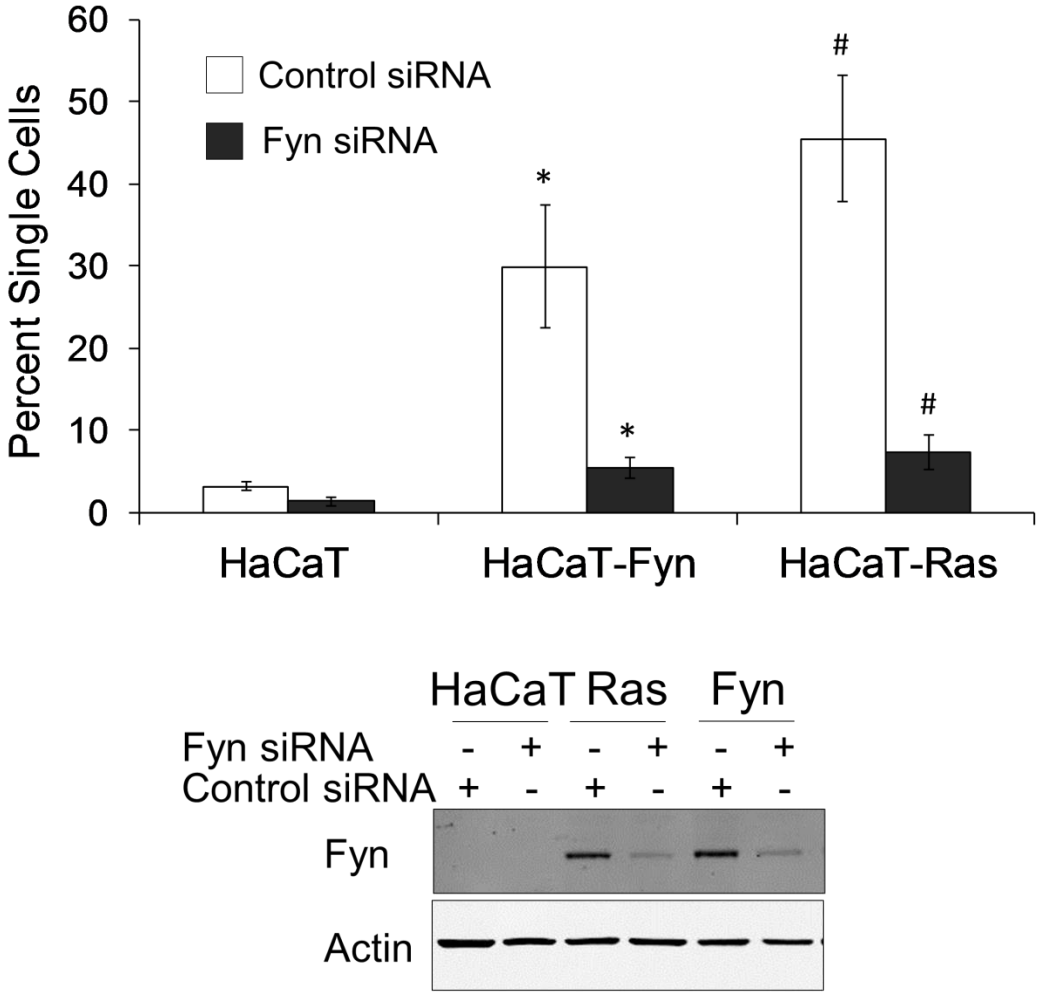

Figure 32: Fyn Knockdown Induces Cell-Cell Adhesion in HaCaT-Fyn and HaCaT-Ras Cells

Cell-cell adhesion was measured 72 hours after transfection of HaCaT, HaCaT-Fyn and HaCaT-Ras cells with control or Fyn siRNA. The Western blot verifying Fyn knockdown is shown below. Cell-cell adhesion was significantly increased in the HaCaT-Fyn cells (*$p<0.01$) and the HaCaT-Ras cells ($^{\#}p<0.001$) following Fyn knockdown. Data shown is a representative experiment that was performed in duplicate.

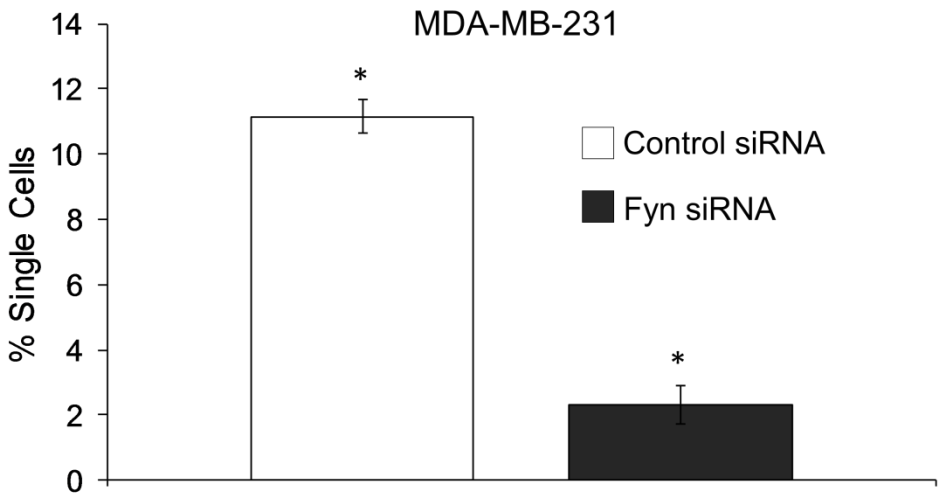

Figure 33: Fyn Knockdown Induces Cell-Cell Adhesion in MDA-MB-231 Cells

Cell-cell adhesion was measured 72 hours after transfection with Fyn siRNA. Cell-cell adhesion was significantly increased in the MDA-MB231 cells (*$p<0.05$) following Fyn knockdown. Data shown is a representative experiment that was performed in duplicate.

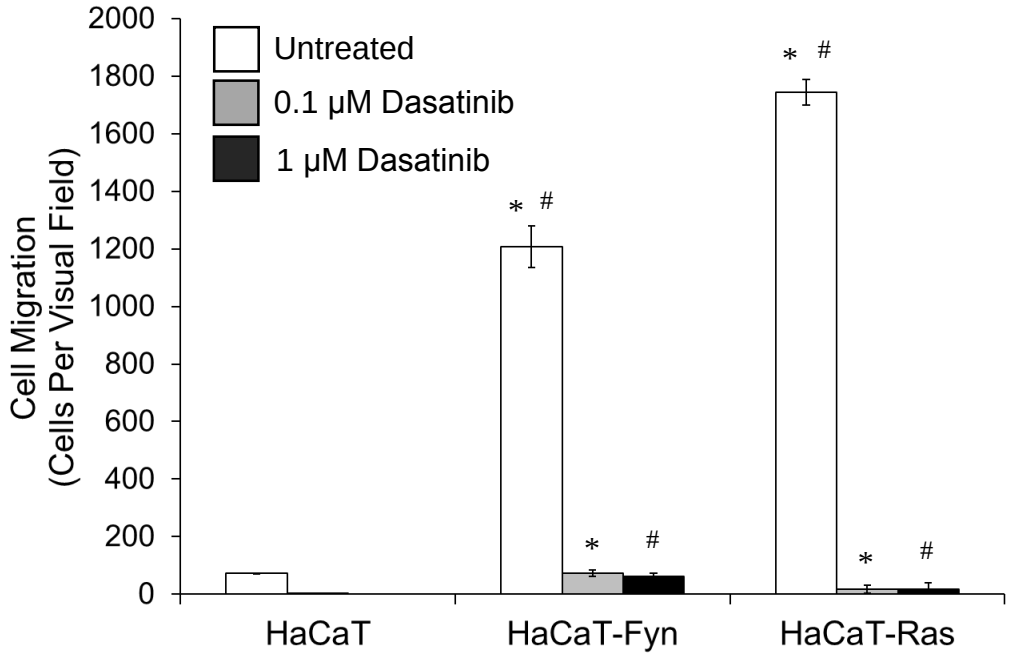

Figure 34: Dasatinib Treatment Inhibits Migration in HaCaT-Fyn and HaCaT-Ras Cells

HaCaT, HaCaT-Fyn and HaCaT-Ras cells were untreated or treated with 0.1 μM or 1.0 μM Dasatinib for 24 hours. Note migration in the HaCaT-Fyn and HaCaT-Ras cells was significantly inhibited by 0.1 μM Dasatinib treatment (*$p<0.001$) and 1.0 μM Dasatinib treatment ($^{\#}p<0.001$). Data shown is a representative experiment that was performed in duplicate.

5.3 Dasatinib Treatment and Fyn Inhibition Induces the Formation of F-actin

Dasatinib treatment upregulated cell-cell adhesion and this change appeared to be stable for as long as the cells were cultured in the drug (Figure 41). Keratinocytes have two main junctions responsible for maintaining cell-cell adhesion, the desmosome and the adherens junction. Because Dasatinib did not restore pan-cytokeratin expression (Figure 35), we concluded that the desmosome was most likely not mediating the Dasatinib-induced change in cell-cell adhesion. To assess whether changes in cell-cell adhesion following Dasatinib exposure were occurring through the actin-based adherens junction, we stained for polymerized F-actin using Rhodamine-phalloidin. Following treatment with 1 μM Dasatinib, the HaCaT-Ras cells rapidly increased levels of F-actin from 5 minutes to 1 hour, and F-actin levels remained elevated approximately 10-fold at 24 hours (Figure 36). We also biochemically fractionated free G-actin and polymerized F-actin and quantified them by Western blotting. Dasatinib increased the F-actin/G-actin ratio in HaCaT-Ras cells, while total actin remained unchanged, and Dasatinib did not alter the F-actin/G-actin ratio in HaCaT cells (Figure 37). Because Dasatinib can inhibit multiple kinases, the induction of F-actin we observed may not be due solely to inhibition of Fyn. Therefore we used Fyn siRNA to reduce Fyn levels and test whether direct Fyn inhibition is sufficient to induce F-actin formation. Fyn knockdown significantly increased F-actin levels in HaCaT-Ras cells ($p<0.001$) (Figure 38) and MDA-MB-231

cells ($p<0.01$) (Figure 43) (Yadav and Denning, 2011). Thus, inhibition of Fyn is sufficient to increase F-actin levels.

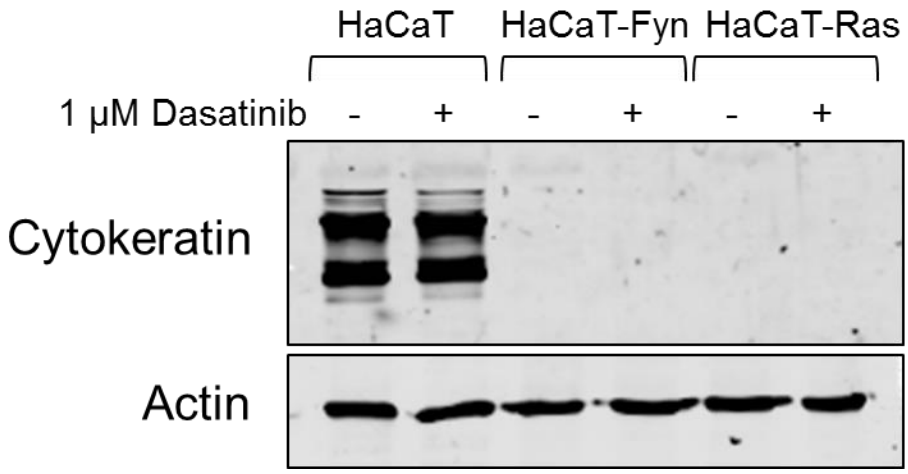

Figure 35: Dasatinib Treatment Does Not Restore Cytokeratin Expression in HaCaT-Fyn or HaCaT-Ras Cells

Following treatment with 1 μM Dasatinib for 24 hours, protein levels of pan-cytokeratin were measured using Western blot techniques on lysates from HaCaT, HaCaT-Fyn and HaCaT-Ras cells. β-actin was used as a loading control. Data shown is a representative experiment that was performed in duplicate.

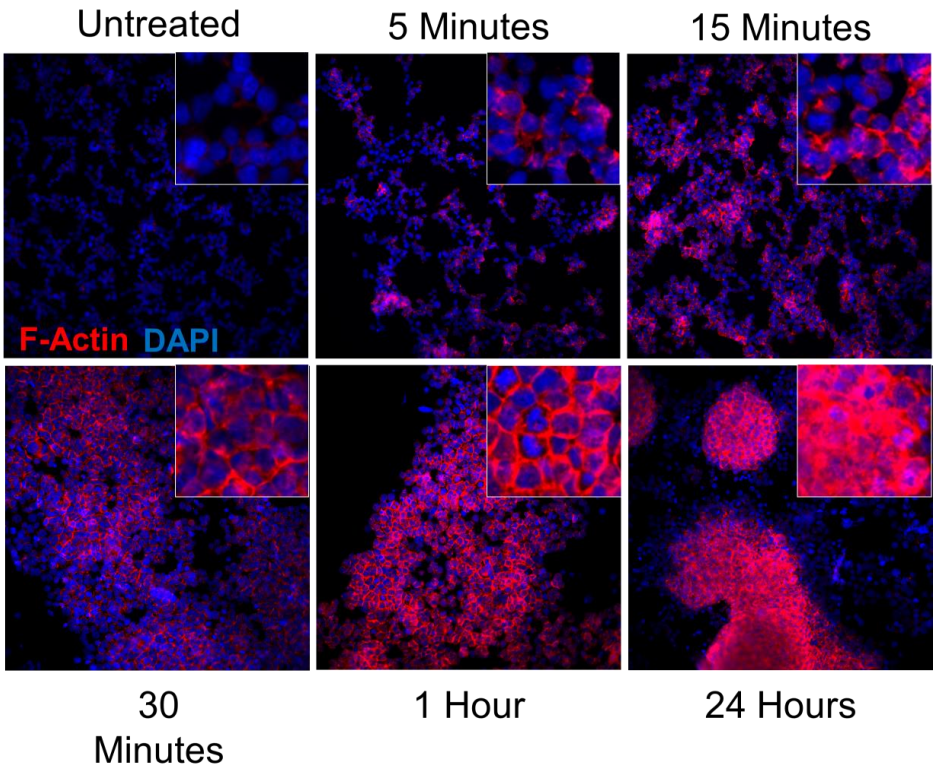

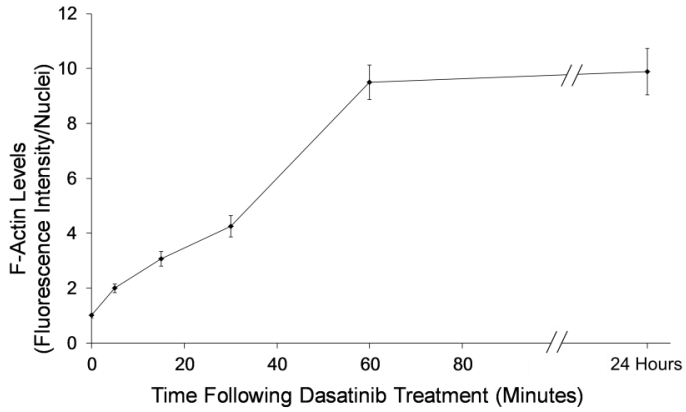

Figure 36: Dasatinib Treatment Increases F-actin Levels in HaCaT-Ras Cells

HaCaT-Ras cells were treated with 1.0 µM Dasatinib for the indicated times and then stained w ith Rhodamine-phalloidin and DAPI. The insert in the upper right of each picture shows higher magnification. Quantitation of Rhodamine-phalloidin staining normalized to the number of DAPI nuclei is shown in the graph. Data shown is a representative experiment that was performed in triplicate.

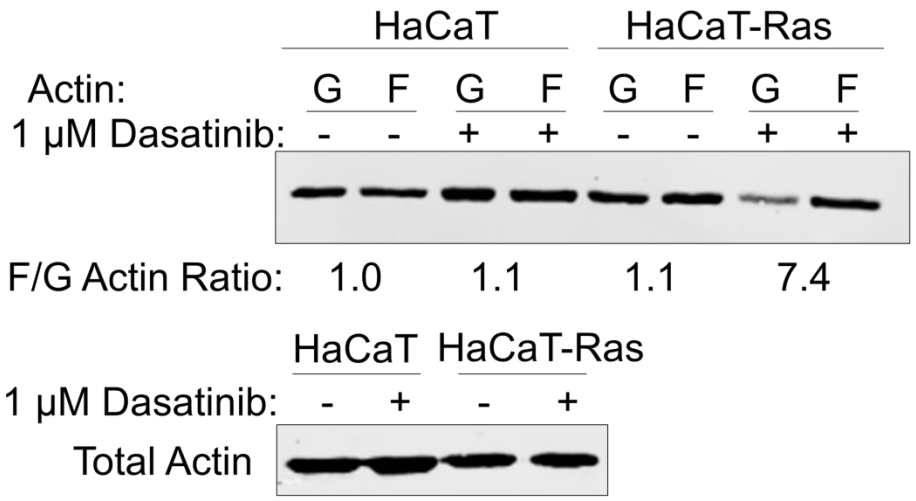

Figure 37: Dasatinib Treatment Increases the F-actin Fraction in HaCaT-Ras Cells

HaCaT and HaCaT-Ras cells were treated with or without 1.0 µM Dasatinib for 30 minutes and fractionated into soluble (G-actin) and insoluble (F-actin) fractions. Shown is a Western blot for F-actin, G-actin and total actin. Data shown is a representative experiment that was performed in duplicate.

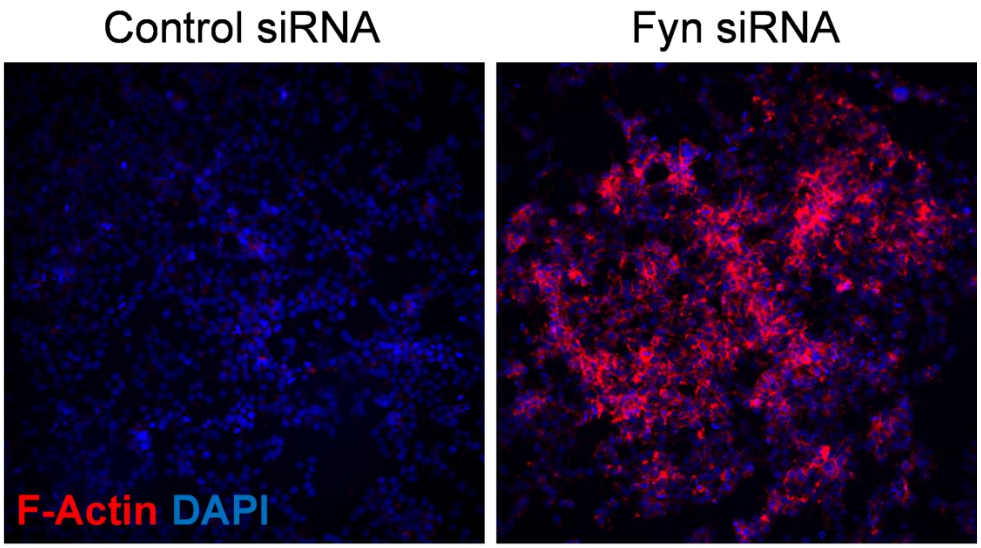

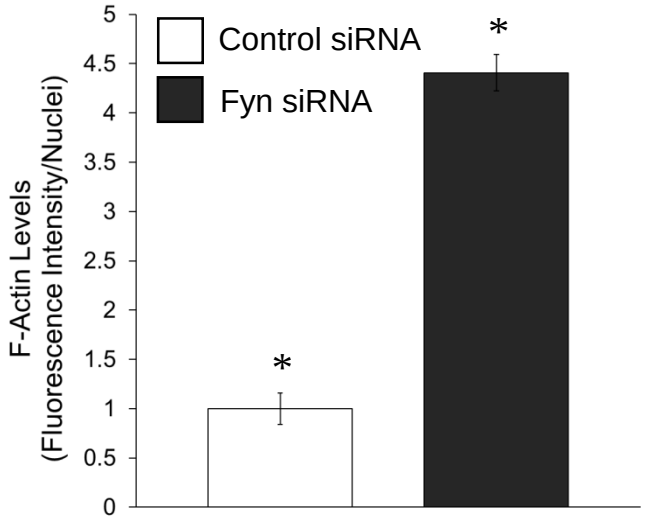

Figure 38: Fyn Knockdown Increases F-actin in HaCaT-Ras Cells

HaCaT-Ras cells were transfected with control or Fyn siRNA and stained with Rhodamine-phalloidin and DAPI after 72 hours. Quantitation of Rhodamine-phalloidin staining normalized to the number of DAPI nuclei indicates F-actin is significantly increased following Fyn knockdown (*$p<0.001$). Data shown is a representative experiment that was performed in triplicate.

5.4 Dasatinib Treatment Induces the Formation of Stable Adherens Junctions

To determine if increased F-actin colocalized with the cytoskeletal linker catenins found in the adherens junction, we performed immunofluorescent staining for F-actin and α-catenin, β-catenin or p120catenin (Figure 39). Prior to Dasatinib exposure, α-catenin, β-catenin and p120catenin were diffusely localized in HaCaT-Ras cells (Figure 40). However, treatment with 1 μM Dasatinib for one hour resulted in translocation of these catenins to the plasma membrane, where α-catenin, β-catenin and p120catenin colocalized with F-actin (Figures 39 & 40, data not shown for α-catenin and β-catenin). These results indicate that Dasatinib treatment was increasing cell-cell adhesion by inducing the formation of stable adherens junctions.

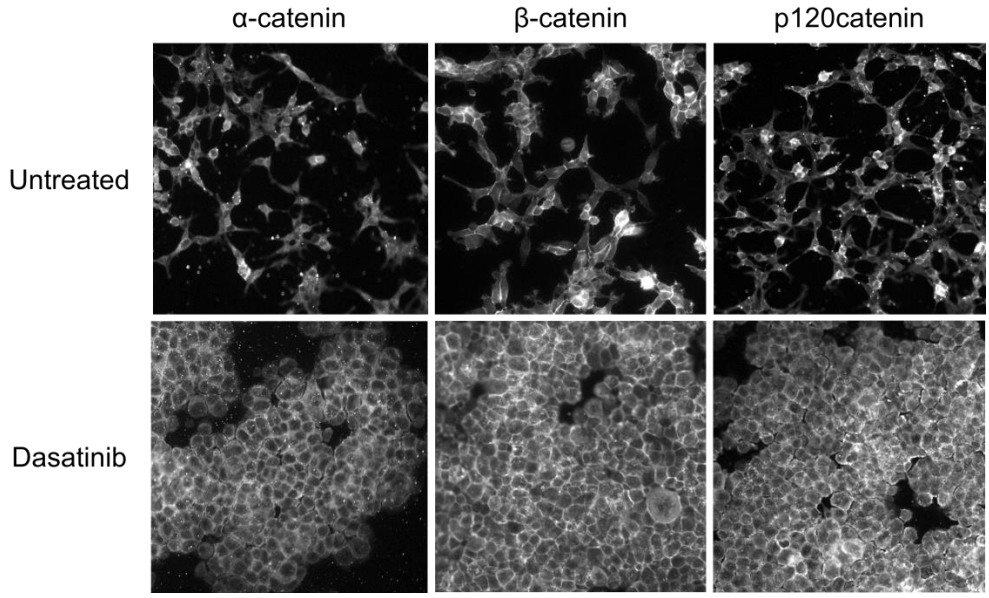

Figure 39: Dasatinib Treatment Results in Localization of Adherens Junction Components to the Cell Membrane

HaCaT-Ras cells remained untreated or were treated with 1 μM Dasatinib for 30 minutes. Shown is immunofluorescent staining for three components of the adherens junction, α-catenin, β-catenin and p120catenin. Data shown is a representative experiment that was performed in triplicate.

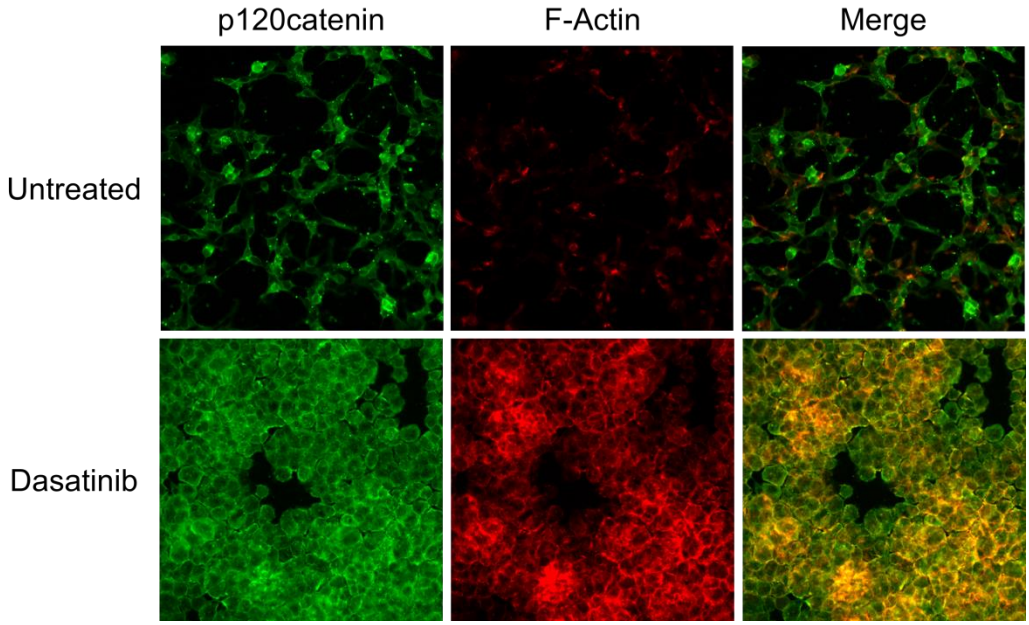

Figure 40: Dasatinib Treatment Results in the Formation of Stable Adherens Junctions in HaCaT-Ras Cells

Staining for p120catenin and F-actin (stained with Rhodamine-phalloidin) in HaCaT-Ras cells following 30 minutes of 1 μM Dasatinib exposure is shown. Note that Dasatinib induces colocalization between p120catenin and the cortical F-actin cytoskeleton. Data shown is a representative experiment that was performed in triplicate.

5.5 Fyn Inhibition Upregulates F-actin By Release of Rho Inhibition

The Rho family of GTPases regulates the stability of the actin cytoskeleton, with Rho activity increasing levels of actin stress fibers (Menke and Giehl, 2012, Kaibuchi, Kuroda and Amano, 1999). Since Dasatinib rapidly induced F-actin levels in HaCaT-Ras cells, we tested if Dasatinib-induced F-actin was dependent on Rho signaling. Pretreatment of HaCaT-Ras cells with 20 μM Y27632, an inhibitor of the Rho effector ROCK (also known as Rho-associated protein kinase), blocked Dasatinib's ability to upregulate F-actin (Figure 41). Similarly, pretreatment of HaCaT-Fyn cells and MDA-MB-231 cells with 20 μM Y27632 also blocked Dasatinib's induction of F-actin (Figures 42 & 43). Treatment of HaCaT cells with Dasatinib did not increase F-actin levels and Y27632 exposure only slightly decreased levels of F-actin (Figure 44). These results suggest that Fyn activity inhibits Rho function and Dasatinib releases this inhibition, inducing upregulation of the F-actin cytoskeleton.

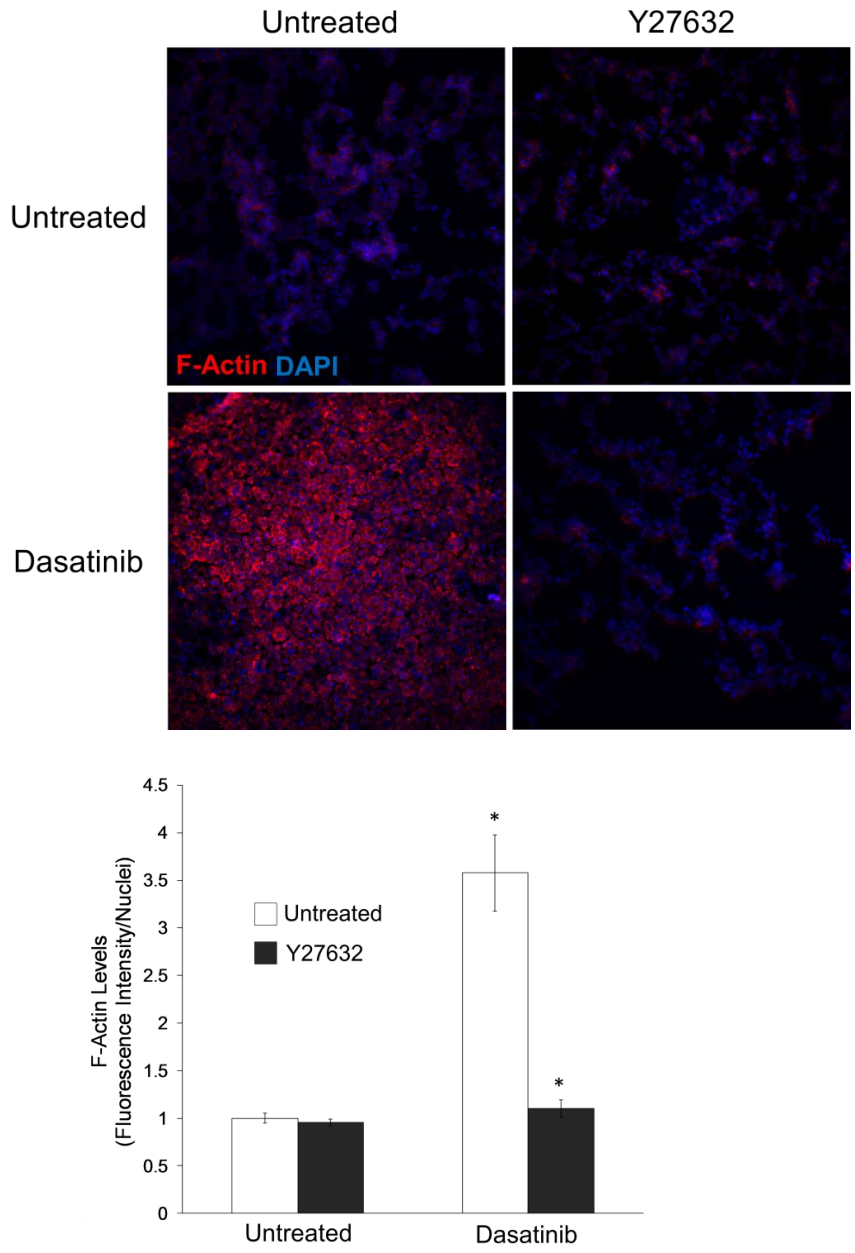

Figure 41: Co-Treatment with a ROCK Inhibitor Blocks Dasatinib-Induced F-actin in HaCaT-Ras Cells

HaCaT-Ras cells were pre-treated with 20 μM Y27632, an inhibitor of ROCK, for 20 minutes, followed by cotreatment with 1 μM Dasatinib for 30 minutes. Staining for F-actin using Rhodamine-phalloidin indicated that Y27632 significantly inhibited (*$p<0.001$) the Dasati nib-mediated increase in F-actin. Quantitation of Rhodamine-phalloidin staining normalized to the number of DAPI nuclei is shown below. Data shown is a representative experiment that was performed in triplicate.

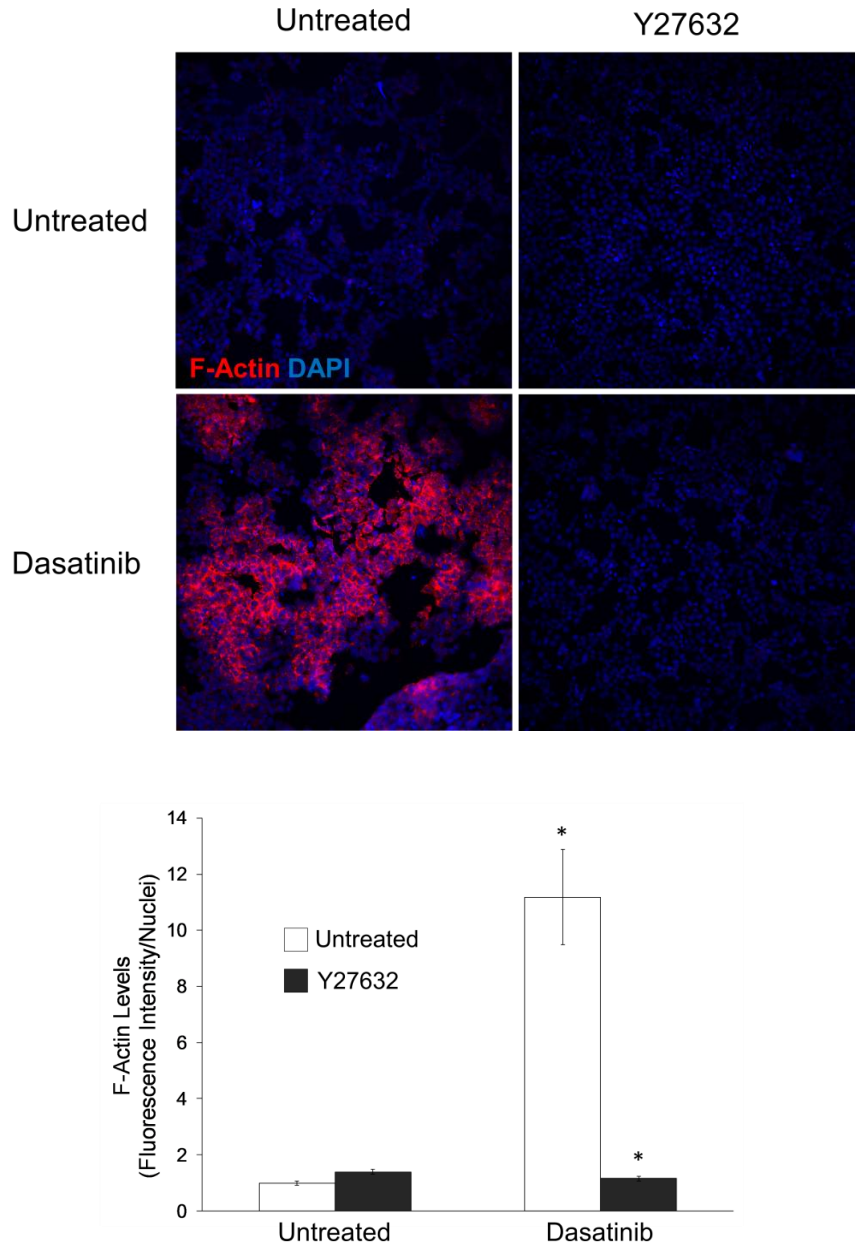

Figure 42: Co-Treatment with a ROCK Inhibitor Blocks Dasatinib-Induced F-actin in HaCaT-Fyn Cells

HaCaT-Fyn cells were pre-treated with 20 μM Y27632 for 20 minutes followed by cotreatment with 1 μM Dasatinib for 30 minutes. Staining for F-actin using Rhodamine-phalloidin indicated that Y27632 cotreatment significantly inhibited (*$p<0.001$) the Dasatinib-mediated increase in F-actin. Quantitation of Rhodamine-phalloidin staining normalized to the number of DAPI nuc lei is shown below. Data shown is a representative experiment that was performed in triplica te.

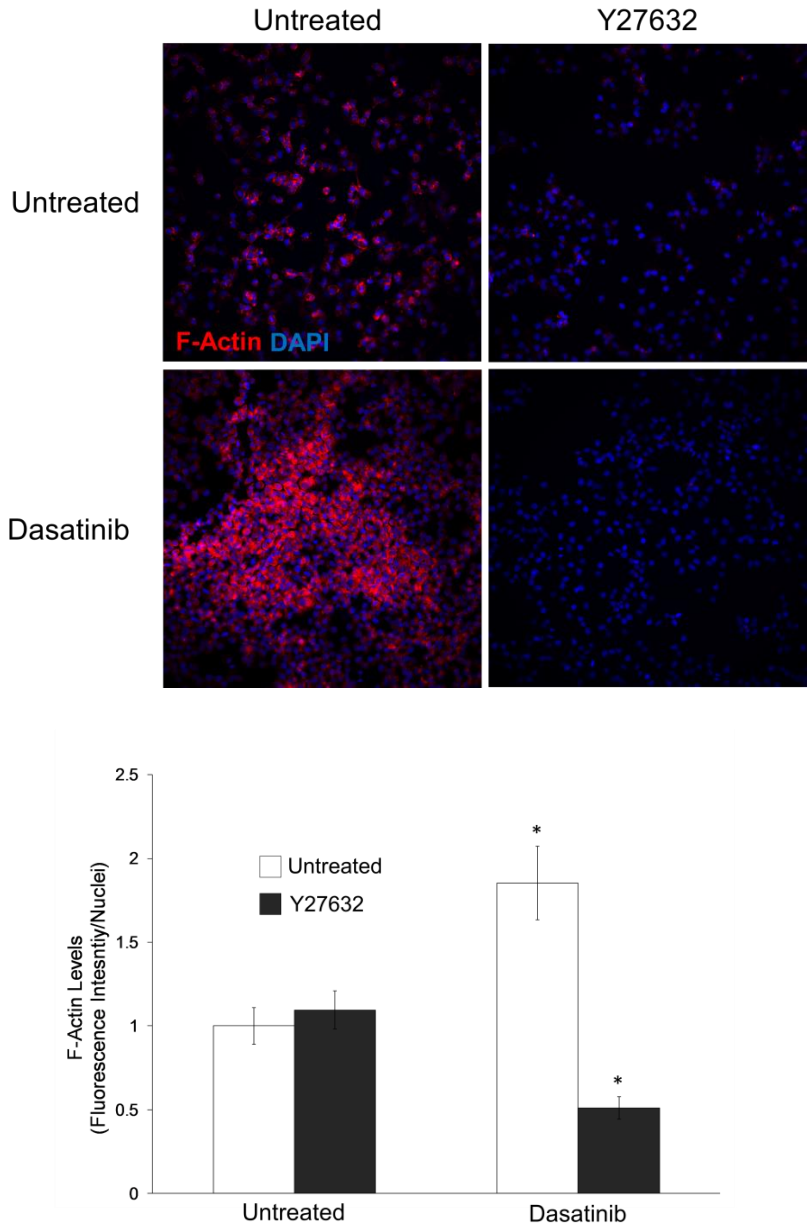

Figure 43: Co-Treatment with a ROCK Inhibitor Blocks Dasatinib-Induced F-actin in MDA-MB-231 Cells

MDA-MB-231 cells were pre-treated with 20μM Y27632, an inhibit or of the Rho effector protein ROCK, for twenty minutes, followed by cotreatment with 1μM Dasatinib for 30 minutes. Staining for F-actin using Rhodamine-phalloidin indicated that Y27632 cotreatment significantly inhibited (*$p<0.001$) the Dasatinib-mediated increase in F-actin. Quantitation of Rhodamine-phalloidin staining normalized to the number of DAPI nuclei is shown below. Data shown is a representative experiment that was performed in duplicate.

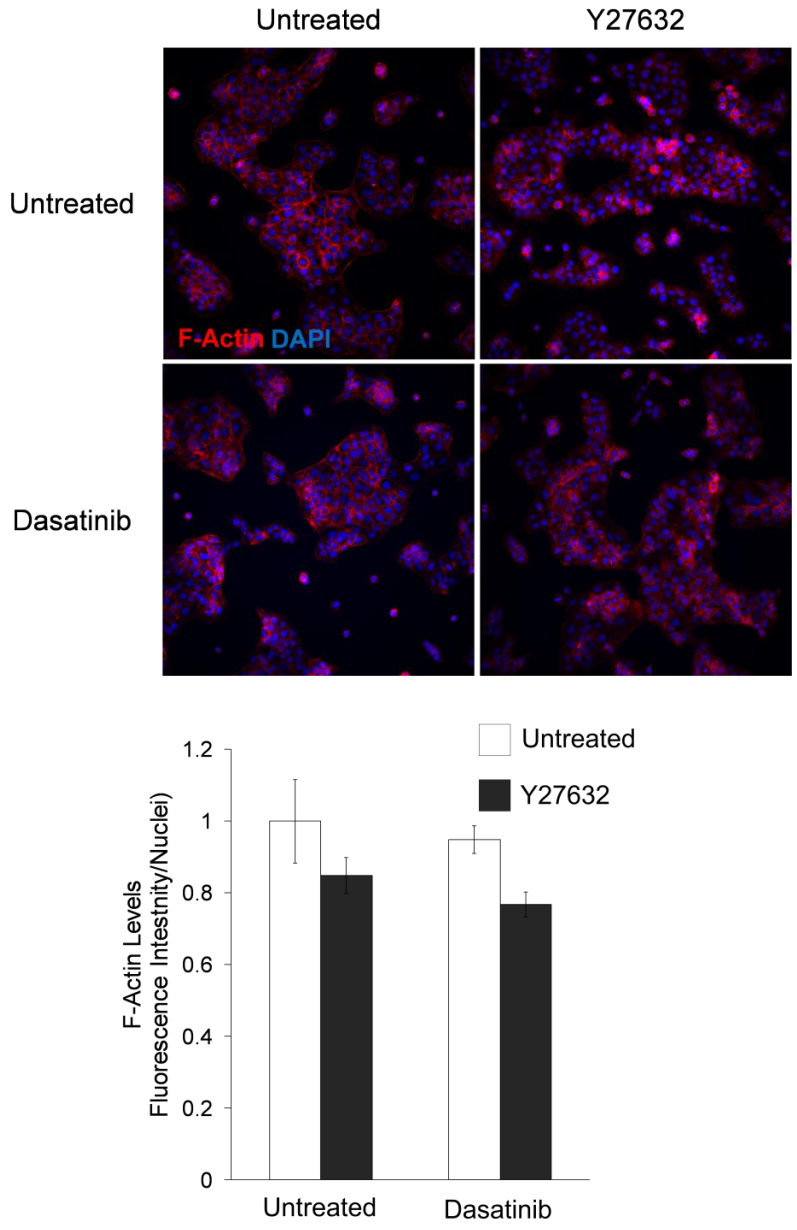

Figure 44: Dasatinib Treatment Does Not Alter F-actin in HaCaT Cells and Y27632 Only Slightly Decreases F-actin Levels

HaCaT cells were pre-treated with 20μM Y27632, an inhibitor of the Rho effector protein ROCK, for twenty minutes, followed by cotreatment with 1μM Dasatinib for 30 minutes. Staining for F-actin using Rhodamine-phalloidin indicated that neither Dasatinib nor Y27632 treatment significantly reduced levels of F-actin. Quantitation of Rhodamine-phalloidin staining normalized to the number of DAPI nuclei is sh own below. Data shown is a representative experiment that was performed in duplicate.

5.6 Increased F-actin Polymerization Drives the Increase in Cell-Cell Adhesion

In our previous experiments blocking Dasatinib's effects on F-actin through ROCK inhibition, we observed the cells no longer formed aggregates in the cell culture plate (Figures 41 & 42), suggesting that the increase in cell-cell adhesion required or was driven by the increase in F-actin. To explore this possibility, we first determined that Y27632 pre-treatment prevented an increase in cell-cell adhesion following Dasatinib treatment in HaCaT-Ras cells by performing a cell-cell adhesion assay (Figure 45). We then pretreated HaCaT-Ras cells with 0.1 μg/mL Cytochalasin D for 30 minutes to prevent actin polymerization and treated the cells with Dasatinib. Pretreatment with Cytochalasin D blocked the Dasatinib-induced increase in cell-cell adhesion in HaCaT-Ras cells (Figure 45). Furthermore, disruption of cell-cell adhesion by culturing cells in low Ca^{+2} media did not prevent Dasatinib-induced F-actin levels (Figure 46). Together, these results indicate that actin polymerization is necessary to allow the increase in cell-cell adhesion induced by Dasatinib in HaCaT-Ras cells.

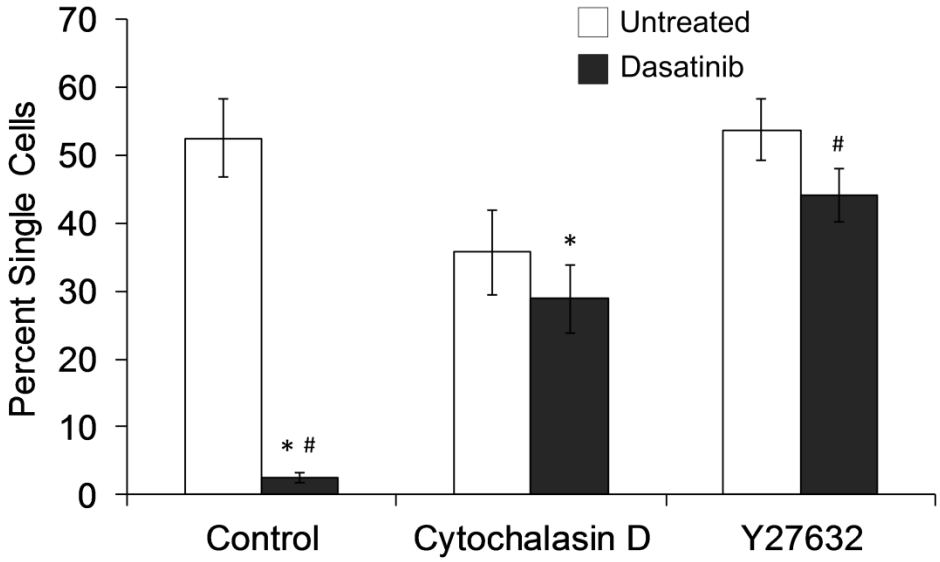

Figure 45: Blocking Actin Polymerization or ROCK Activity Prevents the Dasatinib-Induced Increase in Cell-Cell Adhesion

HaCaT-Ras cells were pretreated with either 0.1 μg/mL Cytochalasin D or 20 μM Y27632 for 20 minutes followed by 30 minutes of 1 μM Dasatinib exposure. Cell-cell adhesion was assayed using the dispase assay. Dasatinib-mediated cell-cell adhesion in HaCaT-Ras cells was significantly inhibited by both Cytochalasin D (*$p<0.001$) and Y27632 ($^{\#}p<0.001$). Data shown is a representative experiment that was performed in duplicate.

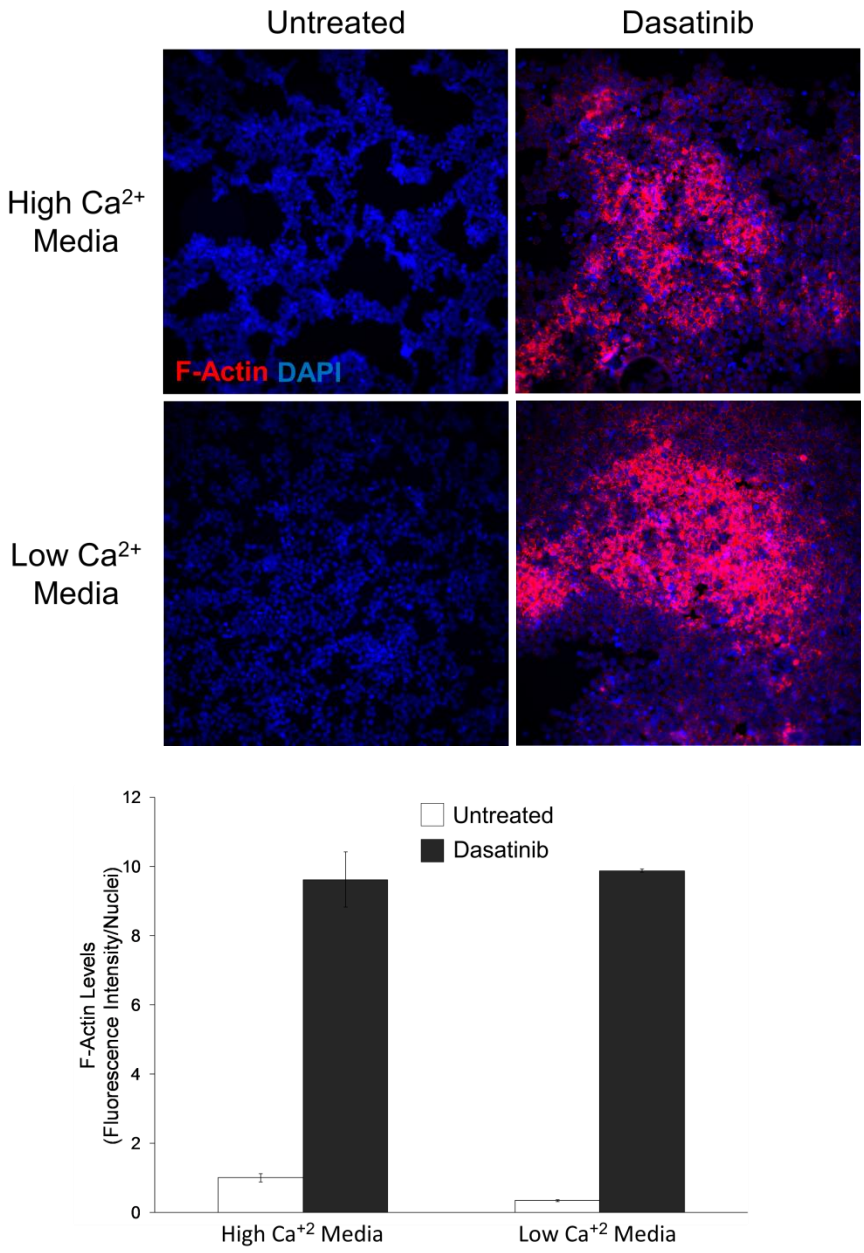

Figure 46: Culture in Low Ca^{+2} Media Does Not Prevent Dasatinib-Induced F-actin Upregulation

HaCaT-Ras cells were treated with 1 μM Dasatinib for 30 minutes in either high Ca^{2+} media (DMEM) or low Ca^{2+} media (Media 154) and stained with Rhodamine-phalloidin. Quantitation of Rhodamine-phalloidin staining normalized to the number of DAPI nuclei is shown below. Data shown is a representative experiment that was performed in triplicate.

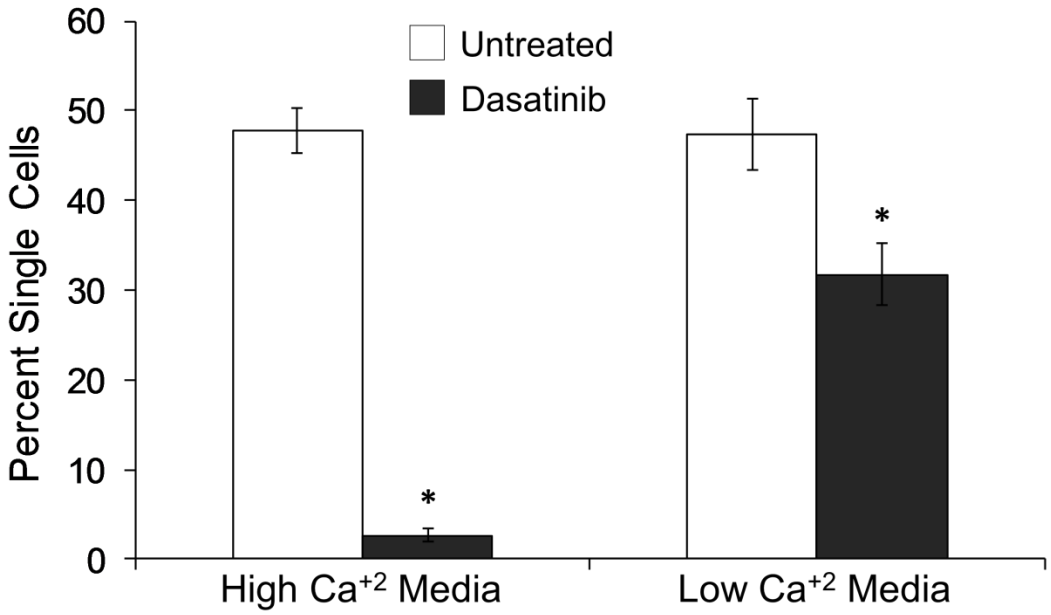

Figure 47: Culture in Low Ca^{+2} Media Prevents Dasatinib-Induced Cell-Cell Adhesion

HaCaT-Ras cells were treated with 1 μM Dasatinib for 30 minutes in either high Ca^{2+} or low Ca^{2+} media and assayed for cell-cell adhesion. Low Ca^{2+} media significantly inhibited Dasatinib-induced cell-cell adhesion (*$p<0.001$). Data shown is a representative experiment that was performed in duplicate.

5.7 Summary

Following Dasatinib treatment the HaCaT-Ras and HaCaT-Fyn cells underwent a marked change in appearance (Figure 20), but this change was not accompanied by a reduction in cell viability or increase in apoptosis compared to the parental HaCaT cells (Figures 24 & 28). However, Fyn inhibition using Dasatinib and siRNA increased cell-cell adhesion in HaCaT-Ras, HaCaT-Fyn and MDA-MB-231 cells, all of which have upregulated Fyn expression (Figures 31, 32 & 33). When cells acquire the ability to migrate they must downregulate their adhesion structures and reduce the stability of the actin cytoskeleton. Increased Fyn activity is sufficient to increase the migratory capacity of HaCaT cells, and Dasatinib treatment, in turn, is sufficient to inhibit this migration (Figure 34) (Yadav and Denning, 2011). Following Dasatinib exposure, the cells expressing high levels of Fyn upregulated the levels of polymerized F-actin, and this F-actin co-localized with catenin members of the adherens junction, suggesting increased stable cell-cell adhesion through the adherens junction (Figures 36, 38 & 40). Furthermore, inhibition of the Rho pathway prevented this increase in F-actin following Dasatinib treatment (Figure 41). These results suggest that increased Fyn is inhibiting Rho to decrease levels of F-actin, decreasing the stability of cell-cell adhesions and increasing the migratory capacity of the cells. Dasatinib treatment inhibits Fyn to restore Rho activity, increasing levels of F-actin to drive the formation of stable adherens junctions.

CHAPTER VI

TARGETING FYN IN A UV MODEL OF SKIN CARCINOGENESIS

6.1 Abstract

cSCC is the second most common type of skin cancer with over 700,000 diagnoses made every year in the United States of America alone, and this number is only growing (Weinstock, 1989). Despite the high rate of diagnosis, most cSCCs are successfully treated with surgical excision and only 1% of cases result in mortality (LeBoeuf and Schmults, 2011, Newman, 1991). However, patients diagnosed with cSCC are at higher lifelong risk for secondary tumors and these recurrences are usually more malignant (Veness et al, 2003). There are currently no treatment therapies that target the molecular mechanism of cSCC tumorigenesis. By developing specific therapeutic protocols, we may reduce some of the physical deformity created by current treatment protocols, reduce tumor recurrence and potentially develop an intervention strategy, greatly reducing the economic strain created by current therapies (Clayman et al, 2005).

The introduction of active Fyn in the epidermis of a murine model results in the formation of actinic keratoses and SCCs (Zhao et al, 2009). We used an *in vivo* model of

UV-induced skin tumors in SKH1 hairless mice and followed each UV exposure with 10 nmole or 100 nmole topical Dasatinib treatment (Figure 48). Following 23 weeks of UV exposure, the mice treated with Dasatinib had a significant reduction in total tumor burden, suggesting SFK inhibition may be an effective method of tumor prevention (Figure 49).

6.2 Treatment with Dasatinib Reduces Total Tumor Burden in a UV-Model of Skin Carcinogenesis

The results thus far demonstrate that Ras-mediated Fyn upregulation results in decreased cell-cell adhesion and an increased migratory potential, two cancer-associated phenotypes. The identification of EMT markers in cSCC significantly increases the risk of cancer associated mortality (Clayman et al, 2005). Furthermore, Fyn is over-expressed in human cSCC and is oncogenic in mouse epidermis (Zhao et al, 2009). To test if inhibiting Fyn might mitigate UV-induced skin carcinogenesis, we exposed three groups of SKH1 hairless mice (12 mice/group) to increasing doses of UVB (30 mJ/cm² - 150 mJ/cm²) three times a week for 23 weeks. Immediately following each UVB exposure we administered a topical dose of acetone, 10 nmole Dasatinib in acetone or 100 nmole Dasatinib in acetone to each group (Figure 48). Dasatinib was applied after UVB exposure to avoid any sunscreen effects. After 23 weeks of UV exposure, the mice were allowed to recover for a week before tumor analysis. Both Dasatinib treatments significantly reduced the total tumor burden per mouse ($p<0.05$) (Figure 49). However,

the average size of each tumor did not change significantly (Figure 50). Additionally, there was not difference in the mouse weights between tumor groups, indicating Dasatinib treatment did not decrease the viability of the mice (Figure 54). These results suggest that the tumor burden was primarily lessened by a decrease in the total number of tumors, although this difference was not significant (Figure 51). It is possible that the Dasatinib-treated mice developed fewer total tumors due to higher levels of apoptosis in the UV-damaged cells. Previous studies of Dasatinib-induced apoptosis in HaCaT cells indicated that Dasatinib additively increased levels of apoptosis following UVB exposure (Figure 30). The distribution of benign tumors, atypical benign tumors and squamous cell carcinomas that arose in the control or Dasatinib treated groups was similar (Figure 52b), indicating that there was not a significant difference in tumor histopathology between groups (Figure 52a). Staining for the differentiation marker Keratin 1 exposed a significant difference in the differentiation status of tumors between the groups, with more poorly differentiated tumors in the Dasatinib-treated groups (Figure 53).

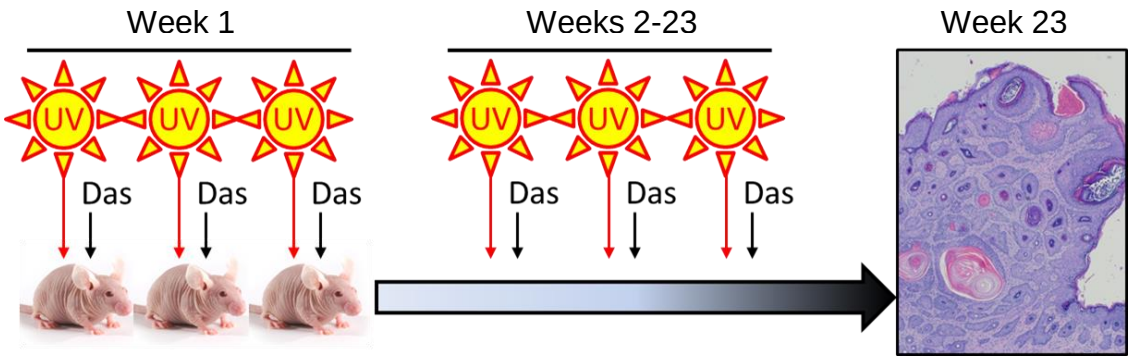

Figure 48: *In Vivo* Model of UV-Induced Skin Carcinogenesis with Dasatinib treatment

Schematic describing UV exposure and Dasatinib treatment in the SKH1 mouse model. Three groups of mice were exposed to increasing doses of UVB (30 mJ/cm² - 150 mJ/cm²) three times a week for 23 weeks, followed by topical treatment with acetone, 10 nmole Dasatinib in acetone or 100 nmole Dasatinib in acetone. Mice were allowed to recover for 1 week before tumor analysis. Figure courtesy of Dr. Mitchell F. Denning.

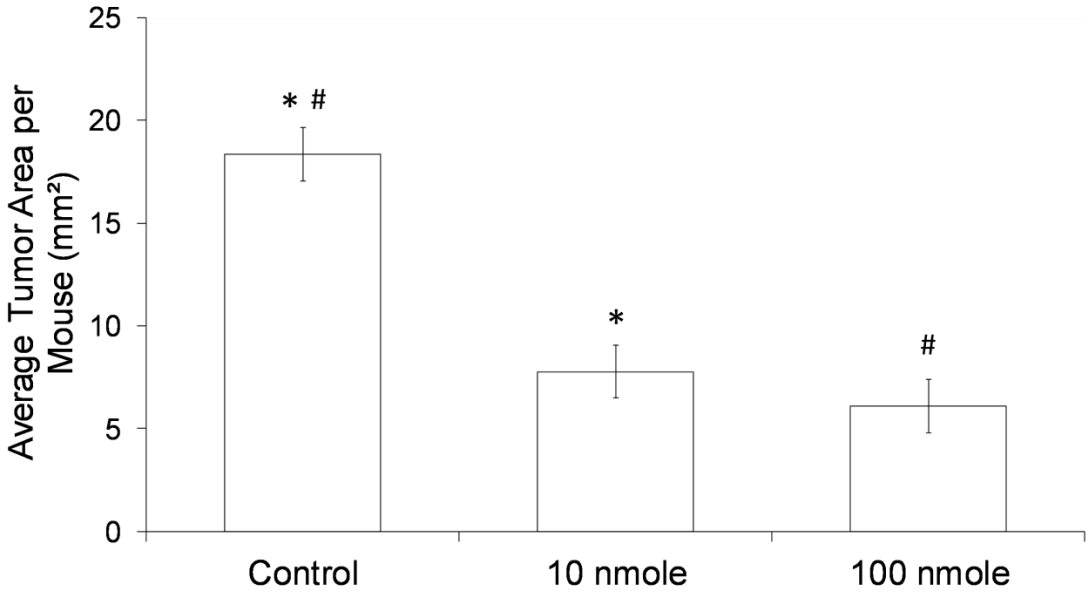

Figure 49: Dasatinib Treatment Following UV Exposure Reduces Total Tumor Burden

Three groups of twelve SKH1 mice were exposed to increasing doses of UVB (30 mJ/cm² - 150 mJ/cm²) 3x a week for 23 weeks. Each UVB exposure was immediately followed by treatment with acetone alone (control), 10 nmole Dasatinib or 100 nmole Dasatinib, and tumor size and number was quantified after 24 weeks. Total tumor burden was significantly reduced by both the 10 nmole treatment ($^{*}p<0.05$) and 100 nmole treatment ($^{\#}p<0.01$).

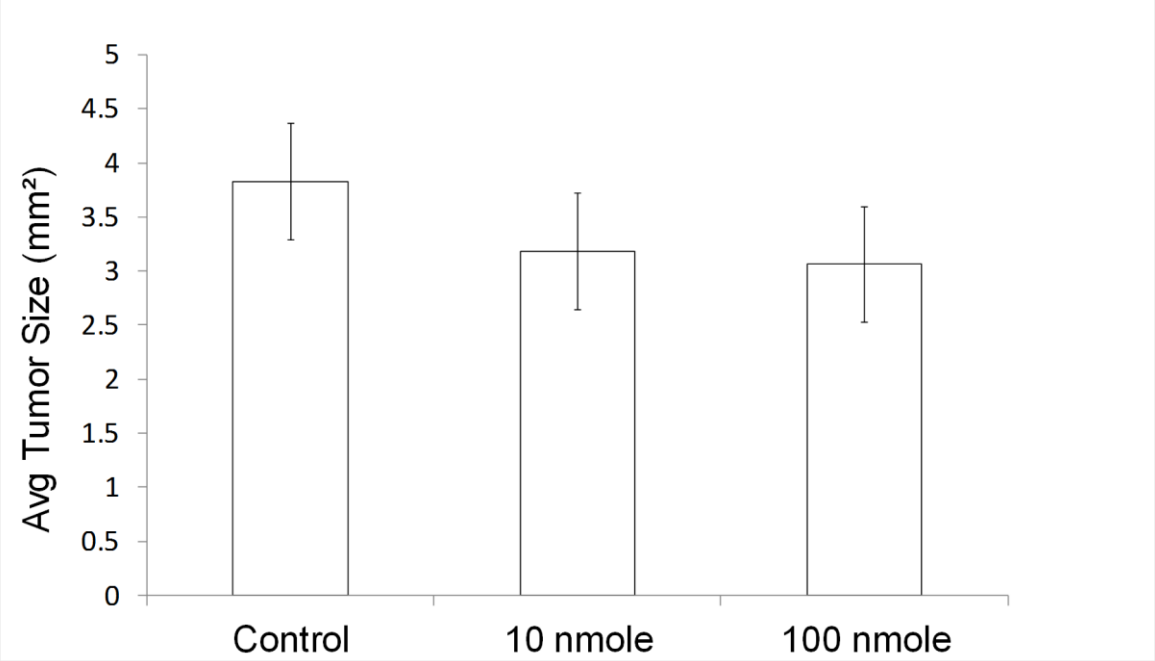

Figure 50: Dasatinib Treatment Following UV Exposure Did Not Decrease Tumor Size

Average tumor size per mouse in each treatment group is shown.

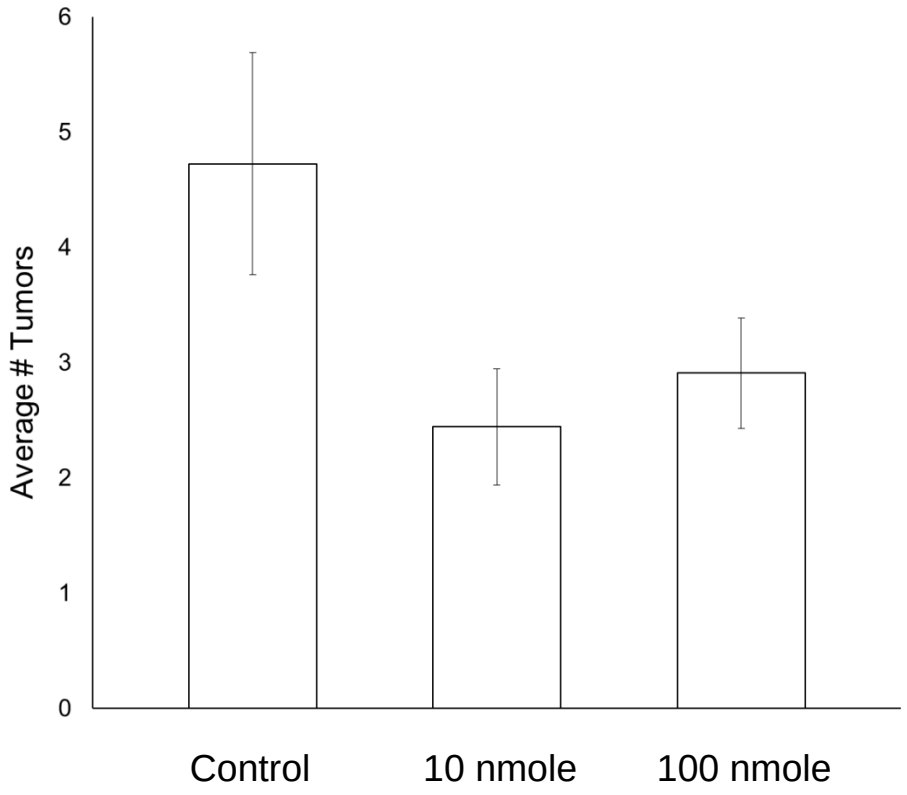

Figure 51: Dasatinib Treatment Following UV Exposure Reduced Tumor Number

Average number of tumors per mouse in each treatment group is shown.

A.

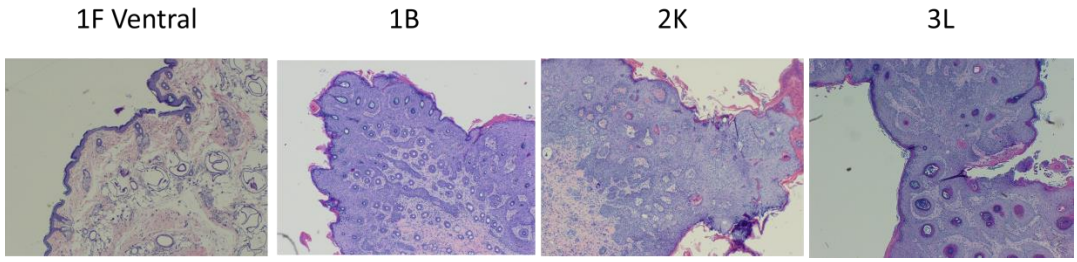

B.

	Benign Tumors	Atypical Benign Tumors	Squamous Cell Carcinoma
Untreated	13	10	0
10 nmole Dasatinib	14	6	6
100 nmole Dasatinib	15	10	2

Figure 52: Dasatinib Treatment Did Not Alter Distribution of Tumor Types Following UV Exposure

A. One week after the end of UV exposure tumors were taken for histopathology. Shown are representative hematoxylin and eosin (H&E) stained sections of UV-irradiated dorsal epidermis (IF Ventral), a benign papilloma (1B), a progressing papilloma (2K) and a squamous cell carcinoma (3L).
B. Histology of UV-induced SKH1 mouse tumors is summarized for each treatment group based on analysis of H&E stained tumor sections.

A.

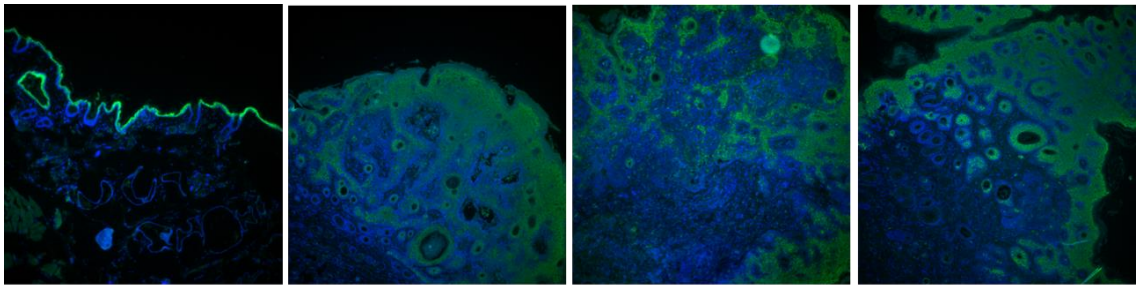

1F Ventral
K1 Positive

1B
K1 Positive

2K
Patchy Loss

3L
Patchy Loss

B.

	K1 Positive	Patchy Loss	Loss in Deep Tumor	Complete Loss
Untreated	6	2	0	2
10 nmole Dasatinib	0	4	3	0
100 nmole Dasatinib	1	5	2	1

Figure 53: Dasatinib Treatment Resulted in Tumors with Decreased Differentiation Status

A. Tumors were stained for Keratin 1 expression. Shown are representative immunofluorescent stained sections of UV-irradiated dorsal epidermis (IF Ventral), a benign papilloma (1B), a progressing papilloma (2K) and a squamous cell carcinoma (3L) with corresponding analysis of K1 expression.
B. Staining of UV-induced SKH1 mouse tumors is summarized for each treatment group based on analysis of Keratin 1 sta ined tumor sections. Dasatinib treatment resulted in significantly more tumors with loss of K1 staining ($p<0.005$). Statistical analysis was performed using Fisher's Exact Test.

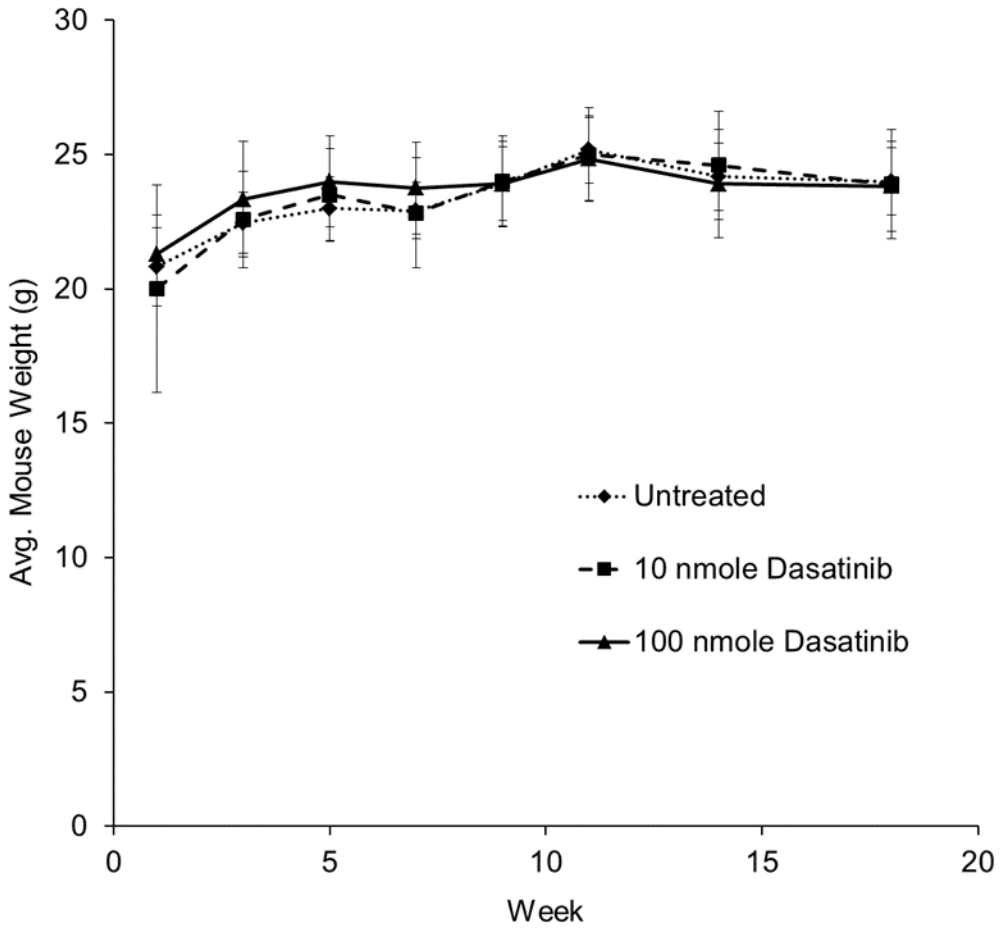

Figure 54: Dasatinib Treatment Did Not Alter Mouse Weight

Mice were weighed during the duration of the experiment on the dates indicated. Weights are shown in grams. UVB exposure began at week 1 and ended at week 23.

6.3 Summary

UVB exposure is the most common carcinogen driving the formation of cSCCs (Alam and Ratner, 2001). We exposed 36 SKH1 hairless mice to increasing doses of UVB and followed each exposure with two different cutaneous Dasatinib doses (10 and 100 nmole). After 23 weeks all of the mice had developed skin tumors, but both Dasatinib treatments resulted in a significant reduction in total tumor burden (Figure 49). The tumor sizes did not vary between treatment groups, but the 10 nmole and 100 nmole treatments both caused a reduction in the number of tumors that formed (Figure 50 & 51). There was also no difference in the distribution of benign and malignant tumors between groups (Figure 52). However, there was a significant increase in poorly differentiated tumors in the Dasatinib treated mice (Figure 53). Although Dasatinib treatment did reduce total tumor burden, further studies with longer time points are required to investigate how SFK inhibition alters the malignant potential of the tumors that do form.

CHAPTER VII

DISCUSSION

7.1 *FYN* Expression May Be Regulated by the Transcription Factor Lef-1

Fyn over-expression has been detected in many different human malignancies, including cSCC, glioblastoma multiforme, head and neck squamous cell carcinoma, melanoma, pancreatic and prostate cancer (Zhao et al, 2009, Saito et al, 2010, Ban et al, 2008, Lu et al, 2009, Posadas et al, 2009, Talantov et al, 2005). However, the signaling mechanism governing *FYN* transcriptional regulation has only been described in CML, where BCR-ABL drives ROS production to activate the transcription factors Egr and Sp1, increasing *FYN* expression (Gao et al, 2009). A previous graduate student, Vipin Yadav, found that the introduction of active H-Ras(G12V) to the HaCaT keratinocyte cell line resulted in upregulation of Fyn expression through a PI3K/Akt dependent mechanism (Yadav and Denning, 2011). Using RT-qPCR techniques I found that *FYN* was selectively upregulated over 200-fold (Figure 6). However, depletion of ROS in the cell culture media did not decrease activity at the *FYN* promoter, suggesting *FYN* expression was being regulated by a different mechanism than that identified in CML (Figure 8).

The gene encoding *FYN* is located on chromosome 6q21 and spans approximately 213,120 base pairs. 14 exons spliced from *FYN*'s mRNA transcript are translated to a protein that is 537 amino acids long. Using luciferase reporter constructs, we identified the region between -100 and -50 bases upstream of the transcription start site as necessary for *FYN* upregulation in HaCaT-Ras cells (Figure 9). Mutation of the GA sequence located -74 bases upstream of the transcription start site abolished *FYN* expression, underlining the importance of this region in *FYN* regulation (Figure 10). It is worth nothing that this site is different than that identified by Gao et al. in their paper describing ROS-mediated *FYN* transcriptional regulation (Figure 55) (Gao et al, 2009).

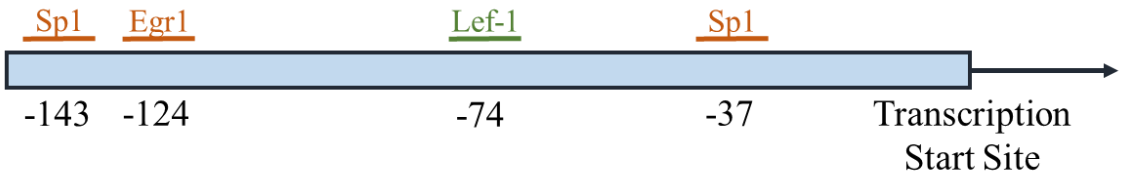

Figure 55: Diagram of Transcription Factor Binding to the *FYN* Promoter

Transcription factor binding sites in the *FYN* promoter identified in our work and work performed by the Chandra lab are diagramed in the figure above. Luciferase reporter analysis and EMSA identified Lef-1 (green) as the transcription factor binding -74 base pairs upstream of the transcription start site and mediating *FYN* upregulation in Ras-transformed keratinocytes. Luciferase reporter analysis and ChIP identified Sp1 and Egr1 (orange) as the transcription factors binding -147-138, -41-32 and -128-120 base pairs (respectively) upstream of the transcription start site and mediating *FYN* upregulation in BCR-ABL-transformed leukemic cells.

Vipin Yadav found that the PI3K/Akt pathway was mediating Fyn upregulation in Ras-transformed HaCaT cells (Yadav and Denning, 2011). Akt plays many important roles in the cell, inhibiting apoptosis and regulating cell proliferation, autophagy and metabolism. Akt activity has been associated with dozens of transcription factors, and four of these proteins were also predicted to bind near the site necessary for *FYN* upregulation in our system, -74 base pairs upstream of the transcription start site. These transcription factors were GATA-1, GATA-2, GATA-3 and Lef-1 (Zhao et al, 2006, Menghini et al, 2005, Song, Hollstein and Xu, 2007, Huang et al, 2012). Initial EMSA analysis of transcription factor binding suggested Lef-1 may be binding to the site of interest in HaCaT-Ras cells (Figure 16). However, knocking down Lef-1 in HaCaT-Ras cells did not decrease *FYN* mRNA levels (Figure 17). Lef-1 is a member of the TCF family of transcription factors, and these proteins are capable of functionally substituting for each other *in vivo* (Staal and Clevers, 2000). Therefore we also knocked down an essential binding partner for Lef-1/TCF transcriptional regulation, β-catenin. Knockdown of β-catenin also did not decrease *FYN* mRNA levels (Figure 18). Together, these results contradict our EMSA findings that suggest Lef-1 was mediating *FYN* upregulation in HaCaT-Ras cells. This discrepancy could be the result of many different factors. Our knock-down may not have been complete enough to reduced Lef-1 or β-catenin activity below what is necessary to see loss of *FYN* transcription, or other closely related proteins such as TCF7 may have replaced Lef-1 in regulating *FYN* over-expression in the HaCaT-Ras cells. Alternatively, our largest reporter plasmid contained 2,000 base pairs of the *FYN* promoter. Although

this region surely contains some regulatory elements regarding *FYN* transcription, it may not have encompassed enhancers or other regions of importance further upstream or downstream of this segment that play important roles in *FYN* regulation *in vivo.* Additionally, our *in vitro* EMSA results may have identified a potential interaction between Lef-1 and the *FYN* promoter that is not occurring *in vivo* in our HaCaT-Ras cells due to signaling mechanisms that were not detected following the introduction of reporter plasmids.

7.2 Increased Fyn Activity is Sufficient to Induce EMT in Keratinocytes

Fyn has previously been described as an initiator of EMT (Saito et al, 2010, Lewin et al, 2010). Increased Fyn activity has been implicated in the increased migratory potential of melanoma and prostate cancer cells, as well as increased metastasis in oral and pancreatic tumors (Saito et al, 2010, Jensen et al, 2011, Huang et al, 2003, Chen et al, 2009b, Li et al, 2003). Additionally, studies have uncovered a role for Fyn in the down-regulation of E-cadherin in A549 lung cancer cells, and inhibition of Src in Ras-transformed HaCaT cells stabilized E-cadherin at the cell membrane, implicating SFKs like Fyn as negative regulators of E-cadherin stability (Kim et al, 2011, Alt-Holland et al, 2008). Fyn is also capable of phosphorylating β-catenin at two sites that break the connection between β-catenin and both E-cadherin and the actin cytoskeleton. These phosphorylation events free β-catenin from the cell membrane, allowing its translocation to the nucleus and

upregulation of TCF/LEF target genes (Piedra et al, 2003, Castano et al, 2007). In HaCaT cells, increased Fyn expression resulted in the downregulation of E-cadherin and cytokeratin, upregulation of vimentin and the transition from a cobblestone, epithelial morphology to a small, stellate, mesenchymal morphology, all of which are markers of EMT (Figures 19 & 20). We used RT-qPCR to analyze the mRNA levels of three transcription factors considered master regulators of EMT: Slug, Snail and Twist. Both the HaCaT-Fyn and HaCaT-Ras cells had upregulated expression levels of Twist over 40-fold, suggesting this was the mechanism driving EMT in these cells (Figure 23). Although EMT is a normal process in embryogenesis and wound healing, the acquisition of a mesenchymal, migratory phenotype is considered an important step in the progression of epithelial malignancies (Radisky, 2005, Kalluri and Weinberg, 2009b). In cSCC, the identification of invasion or a migratory capacity decreases the predicted three year disease free survival rate by thirty percent (Clayman et al, 2005). Therefore, the identification of Fyn as a potential driver of EMT in cSCC is an important contribution to our understanding of the development of particularly malignant skin tumors.

Due to Fyn's ability to induce EMT in keratinocytes, we chose to block Fyn activity using Dasatinib, an inhibitor of SFKs, BCR-ABL and other kinases (Aguilera and Tsimberidou, 2009). Although Dasatinib treatment did not reverse expression of the markers of EMT, it did inhibit cell migration and promote cell-cell adhesion, two important features of the EMT phenotype (Figures 22, 31 & 34). RT-qPCR analysis of

expression levels of Slug, Snail and Twist following 24 hours in 1 μM Dasatinib showed no reduction of expression to levels comparable to those in the parental HaCaT cells (Figure 23). Therefore, it is possible that once the cells had undergone EMT, positive feedback mechanisms were activated to drive and maintain the mesenchymal phenotype, and inhibition of Fyn was no longer sufficient to reverse EMT (Saunders and McClay, 2014).

7.3 Dasatinib Treatment Decreases Cell Viability to a Similar Extent in Parental and Transformed Keratinocytes

Reduced Fyn signaling, either directly or using the SFK inhibitor Dasatinib, results in decreased cellular proliferation in several cell systems, including osteoclasts and T-cells, among others (Singh et al, 2012, Kim et al, 2010, Schade et al, 2008, Ninio-Many et al, 2013). Other groups have also shown that Fyn activity inhibits apoptosis and promotes cell survival, either by upregulating Sam68 and HnRNPA2B1 activity or by preventing PIKE-A cleavage to increase Akt activity and prevent cell death (Chen et al, 2011, Tang, Feng and Ye, 2007). Following 24 hours in 0.1 μM or 1 μM Dasatinib, we saw a similar decrease in cell viability between the parental HaCaT and HaCaT-Ras cells (Figure 24). We could not detect a decrease in proliferation using DNA quantitation or radioactive thymidine incorporation upon Dasatinib exposure (Figures 25 & 26). Finally, treatment with Dasatinib induced apoptosis in both cell lines to a similar extent and did not induce autophagy (Figure 28 & 29). From these results it appears likely that upregulated Fyn

activity is not increasing proliferation or resistance to apoptosis in HaCaT-Ras cells. Instead of acting as a survival factor, our results indicate that increased Fyn signaling is decreasing the strength of cell-cell adhesions and increasing cell motility, promoting the transition to a mesenchymal phenotype.

7.4 Dasatinib Treatment Results in Increased Cell-Cell Adhesion

During KC differentiation, Fyn is involved in the formation of adherens junctions, recruiting junctional components and inducing signaling pathways that control the differentiation program (Calautti et al, 1995, Tu et al, 2008, Cabodi et al, 2000). However, in KC transformation and oncogenesis, Fyn activity has been implicated in the dissolution of cell-cell adhesion structures and an increased migratory phenotype (Owens et al, 2000, Roura et al, 1999). Fyn activity is also associated with both the formation and dissolution of focal adhesions, and to a lesser extent hemidesmosomes and desmosomes (Rengifo-Cam et al, 2004, Zeng et al, 2003, Sharma and Mayer, 2008, Peng and Guan, 2011, Schober et al, 2007, Mariotti et al, 2001, Spinardi et al, 2004, Gagnoux-Palacios et al, 2003). Treatment with 0.1 μM or 1 μM Dasatinib did not increase cell-cell adhesion in the parental HaCaT cells, most likely because these cells already had a robust cortical F-actin cytoskeleton and strong cell-cell adhesion (Figures 31 & 44). However, in keratinocytes stably expressing active Fyn (HaCaT-Fyn cells) or Ras (HaCaT-Ras cells), Dasatinib exposure rapidly increased cell-cell adhesion over 6-fold (Figure 31).

Fyn knockdown using siRNA had a similar result, demonstrating that Fyn inhibition is sufficient to induce an increase in cell-cell adhesion (Figure 32). These findings apply to cell types other than keratinocytes, as Fyn knockdown in MDA-MB-231 breast cancer epithelial cells also increased cell-cell adhesion (Figure 33). Our results support a previously established role for Fyn in the turnover of adherens junctions through phosphorylation of p120catenin and β-catenin, ultimately causing dissociation of the adherens junction complex from the actin cytoskeleton and loss of cell-cell adhesion (Calautti et al, 1998, Piedra et al, 2003, Lilien and Balsamo, 2005, Castano et al, 2007).

In conjunction with an increase in cell-cell adhesion following Dasatinib treatment in HaCaT-Ras and HaCaT-Fyn cells (Figure 31 & 32), we also observed an interesting change in the cell's ability to remain adhered to the culture plate. In cultures with high cell density we observed Dasatinib treatment induced cell-cell adhesion, and these tight clumps of cells were easily dislodged from the plastic, resulting in floating rafts of cells that remained adhered to each other but not to the matrix. We have generated two hypotheses that may account for this change in cell-cell adhesion. First, although the strength and number of cell-matrix adhesions may not been altered, the increase in cell-cell adhesion may reduce the cell's ability to remain adhered following the physical dislodgement induced by the media moving around in the plate. Second, a great deal of cross-talk occurs between the cell-cell adhesion complexes and cell-matrix complexes. Increased Fyn activity has been shown to shift the actin cytoskeleton, an important

stabilizing component of adhesion complexes, away from adherens junctions and toward focal adhesions (Rengifo-Cam et al, 2004). Therefore, following Fyn inhibition, increased stability at the adherens junction may signal for decreased stability at the focal adhesion, resulting in decreased adherence to the matrix and an increase in cell detachment, thus resulting in the floating rafts of cells that we observed. Although we have not studied Dasatinib's ability to alter cell-matrix adhesion in HaCaT-Ras and HaCaT-Fyn cells, it remains an interesting avenue of research that may shed additional light on the role of Fyn as a target in cSCCs.

It is important to note that Dasatinib is not a specific inhibitor of Fyn; instead it decreases the activity of all SFKs, BCR-ABL and other tyrosine kinases (Figure 21) (Aguilera and Tsimberidou, 2009, Lombardo et al, 2004). However, our Dasatinib treatment results can be primarily attributed to inhibition of Fyn activity, as it is the only SFK differentially regulated between our parental HaCaT and HaCaT-Ras cells, and results similar to those seen with Dasatinib treatment were observed with Fyn knockdown using siRNA. Additionally, the introduction of active Fyn was sufficient to drive EMT in HaCaT cells, and Dasatinib treatment of these HaCaT-Fyn cells promoted cell-cell adhesion and increased F-actin levels. Dasatinib also requires a much lower *in vitro* IC_{50} to inhibit SFKs (0.5 nM) than any of its other targets (Aguilera and Tsimberidou, 2009, Lombardo et al, 2004). This IC_{50} was determined in a test tube, where lower concentrations of the inhibitor are required to out-compete ATP from the SFK binding site. In cells, higher

concentrations of ATP competitive kinase inhibitors are required due to the higher intracellular levels of ATP (1-10 mM). The concentrations of Dasatinib used in our experiments (0.1 and 1 μM) are comparable to those used in other studies to treat cells in culture (Li et al, 2010, Buettner et al, 2008).

7.5 Dasatinib Treatment Results in Increased Polymerized F-actin, Driving the Formation of Adherens Junctions

EMT is commonly associated with an increase in the dynamic nature of the actin cytoskeleton, resulting in loss of cell-cell adhesion, cell detachment and migration (Radisky, 2005, Kalluri and Weinberg, 2009b). Fyn activity has been implicated in the dissolution of cell-cell adhesions, phosphorylating β-catenin and p120catenin to induce rearrangement of the actin cytoskeleton away from adherens junctions and toward focal contacts, a premature form of focal adhesions (Rengifo-Cam et al, 2004). Following Dasatinib exposure in the HaCaT-Ras cells, we could not detect an increase in the expression of the cytokeratins either by Western blot or immunofluorescent staining (Figure 35, data not shown), making the formation of desmosomes an unlikely mechanism of Dasatinib-induced cell-cell adhesion. In contrast, levels of polymerized F-actin increased as early as five minutes after Dasatinib exposure, continued to increase for 6 hours and remained elevated for over 24 hours (Figure 36). This increase in F-actin was also seen in HaCaT-Ras cells following Fyn knockdown using siRNA, indicating that Fyn inhibition is sufficient to cause these changes (Figure 38). Furthermore, the F-

actin induced by Dasatinib formed a cortical cytoskeleton that colocalized with the adherens junction proteins α-catenin, β-catenin and p120catenin, suggesting the formation of stable adherens junctions (Figure 40). It is worth noting that the parental HaCaT cells had higher levels of F-actin prior to treatment, and Dasatinib exposure did not alter the levels of polymerized actin (Figure 44). This suggests that Dasatinib's effects are not universal on all cell types. Instead, Dasatinib treatment acts to upregulate the F-actin cytoskeleton and cell-cell adhesion in cancer cells that have undergone some degree of EMT.

The ability of the Rho family of proteins to regulate actin stability has been well established (Owens et al, 2000, Grosheva et al, 2001, Cozzolino et al, 2003, Menke and Giehl, 2012, Wildenberg et al, 2006). Rho acts to increase the formation of actin stress fibers, while its family member Rac decreases the stability of cell-cell adhesions and indirectly decreases the stability of the actin cytoskeleton (Lamouille, Xu and Derynck, 2014, Whale et al, 2011). Previous work in oligodendrocytes has uncovered a relationship between Fyn activity and actin stability, where Fyn phosphorylates p190RhoGAP to inhibit Rho, ultimately causing disassembly of the actin cytoskeleton (Wolf et al, 2001, Liang, Draghi and Resh, 2004). In HaCaT-Ras cells, following inhibition of the downstream Rho effector protein ROCK, Dasatinib exposure no longer upregulated levels of F-actin (Figure 41). These results suggest that, in keratinocytes, Fyn inhibits Rho activity, and Dasatinib treatment releases this inhibition to activate Rho,

ultimately promoting actin cytoskeletal stability. This dependence on ROCK for Dasatinib-induced F-actin was also seen in HaCaT-Fyn and MDA-MB-231 cells (Figures 42 & 43).

The existing body of literature concerning Fyn's role in cell-cell adhesion suggests that Fyn acts primarily at the adhesion complex itself, phosphorylating target proteins to either increase or decrease the stability of the junctions (Calautti et al, 2002, Piedra et al, 2003). Therefore, we expected that Dasatinib treatment would initially act at the adherens junction, increasing the stability of the adhesion and activating signaling cascades that resulted in F-actin upregulation. This, however, is not what we observed. Instead, following pretreatment with the ROCK inhibitor Y27632 the cells no longer formed aggregates in the cell culture plate upon Dasatinib exposure, suggesting increased F-actin was necessary for the increase in cell-cell adhesion (Figure 41). To test whether adherens junction formation or F-actin stability was initiated before junctional adhesion, we pretreated the cells with Cytochalasin D, a mycotoxin that prevents actin polymerization. This pretreatment blocked Dasatinib's ability to increase cell-cell adhesion in the HaCaT-Ras cells, further suggesting that actin polymerization was required for formation of cell-cell adhesive structures (Figure 45). We then cultured the cells in low Ca^{+2} media, cell culture conditions that block the formation of Ca^{+2}-dependent cadherin-based adhesions such as adherens junctions and desmosomes. Culture in low Ca^{+2} conditions did not prevent the Dasatinib-induced increase in F-actin,

indicating that loss of cell-cell adhesion was not sufficient to block the polymerization of cortical F-actin (Figure 46). Together these results suggest that the increase in cell-cell adhesion through the adherens junction by Dasatinib first required or was being driven by polymerization of the actin cytoskeleton. Increased cell-cell adhesion, in turn, should theoretically decrease the ability of cells with elevated Fyn to detach from surrounding cells, blocking their migratory potential. Additionally, these findings provide mechanistic information on how Dasatinib induces a pronounced cell-clumping phenotype, an observation previously made in other cell types but never characterized (Chan et al, 2012).

7.6 Treatment with Dasatinib Reduces Total Tumor Burden Following Extensive UV Exposure

Twenty-three clinical trials are currently in progress or just concluded (clinicaltrials.gov) to study the results of Dasatinib treatment in solid tumors, including melanoma, prostate cancer, breast, head and neck and colorectal cancers (Montero et al, 2011). Previous investigators have found that transgenic expression of active Fyn in a murine epidermis induced the formation of keratotic tumors and actinic keratoses that progressed to cSCCs (Zhao et al, 2009). Surveys of human cSCCs have also shown increased SFK activity through all layers of the tumor (Ayli et al, 2008). Due to the lack of targeted therapies for cSCC and our findings concerning Fyn's role in keratinocyte migration and the ability to increase cell-cell adhesion following Fyn inhibition, we chose to investigate Dasatinib's

ability to prevent cutaneous tumorigenesis in a UVB mouse model. Dasatinib treatment significantly reduced total tumor burden following extensive UVB exposure, but did not alter tumor size or the general tumor histopathology (Figures 49 & 52), adherens junction makeup or overall keratinocyte acantholysis (data not shown). However, the tumors were analyzed one week after the last Dasatinib exposure, allowing sufficient time for adhesive structures to be re-established between tumor keratinocytes. Our results are consistent with the ability of oral AZD0530, a SFK inhibitor, to reduce chemically induced mouse skin tumors when given by oral gavage (Serrels et al, 2009). Therefore, the use of Dasatinib as a topical therapy may be an effective method to prevent the formation of skin tumors following UV exposure. This treatment is particularly appealing, as a topical therapy is cost effective as well as localized to the site of tumor formation, and requires a lower overall dose, resulting in fewer side effects.

7.7 Significance: Fyn as a Novel Target in cSCCs

In this work we have identified potential transcription factors driving Fyn expression in Ras-transformed keratinocytes, as well as shown that increased Fyn activity is sufficient to induce EMT in keratinocytes. Inhibition of Fyn activity, either using siRNA or the therapeutic Dasatinib, released Rho inhibition and resulted in rapid upregulation of the F-actin cytoskeleton, increasing cell-cell adhesion through the adherens junction and blocking the cell's migratory capacity. Additionally, Dasatinib treatment following UVB

exposure decreased UV-induced tumorigenesis *in vivo*. These findings suggest that Fyn may be an effective therapeutic target in the treatment of cSCC, as it may reduce the danger of cellular invasion and migration, risk factors that dramatically reduce the predicted disease free survival rate among patients.

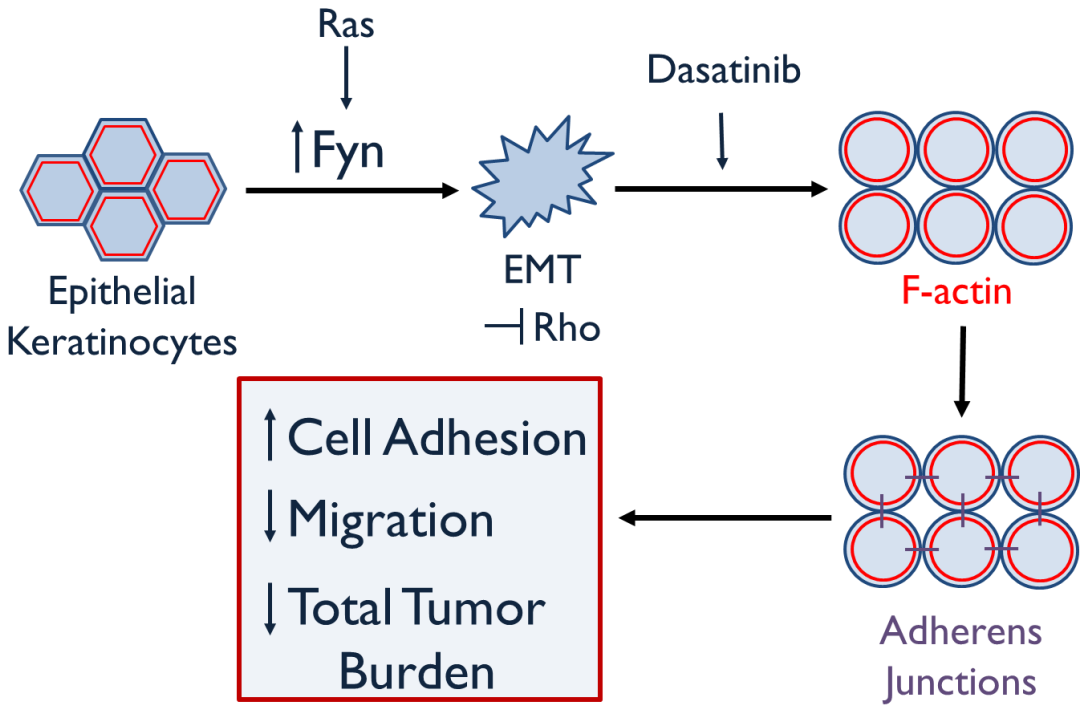

Figure 56: Mechanism of Cell-Cell Adhesion Following Fyn Inhibition

Increased Fyn activity, potentially through an increase in Ras signaling, induces keratinocytes to undergo EMT and inhibits Rho activity. Dasatinib treatment inhibits Fyn, releasing this inhibition of Rho to increase the stable F-actin cytoskeleton. This increase in F-actin stabilizes the formation of adherens junctions, resulting in increased cell-cell adhesion and decreased migration. Inhibition of SFK activity using Dasatinib also results in decreased total tumor burden following extensive UV exposure in a murine model.

BIBLIOGRAPHY:

Aguilera DG, Tsimberidou AM (2009). Dasatinib in chronic myeloid leukemia: A review. *Ther Clin Risk Manag* 5: 281-9.

Alam M, Ratner D (2001). Cutaneous squamous-cell carcinoma. *N Engl J Med* 344: 975-83.

Alema S, Salvatore AM (2007). p120 catenin and phosphorylation: Mechanisms and traits of an unresolved issue. *Biochim Biophys Acta* 1773: 47-58.

Allen TD, Potten CS (1974). Fine-structural identification and organization of the epidermal proliferative unit. *J Cell Sci* 15: 291-319.

Alt-Holland A, Shamis Y, Riley KN, DesRochers TM, Fusenig NE, Herman IM, Garlick JA (2008). E-cadherin suppression directs cytoskeletal rearrangement and intraepithelial tumor cell migration in 3D human skin equivalents. *J Invest Dermatol* 128: 2498-507.

Anastasiadis PZ, Moon SY, Thoreson MA, Mariner DJ, Crawford HC, Zheng Y, Reynolds AB (2000). Inhibition of RhoA by p120 catenin. *Nat Cell Biol* 2: 637-44.

Anastasiadis PZ, Reynolds AB (2001). Regulation of rho GTPases by p120-catenin. *Curr Opin Cell Biol* 13: 604-10.

Ansieau S, Bastid J, Doreau A, Morel AP, Bouchet BP, Thomas C, Fauvet F, Puisieux I, Doglioni C, Piccinin S, *et al* (2008). Induction of EMT by twist proteins as a collateral effect of tumor-promoting inactivation of premature senescence. *Cancer Cell* 14: 79-89.

Anwar J, Wrone DA, Kimyai-Asadi A, Alam M (2004). The development of actinic keratosis into invasive squamous cell carcinoma: Evidence and evolving classification schemes. *Clin Dermatol* 22: 189-96.

Araujo J, Logothetis C (2010). Dasatinib: A potent SRC inhibitor in clinical development for the treatment of solid tumors. *Cancer Treat Rev* 36: 492-500.

Avizienyte E, Frame MC (2005). Src and FAK signalling controls adhesion fate and the epithelial-to-mesenchymal transition. *Curr Opin Cell Biol* 17: 542-7.

Ayli EE, Li W, Brown TT, Witkiewicz A, Elenitsas R, Seykora JT (2008). Activation of src-family tyrosine kinases in hyperproliferative epidermal disorders. *J Cutan Pathol* 35: 273-7.

Ban K, Gao Y, Amin HM, Howard A, Miller C, Lin Q, Leng X, Munsell M, Bar-Eli M, Arlinghaus RB, Chandra J (2008). BCR-ABL1 mediates up-regulation of fyn in chronic myelogenous leukemia. *Blood* 111: 2904-8.

Barbacid M (1987). Ras genes. *Annu Rev Biochem* 56: 779-827.

Behrens J, Vakaet L, Friis R, Winterhager E, Van Roy F, Mareel MM, Birchmeier W (1993). Loss of epithelial differentiation and gain of invasiveness correlates with tyrosine phosphorylation of the E-cadherin/beta-catenin complex in cells transformed with a temperature-sensitive v-SRC gene. *J Cell Biol* 120: 757-66.

Bhawan J (2007). Squamous cell carcinoma in situ in skin: What does it mean? *J Cutan Pathol* 34: 953-5.

Bjorge JD, Jakymiw A, Fujita DJ (2000). Selected glimpses into the activation and function of src kinase. *Oncogene* 19: 5620-35.

Boukamp P (2005). Non-melanoma skin cancer: What drives tumor development and progression? *Carcinogenesis* 26: 1657-67.

Bourguignon LY, Wong G, Earle C, Krueger K, Spevak CC (2010). Hyaluronan-CD44 interaction promotes c-src-mediated twist signaling, microRNA-10b expression, and RhoA/RhoC up-regulation, leading to rho-kinase-associated cytoskeleton activation and breast tumor cell invasion. *J Biol Chem* 285: 36721-35.

Bouwes Bavinck JN, Hardie DR, Green A, Cutmore S, MacNaught A, O'Sullivan B, Siskind V, Van Der Woude FJ, Hardie IR (1996). The risk of skin cancer in renal transplant recipients in queensland, australia. A follow-up study. *Transplantation* 61: 715-21.

Brandt D, Gimona M, Hillmann M, Haller H, Mischak H (2002). Protein kinase C induces actin reorganization via a src- and rho-dependent pathway. *J Biol Chem* 277: 20903-10.

Brignatz C, Paronetto MP, Opi S, Cappellari M, Audebert S, Feuillet V, Bismuth G, Roche S, Arold ST, Sette C, Collette Y (2009). Alternative splicing modulates autoinhibition and SH3 accessibility in the src kinase fyn. *Mol Cell Biol* 29: 6438-48.

Bromann PA, Korkaya H, Courtneidge SA (2004). The interplay between src family kinases and receptor tyrosine kinases. *Oncogene* 23: 7957-68.

Brown K, Buchmann A, Balmain A (1990). Carcinogen-induced mutations in the mouse c-ha-ras gene provide evidence of multiple pathways for tumor progression. *Proc Natl Acad Sci U S A* 87: 538-42.

Brownlow N, Mol C, Hayford C, Ghaem-Maghami S, Dibb NJ (2009). Dasatinib is a potent inhibitor of tumour-associated macrophages, osteoclasts and the FMS receptor. *Leukemia* 23: 590-4.

Brunton VG, Avizienyte E, Fincham VJ, Serrels B, Metcalf CA,3rd, Sawyer TK, Frame MC (2005). Identification of src-specific phosphorylation site on focal adhesion kinase: Dissection of the role of src SH2 and catalytic functions and their consequences for tumor cell behavior. *Cancer Res* 65: 1335-42.

Buettner R, Mesa T, Vultur A, Lee F, Jove R (2008). Inhibition of src family kinases with dasatinib blocks migration and invasion of human melanoma cells. *Mol Cancer Res* 6: 1766-74.

Butani AK, Arbesfeld DM, Schwartz RA (2005). Premalignant and early squamous cell carcinoma. *Clin Plast Surg* 32: 223-35.

Cabodi S, Calautti E, Talora C, Kuroki T, Stein PL, Dotto GP (2000). A PKC-h/fyn-dependent pathway leading to keratinocyte growth arrest and differentiation. *Mol Cell* 6: 1121-9.

Calautti E, Cabodi S, Stein PL, Hatzfeld M, Kedersha N, Paolo DG (1998). Tyrosine phosphorylation and src family kinases control keratinocyte cell-cell adhesion. *J Cell Biol* 141: 1449-65.

Calautti E, Grossi M, Mammucari C, Aoyama Y, Pirro M, Ono Y, Li J, Dotto GP (2002). Fyn tyrosine kinase is a downstream mediator of rho/PRK2 function in keratinocyte cell-cell adhesion. *J Cell Biol* 156: 137-48.

Calautti E, Missero C, Stein PL, Ezzell RM, Dotto GP (1995). Fyn tyrosine kinase is involved in keratinocyte differentiation control. *Genes Dev* 9: 2279-91.

Campbell C, Quinn AG, Ro YS, Angus B, Rees JL (1993). p53 mutations are common and early events that precede tumor invasion in squamous cell neoplasia of the skin. *J Invest Dermatol* 100: 746-8.

Cary LA, Chang JF, Guan JL (1996). Stimulation of cell migration by overexpression of focal adhesion kinase and its association with src and fyn. *J Cell Sci* 109 (Pt 7): 1787-94.

Cary LA, Klinghoffer RA, Sachsenmaier C, Cooper JA (2002). SRC catalytic but not scaffolding function is needed for integrin-regulated tyrosine phosphorylation, cell migration, and cell spreading. *Mol Cell Biol* 22: 2427-40.

Castano J, Solanas G, Casagolda D, Raurell I, Villagrasa P, Bustelo XR, Garcia dH, Dunach M (2007). Specific phosphorylation of p120-catenin regulatory domain differently modulates its binding to RhoA. *Mol Cell Biol* 27: 1745-57.

Chan D, Tyner JW, Chng WJ, Bi C, Okamoto R, Said J, Ngan BD, Braunstein GD, Koeffler HP (2012). Effect of dasatinib against thyroid cancer cell lines in vitro and a xenograft model in vivo. *Oncol Lett* 3: 807-15.

Chen Y, Chen CH, Tung PY, Huang SH, Wang SM (2009a). An acidic extracellular pH disrupts adherens junctions in HepG2 cells by src kinases-dependent modification of E-cadherin. *J Cell Biochem* 108: 851-9.

Chen ZY, Cai L, Bie P, Wang SG, Jiang Y, Dong JH, Li XW (2009b). Roles of fyn in pancreatic cancer metastasis. *J Gastroenterol Hepatol* 25: 293-301.

Chen ZY, Cai L, Zhu J, Chen M, Chen J, Li ZH, Liu XD, Wang SG, Bie P, Jiang P, Dong JH, Li XW (2011). Fyn requires HnRNPA2B1 and Sam68 to synergistically regulate apoptosis in pancreatic cancer. *Carcinogenesis* 32: 1419-26.

Cheng GZ, Zhang WZ, Sun M, Wang Q, Coppola D, Mansour M, Xu LM, Costanzo C, Cheng JQ, Wang LH (2008). Twist is transcriptionally induced by activation of STAT3 and mediates STAT3 oncogenic function. *J Biol Chem* 283: 14665-73.

Clark K, Langeslag M, Figdor CG, van Leeuwen FN (2007). Myosin II and mechanotransduction: A balancing act. *Trends Cell Biol* 17: 178-86.

Clayman GL, Lee JJ, Holsinger FC, Zhou X, Duvic M, El-Naggar AK, Prieto VG, Altamirano E, Tucker SL, Strom SS, Kripke ML, Lippman SM (2005). Mortality risk from squamous cell skin cancer. *J Clin Oncol* 23: 759-65.

Colicelli J (2004). Human RAS superfamily proteins and related GTPases. *Sci STKE* 2004: RE13.

Cozzolino M, Stagni V, Spinardi L, Campioni N, Fiorentini C, Salvati E, Alema S, Salvatore AM (2003). p120 catenin is required for growth factor-dependent cell motility and scattering in epithelial cells. *Mol Biol Cell* 14: 1964-77.

Croxton R, Ma Y, Cress WD (2002). Differences in DNA binding properties between E2F1 and E2F4 specify repression of the mcl-1 promoter. *Oncogene* 21: 1563-70.

Dajee M, Tarutani M, Deng H, Cai T, Khavari PA (2002). Epidermal ras blockade demonstrates spatially localized ras promotion of proliferation and inhibition of differentiation. *Oncogene* 21: 1527-38.

Davidson D, Viallet J, Veillette A (1994). Unique catalytic properties dictate the enhanced function of p59fynT, the hemopoietic cell-specific isoform of the fyn tyrosine protein kinase, in T cells. *Mol Cell Biol* 14: 4554-64.

D'Costa AM, Robinson JK, Maududi T, Chaturvedi V, Nickoloff BJ, Denning MF (2006). The proapoptotic tumor suppressor protein kinase C-δ is lost in human squamous cell carcinomas. *Oncogene* 25: 378-86.

Demetri GD, Lo Russo P, MacPherson IR, Wang D, Morgan JA, Brunton VG, Paliwal P, Agrawal S, Voi M, Evans TR (2009). Phase I dose-escalation and pharmacokinetic study of dasatinib in patients with advanced solid tumors. *Clin Cancer Res* 15: 6232-40.

Denning MF, Dlugosz AA, Williams EK, Szallasi Z, Blumberg PM, Yuspa SH (1995). Specific protein kinase C isozymes mediate the induction of keratinocyte differentiation markers by calcium. *Cell Growth Differ* 6: 149-57.

Diepgen TL, Mahler V (2002). The epidemiology of skin cancer. *Br J Dermatol* 146 Suppl 61: 1-6.

Dotto GP (1999). Signal transduction pathways controlling the switch between keratinocyte growth and differentiation. *Crit Rev Oral Biol Med* 10: 442-57.

Downward J (2003). Targeting RAS signalling pathways in cancer therapy. *Nat Rev Cancer* 3: 11-22.

Drosten M, Lechuga CG, Barbacid M (2013a). Genetic analysis of ras genes in epidermal development and tumorigenesis. *Small GTPases* 4: .

Drosten M, Lechuga CG, Barbacid M (2013b). Ras signaling is essential for skin development. *Oncogene*.

Eckert RL (1989). Structure, function, and differentiation of the keratinocyte. *Physiol Rev* 69: 1316-46.

Eckert RL, Rorke EA (1989). Molecular biology of keratinocyte differentiation. *Environ Health Perspect* 80: 109-16.

Elias PM, Fritsch P, Epstein EH (1977). Staphylococcal scalded skin syndrome. clinical features, pathogenesis, and recent microbiological and biochemical developments. *Arch Dermatol* 113: 207-19.

Enkhbaatar Z, Terashima M, Oktyabri D, Tange S, Ishimura A, Yano S, Suzuki T (2013). KDM5B histone demethylase controls epithelial-mesenchymal transition of cancer cells by regulating the expression of the microRNA-200 family. *Cell Cycle* 12: 2100-12.

Esteban LM, Vicario-Abejon C, Fernandez-Salguero P, Fernandez-Medarde A, Swaminathan N, Yienger K, Lopez E, Malumbres M, McKay R, Ward JM, Pellicer A, Santos E (2001). Targeted genomic disruption of H-ras and N-ras, individually or in combination, reveals the dispensability of both loci for mouse growth and development. *Mol Cell Biol* 21: 1444-52.

Forslind B, Lindberg M, Roomans GM, Pallon J, Werner-Linde Y (1997). Aspects on the physiology of human skin: Studies using particle probe analysis. *Microsc Res Tech* 38: 373-86.

Frame MC (2004). Newest findings on the oldest oncogene; how activated src does it. *J Cell Sci* 117: 989-98.

Frame MC (2002). Src in cancer: Deregulation and consequences for cell behaviour. *Biochim Biophys Acta* 1602: 114-30.

Frisch SM (2008). Caspase-8: Fly or die. *Cancer Res* 68: 4491-3.

Fuchs E (2008). Skin stem cells: Rising to the surface. *J Cell Biol* 180: 273-84.

Fujita Y, Krause G, Scheffner M, Zechner D, Leddy HE, Behrens J, Sommer T, Birchmeier W (2002). Hakai, a c-cbl-like protein, ubiquitinates and induces endocytosis of the E-cadherin complex. *Nat Cell Biol* 4: 222-31.

Gagnoux-Palacios L, Dans M, van't Hof W, Mariotti A, Pepe A, Meneguzzi G, Resh MD, Giancotti FG (2003). Compartmentalization of integrin alpha6beta4 signaling in lipid rafts. *J Cell Biol* 162: 1189-96.

Gao Y, Howard A, Ban K, Chandra J (2009). Oxidative stress promotes transcriptional up-regulation of fyn in BCR-ABL1-expressing cells. *J Biol Chem* 284: 7114-25.

Ghazizadeh S, Taichman LB (2005). Organization of stem cells and their progeny in human epidermis. *J Invest Dermatol* 124: 367-72.

Glick D, Barth S, Macleod KF (2010). Autophagy: Cellular and molecular mechanisms. *J Pathol* 221: 3-12.

Gloster HM,Jr, Brodland DG (1996). The epidemiology of skin cancer. *Dermatol Surg* 22: 217-26.

Gnoni A, Marech I, Silvestris N, Vacca A, Lorusso V (2011). Dasatinib: An anti-tumour agent via src inhibition. *Curr Drug Targets* 12: 563-78.

Goldsmith JF, Hall CG, Atkinson TP (2002). Identification of an alternatively spliced isoform of the fyn tyrosine kinase. *Biochem Biophys Res Commun* 298: 501-4.

Green A (1992). Changing patterns in incidence of non-melanoma skin cancer. *Epithelial Cell Biol* 1: 47-51.

Grewal T, Koese M, Tebar F, Enrich C (2011). Differential regulation of RasGAPs in cancer. *Genes Cancer* 2: 288-97.

Grosheva I, Shtutman M, Elbaum M, Bershadsky AD (2001). p120 catenin affects cell motility via modulation of activity of rho-family GTPases: A link between cell-cell contact formation and regulation of cell locomotion. *J Cell Sci* 114: 695-707.

Guarino M (2010). Src signaling in cancer invasion. *J Cell Physiol* 223: 14-26.

Guarino M, Rubino B, Ballabio G (2007). The role of epithelial-mesenchymal transition in cancer pathology. *Pathology* 39: 305-18.

Hancock JF, Parton RG (2005). Ras plasma membrane signalling platforms. *Biochem J* 389: 1-11.

Harr MW, McColl KS, Zhong F, Molitoris JK, Distelhorst CW (2010). Glucocorticoids downregulate fyn and inhibit IP(3)-mediated calcium signaling to promote autophagy in T lymphocytes. *Autophagy* 6: 912-21.

Hobbs RP, Amargo EV, Somasundaram A, Simpson CL, Prakriya M, Denning MF, Green KJ (2011). The calcium ATPase SERCA2 regulates desmoplakin dynamics and

intercellular adhesive strength through modulation of PKCα signaling. *FASEB J* 25: 990-1001.

Hole PS, Pearn L, Tonks AJ, James PE, Burnett AK, Darley RL, Tonks A (2010). Ras-induced reactive oxygen species promote growth factor-independent proliferation in human CD34+ hematopoietic progenitor cells. *Blood* 115: 1238-46.

Hollstein M, Sidransky D, Vogelstein B, Harris CC (1991). p53 mutations in human cancers. *Science* 253: 49-53.

Houben E, De Paepe K, Rogiers V (2007). A keratinocyte's course of life. *Skin Pharmacol Physiol* 20: 122-32.

Hu P, O'Keefe EJ, Rubenstein DS (2001). Tyrosine phosphorylation of human keratinocyte beta-catenin and plakoglobin reversibly regulates their binding to E-cadherin and alpha-catenin. *J Invest Dermatol* 117: 1059-67.

Huang FI, Chen YL, Chang CN, Yuan RH, Jeng YM (2012). Hepatocyte growth factor activates wnt pathway by transcriptional activation of LEF1 to facilitate tumor invasion. *Carcinogenesis* 33: 1142-8.

Huang J, Asawa T, Takato T, Sakai R (2003). Cooperative roles of fyn and cortactin in cell migration of metastatic murine melanoma. *J Biol Chem* 278: 48367-76.

Huveneers S, Danen EH (2009). Adhesion signaling - crosstalk between integrins, src and rho. *J Cell Sci* 122: 1059-69.

Ilic D, Kanazawa S, Nishizumi H, Aizawa S, Kuroki T, Mori S, Yamamoto T (1997). Skin abnormality in aged fyn-/- fak+/- mice. *Carcinogenesis* 18: 1473-6.

Ingley E (2008). Src family kinases: Regulation of their activities, levels and identification of new pathways. *Biochim Biophys Acta* 1784: 56-65.

International Agency for Research on Cancer Working Group on artificial ultraviolet (UV) light and skin cancer (2007). The association of use of sunbeds with cutaneous malignant melanoma and other skin cancers: A systematic review. *Int J Cancer* 120: 1116-22.

Irby RB, Mao W, Coppola D, Kang J, Loubeau JM, Trudeau W, Karl R, Fujita DJ, Jove R, Yeatman TJ (1999). Activating SRC mutation in a subset of advanced human colon cancers. *Nat Genet* 21: 187-90.

Ise K, Nakamura K, Nakao K, Shimizu S, Harada H, Ichise T, Miyoshi J, Gondo Y, Ishikawa T, Aiba A, Katsuki M (2000). Targeted deletion of the H-ras gene decreases tumor formation in mouse skin carcinogenesis. *Oncogene* 19: 2951-6.

Jensen AR, David SY, Liao C, Dai J, Keller ET, Al-Ahmadie H, Dakin-Hache K, Usatyuk P, Sievert MF, Paner GP, *et al* (2011). Fyn is downstream of the HGF/MET signaling axis and affects cellular shape and tropism in PC3 cells. *Clin Cancer Res* 17: 3112-22.

Jerant AF, Johnson JT, Sheridan CD, Caffrey TJ (2000). Early detection and treatment of skin cancer. *Am Fam Physician* 62: 357,68, 375-6, 381-2.

Jiang W, Ananthaswamy HN, Muller HK, Kripke ML (1999). p53 protects against skin cancer induction by UV-B radiation. *Oncogene* 18: 4247-53.

Joannes A, Grelet S, Duca L, Gilles C, Kileztky C, Dalstein V, Birembaut P, Polette M, Nawrocki-Raby B (2014). Fhit regulates EMT targets through an EGFR/src/ERK/slug signaling axis in human bronchial cells. *Mol Cancer Res*.

Johnson L, Greenbaum D, Cichowski K, Mercer K, Murphy E, Schmitt E, Bronson RT, Umanoff H, Edelmann W, Kucherlapati R, Jacks T (1997). K-ras is an essential gene in the mouse with partial functional overlap with N-ras. *Genes Dev* 11: 2468-81.

Jonason AS, Kunala S, Price GJ, Restifo RJ, Spinelli HM, Persing JA, Leffell DJ, Tarone RE, Brash DE (1996a). Frequent clones of p53-mutated keratinocytes in normal human skin. *Proc Natl Acad Sci U S A* 93: 14025-9.

Jonason AS, Kunala S, Price GJ, Restifo RJ, Spinelli HM, Persing JA, Leffell DJ, Tarone RE, Brash DE (1996b). Frequent clones of p53-mutated keratinocytes in normal human skin. *Proc Natl Acad Sci U S A* 93: 14025-9.

Kaibuchi K, Kuroda S, Amano M (1999). Regulation of the cytoskeleton and cell adhesion by the rho family GTPases in mammalian cells. *Annu Rev Biochem* 68: 459-86.

Kalluri R, Weinberg RA (2009a). The basics of epithelial-mesenchymal transition. *J Clin Invest* 119: 1420-8.

Kalluri R, Weinberg RA (2009b). The basics of epithelial-mesenchymal transition. *J Clin Invest* 119: 1420-8.

Kelfkens G, de Gruijl FR, van der Leun JC (1990). Ozone depletion and increase in annual carcinogenic ultraviolet dose. *Photochem Photobiol* 52: 819-23.

Kern F, Niault T, Baccarini M (2011). Ras and raf pathways in epidermis development and carcinogenesis. *Br J Cancer* 104: 229-34.

Khavari TA, Rinn J (2007). Ras/erk MAPK signaling in epidermal homeostasis and neoplasia. *Cell Cycle* 6: 2928-31.

Kim AN, Jeon WK, Lim KH, Lee HY, Kim WJ, Kim BC (2011). Fyn mediates transforming growth factor-beta1-induced down-regulation of E-cadherin in human A549 lung cancer cells. *Biochem Biophys Res Commun* 407: 181-4.

Kim HJ, Warren JT, Kim SY, Chappel JC, DeSelm CJ, Ross FP, Zou W, Teitelbaum SL (2010). Fyn promotes proliferation, differentiation, survival and function of osteoclast lineage cells. *J Cell Biochem* 111: 1107-13.

Kim LC, Song L, Haura EB (2009). Src kinases as therapeutic targets for cancer. *Nat.Rev.Clin.Oncol.* 6: 587-95.

Kim MS, Kim GM, Choi YJ, Kim HJ, Kim YJ, Jin W (2013). C-src activation through a TrkA and c-src interaction is essential for cell proliferation and hematological malignancies. *Biochem Biophys Res Commun* 441: 431-7.

Klein-Szanto AJ (1989). Pathology of human and experimental skin tumors. *Carcinog Compr Surv* 11: 19-53.

Kostic A, Sheetz MP (2006). Fibronectin rigidity response through fyn and p130Cas recruitment to the leading edge. *Mol Biol Cell* 17: 2684-95.

Krause G, Hallek M (2011). On the assessment of dasatinib-induced autophagy in CLL. *Leuk Res* 35: 137-8.

Kripke ML (1988). Impact of ozone depletion on skin cancers. *J Dermatol Surg Oncol* 14: 853-7.

Lamouille S, Xu J, Derynck R (2014). Molecular mechanisms of epithelial-mesenchymal transition. *Nat Rev Mol Cell Biol* 15: 178-96.

Lampugnani MG, Corada M, Andriopoulou P, Esser S, Risau W, Dejana E (1997). Cell confluence regulates tyrosine phosphorylation of adherens junction components in endothelial cells. *J Cell Sci* 110 (Pt 17): 2065-77.

Le XF, Mao W, Lu Z, Carter BZ, Bast RC,Jr. (2010). Dasatinib induces autophagic cell death in human ovarian cancer. *Cancer* 116: 4980-90.

LeBoeuf NR, Schmults CD (2011). Update on the management of high-risk squamous cell carcinoma. *Semin Cutan Med Surg* 30: 26-34.

Lee JH, Pyon JK, Kim DW, Lee SH, Nam HS, Kim CH, Kang SG, Lee YJ, Park MY, Jeong DJ, Cho MK (2010). Elevated c-src and c-yes expression in malignant skin cancers. *J Exp Clin Cancer Res* 29: 116,9966-29-116.

Lee YS, Dlugosz AA, McKay R, Dean NM, Yuspa SH (1997). Definition by specific antisense oligonucleotides of a role for protein kinase C α in expression of differentiation markers in normal and neoplastic mouse epidermal keratinocytes. *Mol Carcinog* 18: 44-53.

Lehembre F, Yilmaz M, Wicki A, Schomber T, Strittmatter K, Ziegler D, Kren A, Went P, Derksen PW, Berns A, Jonkers J, Christofori G (2008). NCAM-induced focal adhesion assembly: A functional switch upon loss of E-cadherin. *EMBO J* 27: 2603-15.

Lentini M, Schepis C, Cuppari DA, Batolo D (2006). Tenascin expression in actinic keratosis. *J Cutan Pathol* 33: 716-20.

Lewin B, Siu A, Baker C, Dang D, Schnitt R, Eisapooran P, Ramos DM (2010). Expression of fyn kinase modulates EMT in oral cancer cells. *Anticancer Res* 30: 2591-6.

Lewis JE, Jensen PJ, Wheelock MJ (1994). Cadherin function is required for human keratinocytes to assemble desmosomes and stratify in response to calcium. *J Invest Dermatol* 102: 870-7.

Li J, Rix U, Fang B, Bai Y, Edwards A, Colinge J, Bennett KL, Gao J, Song L, Eschrich S, *et al* (2010). A chemical and phosphoproteomic characterization of dasatinib action in lung cancer. *Nat.Chem.Biol.* 6: 291-9.

Li W, Marshall C, Mei L, Dzubow L, Schmults C, Dans M, Seykora J (2005). Srcasm modulates EGF and src-kinase signaling in keratinocytes. *J Biol Chem* 280: 6036-46.

Li W, Marshall C, Mei L, Gelfand J, Seykora JT (2007). Srcasm corrects fyn-induced epidermal hyperplasia by kinase down-regulation. *J Biol Chem* 282: 1161-9.

Li X, Yang Y, Hu Y, Dang D, Regezi J, Schmidt BL, Atakilit A, Chen B, Ellis D, Ramos DM (2003). Avß6-fyn signaling promotes oral cancer progression. *J Biol Chem* 278: 41646-53.

Liang X, Draghi NA, Resh MD (2004). Signaling from integrins to fyn to rho family GTPases regulates morphologic differentiation of oligodendrocytes. *J Neurosci* 24: 7140-9.

Lilien J, Balsamo J (2005). The regulation of cadherin-mediated adhesion by tyrosine phosphorylation/dephosphorylation of ß-catenin. *Curr Opin Cell Biol* 17: 459-65.

Liotta LA, Tryggvason K, Garbisa S, Hart I, Foltz CM, Shafie S (1980). Metastatic potential correlates with enzymatic degradation of basement membrane collagen. *Nature* 284: 67-8.

Liu X, Feng R (2010). Inhibition of epithelial to mesenchymal transition in metastatic breast carcinoma cells by c-src suppression. *Acta Biochim Biophys Sin (Shanghai)* 42: 496-501.

Lombardo LJ, Lee FY, Chen P, Norris D, Barrish JC, Behnia K, Castaneda S, Cornelius LA, Das J, Doweyko AM, *et al* (2004). Discovery of N-(2-chloro-6-methyl- phenyl)-2-(6-(4-(2-hydroxyethyl)- piperazin-1-yl)-2-methylpyrimidin-4- ylamino)thiazole-5-carboxamide (BMS-354825), a dual src/abl kinase inhibitor with potent antitumor activity in preclinical assays. *J Med Chem* 47: 6658-61.

Lu KV, Zhu S, Cvrljevic A, Huang TT, Sarkaria S, Ahkavan D, Dang J, Dinca EB, Plaisier SB, Oderberg I, *et al* (2009). Fyn and src are effectors of oncogenic epidermal growth factor receptor signaling in glioblastoma patients. *Cancer Res* 69: 6889-98.

Madison KC (2003). Barrier function of the skin: "La raison d'etre" of the epidermis. *J Invest Dermatol* 121: 231-41.

Mandal M, Myers JN, Lippman SM, Johnson FM, Williams MD, Rayala S, Ohshiro K, Rosenthal DI, Weber RS, Gallick GE, El-Naggar AK (2008). Epithelial to mesenchymal transition in head and neck squamous carcinoma: Association of src activation with E-cadherin down-regulation, vimentin expression, and aggressive tumor features. *Cancer* 112: 2088-100.

Mariner DJ, Davis MA, Reynolds AB (2004). EGFR signaling to p120-catenin through phosphorylation at Y228. *J Cell Sci* 117: 1339-50.

Mariotti A, Kedeshian PA, Dans M, Curatola AM, Gagnoux-Palacios L, Giancotti FG (2001). EGF-R signaling through fyn kinase disrupts the function of integrin α6ß4 at hemidesmosomes: Role in epithelial cell migration and carcinoma invasion. *J Cell Biol* 155: 447-58.

Marks R, Rennie G, Selwood TS (1988). Malignant transformation of solar keratoses to squamous cell carcinoma. *Lancet* 1: 795-7.

Martin FT, Dwyer RM, Kelly J, Khan S, Murphy JM, Curran C, Miller N, Hennessy E, Dockery P, Barry FP, O'Brien T, Kerin MJ (2010). Potential role of mesenchymal stem cells (MSCs) in the breast tumour microenvironment: Stimulation of epithelial to mesenchymal transition (EMT). *Breast Cancer Res Treat* 124: 317-26.

Matsumoto T, Kiguchi K, Jiang J, Carbajal S, Ruffino L, Beltran L, Wang XJ, Roop DR, DiGiovanni J (2004). Development of transgenic mice that inducibly express an active form of c-src in the epidermis. *Mol Carcinog* 40: 189-200.

Melnikova VO, Ananthaswamy HN (2005). Cellular and molecular events leading to the development of skin cancer. *Mutat Res* 571: 91-106.

Menghini R, Marchetti V, Cardellini M, Hribal ML, Mauriello A, Lauro D, Sbraccia P, Lauro R, Federici M (2005). Phosphorylation of GATA2 by akt increases adipose tissue differentiation and reduces adipose tissue-related inflammation: A novel pathway linking obesity to atherosclerosis. *Circulation* 111: 1946-53.

Menke A, Giehl K (2012). Regulation of adherens junctions by rho GTPases and p120-catenin. *Arch Biochem Biophys* 524: 48-55.

Menon GK, Elias PM, Lee SH, Feingold KR (1992). Localization of calcium in murine epidermis following disruption and repair of the permeability barrier. *Cell Tissue Res* 270: 503-12.

Milano V, Piao Y, LaFortune T, de Groot J (2009). Dasatinib-induced autophagy is enhanced in combination with temozolomide in glioma. *Mol Cancer Ther* 8: 394-406.

Mitra SK, Schlaepfer DD (2006). Integrin-regulated FAK-src signaling in normal and cancer cells. *Curr Opin Cell Biol* 18: 516-23.

Montero JC, Seoane S, Ocana A, Pandiella A (2011). Inhibition of SRC family kinases and receptor tyrosine kinases by dasatinib: Possible combinations in solid tumors. *Clin Cancer Res* 17: 5546-52.

Moy RL (2000). Clinical presentation of actinic keratoses and squamous cell carcinoma. *J Am Acad Dermatol* 42: 8-10.

Mullen JT, Feng L, Xing Y, Mansfield PF, Gershenwald JE, Lee JE, Ross MI, Cormier JN (2006). Invasive squamous cell carcinoma of the skin: Defining a high-risk group. *Ann Surg Oncol* 13: 902-9.

Nakamura M, Tokura Y (2011). Epithelial-mesenchymal transition in the skin. *J Dermatol Sci* 61: 7-13.

Nakazawa H, English D, Randell PL, Nakazawa K, Martel N, Armstrong BK, Yamasaki H (1994). UV and skin cancer: Specific p53 gene mutation in normal skin as a biologically relevant exposure measurement. *Proc Natl Acad Sci U S A* 91: 360-4.

Nautiyal J, Majumder P, Patel BB, Lee FY, Majumdar AP (2009). Src inhibitor dasatinib inhibits growth of breast cancer cells by modulating EGFR signaling. *Cancer Lett* 283: 143-51.

Nelson WJ (2009). Remodeling epithelial cell organization: Transitions between front-rear and apical-basal polarity. *Cold Spring Harb Perspect Biol* 1: a000513.

Newman ME (1991). Atlas maps cancer mortality among nonwhites. *J Natl Cancer Inst* 83: 89.

Nie J, Fu X, Han W (2013). Microenvironment-dependent homeostasis and differentiation of epidermal basal undifferentiated keratinocytes and their clinical applications in skin repair. *J Eur Acad Dermatol Venereol* 27: 531-5.

Nikolaou V, Stratigos AJ, Tsao H (2012). Hereditary nonmelanoma skin cancer. *Semin Cutan Med Surg* 31: 204-10.

Ninio-Many L, Grossman H, Shomron N, Chuderland D, Shalgi R (2013). microRNA-125a-3p reduces cell proliferation and migration by targeting fyn. *J Cell Sci* 126: 2867-76.

Oikarinen A, Raitio A (2000). Melanoma and other skin cancers in circumpolar areas. *Int J Circumpolar Health* 59: 52-6.

Okada M (2012). Regulation of the SRC family kinases by csk. *Int J Biol Sci* 8: 1385-97.

Osada S, Hashimoto Y, Nomura S, Kohno Y, Chida K, Tajima O, Kubo K, Akimoto K, Koizumi H, Kitamura Y, *et al* (1993). Predominant expression of the nPKCh, a Ca^{2+}-

independent isoform of protein kinase C in epithelial tissues, in association with epithelial differentiation . *Cell Growth Differ* 4: 167-75.

Owens DW, McLean GW, Wyke AW, Paraskeva C, Parkinson EK, Frame MC, Brunton VG (2000). The catalytic activity of the src family kinases is required to disrupt cadherin-dependent cell-cell contacts. *Mol Biol Cell* 11: 51-64.

Palacios F, Tushir JS, Fujita Y, D'Souza-Schorey C (2005). Lysosomal targeting of E-cadherin: A unique mechanism for the down-regulation of cell-cell adhesion during epithelial to mesenchymal transitions. *Mol Cell Biol* 25: 389-402.

Palomero T, Couronne L, Khiabanian H, Kim MY, Ambesi-Impiombato A, Perez-Garcia A, Carpenter Z, Abate F, Allegretta M, Haydu JE, *et al* (2014). Recurrent mutations in epigenetic regulators, RHOA and FYN kinase in peripheral T cell lymphomas. *Nat Genet* 46: 166-70.

Park SI, Zhang J, Phillips KA, Araujo JC, Najjar AM, Volgin AY, Gelovani JG, Kim SJ, Wang Z, Gallick GE (2008). Targeting SRC family kinases inhibits growth and lymph node metastases of prostate cancer in an orthotopic nude mouse model. *Cancer Res* 68: 3323-33.

Paulsson M (1992). Basement membrane proteins: Structure, assembly, and cellular interactions. *Crit Rev Biochem Mol Biol* 27: 93-127.

Pearce RH, Grimmer BJ (1972). Age and the chemical constitution of normal human dermis. *J Invest Dermatol* 58: 347-61.

Peng X, Guan JL (2011). Focal adhesion kinase: From in vitro studies to functional analyses in vivo. *Curr Protein Pept Sci* 12: 52-67.

Perera E, Sinclair R (2013). An estimation of the prevalence of nonmelanoma skin cancer in the U.S. *F1000Res* 2: 107,107.v1. eCollection 2013.

Piedra J, Miravet S, Castano J, Palmer HG, Heisterkamp N, Garcia dH, Dunach M (2003). p120 catenin-associated fer and fyn tyrosine kinases regulate beta-catenin tyr-142 phosphorylation and beta-catenin-alpha-catenin interaction. *Mol Cell Biol* 23: 2287-97.

Pierceall WE, Goldberg LH, Tainsky MA, Mukhopadhyay T, Ananthaswamy HN (1991). Ras gene mutation and amplification in human nonmelanoma skin cancers. *Mol Carcinog* 4: 196-202.

Playford MP, Schaller MD (2004). The interplay between src and integrins in normal and tumor biology. *Oncogene* 23: 7928-46.

Posadas EM, Al Ahmadie H, Robinson VL, Jagadeeswaran R, Otto K, Kasza KE, Tretiakov M, Siddiqui J, Pienta KJ, Stadler WM, Rinker-Schaeffer C, Salgia R (2009). FYN is overexpressed in human prostate cancer. *BJU Int* 103: 171-7.

Presland RB, Dale BA (2000). Epithelial structural proteins of the skin and oral cavity: Function in health and disease. *Crit Rev Oral Biol Med* 11: 383-408.

Proksch E, Brandner JM, Jensen JM (2008). The skin: An indispensable barrier. *Exp Dermatol* 17: 1063-72.

Radisky DC (2005). Epithelial-mesenchymal transition. *J Cell Sci* 118: 4325-6.

Rajalingam K, Schreck R, Rapp UR, Albert S (2007). Ras oncogenes and their downstream targets. *Biochim Biophys Acta* 1773: 1177-95.

Rasmussen I, Pedersen LH, Byg L, Suzuki K, Sumimoto H, Vilhardt F (2010). Effects of F/G-actin ratio and actin turn-over rate on NADPH oxidase activity in microglia. *BMC Immunol* 11: 44,2172-11-44.

Ratushny V, Gober MD, Hick R, Ridky TW, Seykora JT (2012). From keratinocyte to cancer: The pathogenesis and modeling of cutaneous squamous cell carcinoma. *J Clin Invest* 122: 464-72.

Ravnbak MH (2010). Objective determination of fitzpatrick skin type. *Dan Med Bull* 57: B4153.

Rengifo-Cam W, Konishi A, Morishita N, Matsuoka H, Yamori T, Nada S, Okada M (2004). Csk defines the ability of integrin-mediated cell adhesion and migration in human colon cancer cells: Implication for a potential role in cancer metastasis. *Oncogene* 23: 289-97.

Rivat C, Le Floch N, Sabbah M, Teyrol I, Redeuilh G, Bruyneel E, Mareel M, Matrisian LM, Crawford HC, Gespach C, Attoub S (2003). Synergistic cooperation between the AP-1 and LEF-1 transcription factors in activation of the matrilysin promoter by the src oncogene: Implications in cellular invasion. *FASEB J* 17: 1721-3.

Robert C, Arnault JP, Mateus C (2011). RAF inhibition and induction of cutaneous squamous cell carcinoma. *Curr Opin Oncol* 23: 177-82.

Rogers HW, Weinstock MA, Harris AR, Hinckley MR, Feldman SR, Fleischer AB, Coldiron BM (2010a). Incidence estimate of nonmelanoma skin cancer in the united states, 2006. *Arch Dermatol* 146: 283-7.

Rogers HW, Weinstock MA, Harris AR, Hinckley MR, Feldman SR, Fleischer AB, Coldiron BM (2010b). Incidence estimate of nonmelanoma skin cancer in the united states, 2006. *Arch Dermatol* 146: 283-7.

Roura S, Miravet S, Piedra J, Garcia de Herreros A, Dunach M (1999). Regulation of E-cadherin/catenin association by tyrosine phosphorylation. *J Biol Chem* 274: 36734-40.

Saito YD, Jensen AR, Salgia R, Posadas EM (2010). Fyn: A novel molecular target in cancer. *Cancer* 116: 1629-37.

Salasche SJ (2000). Epidemiology of actinic keratoses and squamous cell carcinoma. *J Am Acad Dermatol* 42: 4-7.

Saunders LR, McClay DR (2014). Sub-circuits of a gene regulatory network control a developmental epithelial-mesenchymal transition. *Development* 141: 1503-13.

Scanlon CS, Van Tubergen EA, Inglehart RC, D'Silva NJ (2013). Biomarkers of epithelial-mesenchymal transition in squamous cell carcinoma. *J Dent Res* 92: 114-21.

Schade AE, Schieven GL, Townsend R, Jankowska AM, Susulic V, Zhang R, Szpurka H, Maciejewski JP (2008). Dasatinib, a small-molecule protein tyrosine kinase inhibitor, inhibits T-cell activation and proliferation. *Blood* 111: 1366-77.

Schaller MD, Hildebrand JD, Parsons JT (1999). Complex formation with focal adhesion kinase: A mechanism to regulate activity and subcellular localization of src kinases. *Mol Biol Cell* 10: 3489-505.

Schenone S, Brullo C, Musumeci F, Biava M, Falchi F, Botta M (2011). Fyn kinase in brain diseases and cancer: The search for inhibitors. *Curr Med Chem* 18: 2921-42.

Schober M, Raghavan S, Nikolova M, Polak L, Pasolli HA, Beggs HE, Reichardt LF, Fuchs E (2007). Focal adhesion kinase modulates tension signaling to control actin and focal adhesion dynamics. *J Cell Biol* 176: 667-80.

Sekulic A, Kim SY, Hostetter G, Savage S, Einspahr JG, Prasad A, Sagerman P, Curiel-Lewandrowski C, Krouse R, Bowden GT, *et al* (2010). Loss of inositol polyphosphate 5-phosphatase is an early event in development of cutaneous squamous cell carcinoma. *Cancer Prev Res (Phila)* 3: 1277-83.

Semba K, Nishizawa M, Miyajima N, Yoshida MC, Sukegawa J, Yamanashi Y, Sasaki M, Yamamoto T, Toyoshima K (1986). Yes-related protooncogene, syn, belongs to the protein-tyrosine kinase family. *Proc Natl Acad Sci U S A* 83: 5459-63.

Serrels A, Canel M, Brunton VG, Frame MC (2011). Src/FAK-mediated regulation of E-cadherin as a mechanism for controlling collective cell movement: Insights from in vivo imaging. *Cell Adh Migr* 5: 360-5.

Serrels B, Serrels A, Mason SM, Baldeschi C, Ashton GH, Canel M, Mackintosh LJ, Doyle B, Green TP, Frame MC, Sansom OJ, Brunton VG (2009). A novel src kinase inhibitor reduces tumour formation in a skin carcinogenesis model. *Carcinogenesis* 30: 249-57.

Sharma A, Mayer BJ (2008). Phosphorylation of p130Cas initiates rac activation and membrane ruffling. *BMC Cell Biol* 9: 50,2121-9-50.

Shima T, Nada S, Okada M (2003). Transmembrane phosphoprotein cbp senses cell adhesion signaling mediated by src family kinase in lipid rafts. *Proc Natl Acad Sci U S A* 100: 14897-902.

Shimokawa M, Haraguchi M, Kobayashi W, Higashi Y, Matsushita S, Kawai K, Kanekura T, Ozawa M (2013). The transcription factor snail expressed in cutaneous squamous cell carcinoma induces epithelial-mesenchymal transition and down-regulates COX-2. *Biochem Biophys Res Commun* 430: 1078-82.

Singh MM, Howard A, Irwin ME, Gao Y, Lu X, Multani A, Chandra J (2012). Expression and activity of fyn mediate proliferation and blastic features of chronic myelogenous leukemia. *PLoS One* 7: e51611.

Sirvent A, Benistant C, Roche S (2012). Oncogenic signaling by tyrosine kinases of the SRC family in advanced colorectal cancer. *Am J Cancer Res* 2: 357-71.

Smit MA, Peeper DS (2008). Deregulating EMT and senescence: Double impact by a single twist. *Cancer Cell* 14: 5-7.

Smith KJ, Haley H, Hamza S, Skelton HG (2009). Eruptive keratoacanthoma-type squamous cell carcinomas in patients taking sorafenib for the treatment of solid tumors. *Dermatol Surg* 35: 1766-70.

Song H, Hollstein M, Xu Y (2007). p53 gain-of-function cancer mutants induce genetic instability by inactivating ATM. *Nat Cell Biol* 9: 573-80.

Spinardi L, Rietdorf J, Nitsch L, Bono M, Tacchetti C, Way M, Marchisio PC (2004). A dynamic podosome-like structure of epithelial cells. *Exp Cell Res* 295: 360-74.

Staal FJ, Clevers H (2000). Tcf/lef transcription factors during T-cell development: Unique and overlapping functions. *Hematol J* 1: 3-6.

Takayama T, Mogi Y, Kogawa K, Yoshizaki N, Muramatsu H, Koike K, Semba K, Yamamoto T, Niitsu Y (1993). A role for the fyn oncogene in metastasis of methylcholanthrene-induced fibrosarcoma A cells. *Int J Cancer* 54: 875-9.

Talantov D, Mazumder A, Yu JX, Briggs T, Jiang Y, Backus J, Atkins D, Wang Y (2005). Novel genes associated with malignant melanoma but not benign melanocytic lesions. *Clin Cancer Res* 11: 7234-42.

Tang X, Feng Y, Ye K (2007). Src-family tyrosine kinase fyn phosphorylates phosphatidylinositol 3-kinase enhancer-activating akt, preventing its apoptotic cleavage and promoting cell survival. *Cell Death Differ* 14: 368-77.

Taniguchi S, Liu H, Nakazawa T, Yokoyama K, Tezuka T, Yamamoto T (2003). p250GAP, a neural RhoGAP protein, is associated with and phosphorylated by fyn. *Biochem Biophys Res Commun* 306: 151-5.

Tao YS, Edwards RA, Tubb B, Wang S, Bryan J, McCrea PD (1996). Beta-catenin associates with the actin-bundling protein fascin in a noncadherin complex. *J Cell Biol* 134: 1271-81.

Thiery JP (2002). Epithelial-mesenchymal transitions in tumour progression. *Nat Rev Cancer* 2: 442-54.

Thomas SM, Brugge JS (1997). Cellular functions regulated by src family kinases. *Annu Rev Cell Dev Biol* 13: 513-609.

Toll A, Masferrer E, Hernandez-Ruiz ME, Ferrandiz-Pulido C, Yebenes M, Jaka A, Tuneu A, Jucgla A, Gimeno J, Baro T, *et al* (2013). Epithelial to mesenchymal transition markers are associated with an increased metastatic risk in primary cutaneous squamous cell carcinomas but are attenuated in lymph node metastases. *J Dermatol Sci* 72: 93-102.

Toll A, Salgado R, Yebenes M, Martin-Ezquerra G, Gilaberte M, Baro T, Sole F, Alameda F, Espinet B, Pujol RM (2010). Epidermal growth factor receptor gene numerical aberrations are frequent events in actinic keratoses and invasive cutaneous squamous cell carcinomas. *Exp Dermatol* 19: 151-3.

Toll A, Salgado R, Yebenes M, Martin-Ezquerra G, Gilaberte M, Baro T, Sole F, Alameda F, Espinet B, Pujol RM (2009). MYC gene numerical aberrations in actinic keratosis and cutaneous squamous cell carcinoma. *Br J Dermatol* 161: 1112-8.

Tse JC, Kalluri R (2007). Mechanisms of metastasis: Epithelial-to-mesenchymal transition and contribution of tumor microenvironment. *J Cell Biochem* 101: 816-29.

Tu CL, Chang W, Bikle DD (2011). The calcium-sensing receptor-dependent regulation of cell-cell adhesion and keratinocyte differentiation requires rho and filamin A. *J Invest Dermatol* 131: 1119-28.

Tu CL, Chang W, Xie Z, Bikle DD (2008). Inactivation of the calcium sensing receptor inhibits E-cadherin-mediated cell-cell adhesion and calcium-induced differentiation in human epidermal keratinocytes. *J Biol Chem* 283: 3519-28.

Tu CL, Oda Y, Komuves L, Bikle DD (2004). The role of the calcium-sensing receptor in epidermal differentiation. *Cell Calcium* 35: 265-73.

Umanoff H, Edelmann W, Pellicer A, Kucherlapati R (1995). The murine N-ras gene is not essential for growth and development. *Proc Natl Acad Sci U S A* 92: 1709-13.

van Erp NP, Gelderblom H, Guchelaar HJ (2009). Clinical pharmacokinetics of tyrosine kinase inhibitors. *Cancer Treat Rev* 35: 692-706.

Varkaris A, Katsiampoura AD, Araujo JC, Gallick GE, Corn PG (2014). Src signaling pathways in prostate cancer. *Cancer Metastasis Rev*.

Veness MJ, Palme CE, Smith M, Cakir B, Morgan GJ, Kalnins I (2003). Cutaneous head and neck squamous cell carcinoma metastatic to cervical lymph nodes (nonparotid): A better outcome with surgery and adjuvant radiotherapy. *Laryngoscope* 113: 1827-33.

Vetter IR, Wittinghofer A (2001). The guanine nucleotide-binding switch in three dimensions. *Science* 294: 1299-304.

Vitale-Cross L, Amornphimoltham P, Fisher G, Molinolo AA, Gutkind JS (2004). Conditional expression of K-ras in an epithelial compartment that includes the stem cells is sufficient to promote squamous cell carcinogenesis. *Cancer Res* 64: 8804-7.

Wadhawan A, Smith C, Nicholson RI, Barrett-Lee P, Hiscox S (2011). Src-mediated regulation of homotypic cell adhesion: Implications for cancer progression and opportunities for therapeutic intervention. *Cancer Treat Rev* 37: 234-41.

Wang Q, Qian J, Wang F, Ma Z (2012). Cellular prion protein accelerates colorectal cancer metastasis via the fyn-SP1-SATB1 axis. *Oncol Rep* 28: 2029-34.

Webb DJ, Donais K, Whitmore LA, Thomas SM, Turner CE, Parsons JT, Horwitz AF (2004). FAK-src signalling through paxillin, ERK and MLCK regulates adhesion disassembly. *Nat Cell Biol* 6: 154-61.

Weinberg RA (2008). Twisted epithelial-mesenchymal transition blocks senescence. *Nat Cell Biol* 10: 1021-3.

Weinstock MA (1989). The epidemic of squamous cell carcinoma. *JAMA* 262: 2138-40.

Whale A, Hashim FN, Fram S, Jones GE, Wells CM (2011). Signalling to cancer cell invasion through PAK family kinases. *Front Biosci (Landmark Ed)* 16: 849-64.

Wildenberg GA, Dohn MR, Carnahan RH, Davis MA, Lobdell NA, Settleman J, Reynolds AB (2006). p120-catenin and p190RhoGAP regulate cell-cell adhesion by coordinating antagonism between rac and rho. *Cell* 127: 1027-39.

Wolf RM, Wilkes JJ, Chao MV, Resh MD (2001). Tyrosine phosphorylation of p190 RhoGAP by fyn regulates oligodendrocyte differentiation. *J Neurobiol* 49: 62-78.

Xie Z, Bikle DD (2007). The recruitment of phosphatidylinositol 3-kinase to the E-cadherin-catenin complex at the plasma membrane is required for calcium-induced phospholipase C-gamma1 activation and human keratinocyte differentiation. *J Biol Chem* 282: 8695-703.

Yadav V, Denning MF (2011). Fyn is induced by ras/PI3K/akt signaling and is required for enhanced invasion/migration. *Mol Carcinog* 50: 346-52.

Yagi R, Waguri S, Sumikawa Y, Nada S, Oneyama C, Itami S, Schmedt C, Uchiyama Y, Okada M (2007). C-terminal src kinase controls development and maintenance of mouse squamous epithelia. *EMBO J* 26: 1234-44.

Yeatman TJ (2004). A renaissance for SRC. *Nat Rev Cancer* 4: 470-80.

Yeo MG, Oh HJ, Cho HS, Chun JS, Marcantonio EE, Song WK (2011). Phosphorylation of ser 21 in fyn regulates its kinase activity, focal adhesion targeting, and is required for cell migration. *J Cell Physiol* 226: 236-47.

Yilmaz M, Christofori G (2009). EMT, the cytoskeleton, and cancer cell invasion. *Cancer Metastasis Rev* 28: 15-33.

Zeisberg M, Neilson EG (2009). Biomarkers for epithelial-mesenchymal transitions. *J Clin Invest* 119: 1429-37.

Zeng L, Si X, Yu WP, Le HT, Ng KP, Teng RM, Ryan K, Wang DZ, Ponniah S, Pallen CJ (2003). PTP alpha regulates integrin-stimulated FAK autophosphorylation and cytoskeletal rearrangement in cell spreading and migration. *J Cell Biol* 160: 137-46.

Zhang S, Yu D (2012). Targeting src family kinases in anti-cancer therapies: Turning promise into triumph. *Trends Pharmacol Sci* 33: 122-8.

Zhao L, Li W, Marshall C, Griffin T, Hanson M, Hick R, Dentchev T, Williams E, Werth A, Miller C, *et al* (2009). Srcasm inhibits fyn-induced cutaneous carcinogenesis with modulation of Notch1 and p53. *Cancer Res* 69: 9439-47.

Zhao W, Kitidis C, Fleming MD, Lodish HF, Ghaffari S (2006). Erythropoietin stimulates phosphorylation and activation of GATA-1 via the PI3-kinase/AKT signaling pathway. *Blood* 107: 907-15.

VITA

The author, Sarah Fenton, was born at the Loyola University Medical Center in Maywood, IL on July 12th, 1986 to Jay and Susan Fenton. She received a Bachelor of Science in Biology from Saint Louis University (St. Louis, MO) in May of 2008.

In July of 2008, Sarah joined the MD/PhD program and began her medical school coursework in the Stritch School of Medicine at Loyola University Medical Center (Maywood, IL). During the summer of 2009 she joined the laboratory of Dr. Mitchell F. Denning for a summer rotation. In 2010 Sarah joined the Denning lab to study the role of Fyn, a Src family tyrosine kinase, in cutaneous squamous cell carcinoma. While at Loyola, Sarah was awarded the Arthur J. Schmitt Dissertation Fellowship and placed first in the 2013 St. Albert's Day Graduate Student Oral Competition. She was also selected to receive a Kligman Travel Fellowship and to give an oral presentation at the 2014 Society for Investigative Dermatology Annual Meeting in Albuquerque, New Mexico.

After completing her Ph.D., Sarah will continue to work on her medical degree with two more years of coursework.